University of Chinese Academy of Sciences

博士学位论文

基于 CRISPR 和等温扩增的新型分子诊断技术以及基于核酸适体的骨桥蛋白检测新方法

作者姓名： Omar Mukama

指导教师: Zhiyuan Li

广州生物医药与健康研究院

学位类别: 理学博士

学科专业: 细胞生物学

培养单位: 中国科学院广州生物医药与健康研究院

2020 年 8 月

Novel Point-of-Care Diagnostics with CRISPR and Isothermal amplification, and an aptamer based detection method for a cancer marker osteopontin

A dissertation submitted to

University of Chinese Academy of Sciences

in partial fulfillment of the requirement

for the degree of

Doctor of Philosophy

in Biochemistry and Molecular Biology

By

Omar Mukama

Supervisor: Professor Zhiyuan Li

Guangzhou Institutes of Biomedicine and Health,

Chinese Academy of Sciences

August, 2020

中国科学院大学

研究生学位论文原创性声明

本人郑重声明：所呈交的学位论文是本人在导师的指导下独立进行研究工作所取得的成果。尽我所知，除文中已经注明引用的内容外，本论文不包含任何其他个人或集体已经发表或撰写过的研究成果。对论文所涉及的研究工作做出贡献的其他个人和集体，均已在文中以明确方式标明或致谢。

作者签名：OMAR MUKAMA

日　期：

中国科学院大学

学位论文授权使用声明

本人完全了解并同意遵守中国科学院有关保存和使用学位论文的规定，即中国科学院有权保留送交学位论文的副本，允许该论文被查阅，可以按照学术研究公开原则和保护知识产权的原则公布该论文的全部或部分内容，可以采用影印、缩印或其他复制手段保存、汇编本学位论文。

涉密及延迟公开的学位论文在解密或延迟期后适用本声明。

作者签名：　　导师签名：

日　期：　　日　期

摘 要

在生物医学和安全性方面，传染病的检测势在必行，因此，快速、灵敏和特异性的诊断仍有待提高。 目前基于 Cas 酶（Cas12a / b，Cas13a / b 和 Cas14）的 CRISPR-Cas 系统在疾病的诊断中得到了发展，Cas 酶通过对靶标进行切割，以及非靶标单链 DNA 进行反式切割，荧光基团标记报告基因单链 DNA，通过反式切割 ssDNA，可以通过荧光读取结果。基于此独特的反式切割特性，我们利用 LbaCas12a，构建了报告基因和激活子 DNA 序列，建立了快速、准确检测核酸的方法。此外，我们结合环介导等温扩增技术（LAMP），以提高测定的灵敏度，设计了一种新型的基于 DNA 探针的侧流生物传感器（LFB）。通过优化，基于 LbaCas12a 的系统对靶序列的识别会诱导报告基因 SSDNA 的反式切割，使 LFB 检测线捕获探针无法检测到报告基因。通过靶向不同的细菌和病毒病原体（HPV 病毒，铜绿假单胞菌, 非洲猪瘟病毒和爱泼斯坦-巴尔病毒），由于 LAMP 的预扩增，在检测时，铜绿假单胞菌和人类乳头瘤病毒分别获得 1×10^{-18} M (1.2 copies)和 3.1×10^{-18} M (1.8 copies)的灵敏度。当在 Cas12a 反应之前进行 PCR 预扩增时，非洲猪瘟病毒和人类疱疹病毒 4 型病毒分别获得了 2.5×10^{-15} M（∽1554.46 拷贝/微升）和 7.1×10-14 M（∽42,000 拷贝/微升）的灵敏度。最重要的是，我们基于 CRISPR 的检测 CIALFB 显示在不到一小时内，有相关菌株和无相关菌株存在的情况下，有很强的特异性。此外，该方法在复杂样品如血清，牛奶和临床样品中也具有适用性，因此，CRISPR-Cas 系统望为现场诊断，治疗和研究病原体提供功能强大，用途广泛且可重新编程的工具，将为疾病的临床评估提供有利手段，并补充克服抗菌素耐药性的现有检测策略。

关键词： CRISPR/Cas12a/b，核酸扩增，侧流生物传感器，疾病预后，适配体

Abstract

The detection of infectious diseases is imperative in biomedicine and safety. Thus, rapid, sensitive and specific diagnostics remains to be accelerated and prioritized. CRISPR-Cas system has been currently exploited in diagnostics based on Cas enzymes (Cas12a/b, Cas13a/b, and Cas14) collateral cleavage of target and non-target ssDNA in the vicinity, an effect which offers a fluorescent readable result from cleavage of a fluorophore-labelled reporter ssDNA. Based on this unique trans-cleavage property, we aimed to construct novel reporter and activator DNA sequences for LbaCas12a rapid and precisely detect cognate nucleic acids. Moreover, we combined loop-mediated isothermal amplification (LAMP) to increase the sensitivity of the assay. We furthermore designed a novel DNA probe-based lateral flow biosensor (LFB) for visual detection and monitoring of reporter sequences trans-cleavage. Under optimized conditions, the target recognition by LbaCas12a/b-based system induced entire trans-cleavage of ssDNA reporters, resulting in short sequences undetectable by the LFB test line capture probe. By targeting different bacterial and viral pathogens (HPV, *P. aeruginosa*, African swine fever virus and Epstein-Barr virus), 1×10^{-18} M (1.2 copies) and 3.1×10^{-18} M (1.8 copies) sensitivities for *P. aeruginosa* and HPV, respectively were obtained due to the LAMP pre-amplification. With PCR pre-amplification prior to Cas12a reaction, 2.5×10^{-15} M (~1554.46 copies/µl) and 7.1×10^{-14} M (~42,000 copies/µl) and sensitivities were achieved for African swine fever virus and Epstein-Barr virus, respectively. Most importantly, our CRISPR based assays showed uncompromised specificity –in the presence of related/unrelated strains- at low-cost in less than an hour for CIALFB. Furthermore, this assay demonstrated applicability in complex samples such as serum, milk and clinical samples. This system promise robust, versatile and reprogrammable tool for Point-of-Care diagnosis, treatment, and study of pathogens. This will pave-the-way forward in the clinical evaluation of disease and complement existing strategies at overcoming antimicrobial resistance.

Furthermore, we presented herein the rapid determination of human osteopontin (OPN) protein, a potential cancer biomarker, which holds substantial promise for point-of-care diagnostics and biomedical applications. To date, most reported platforms for OPN detection are apparatus-dependent, time-consuming, and expensive. Herein, we established a lateral flow biosensor (LFB) for OPN detection. A biotinylated aptamer was used for OPN pre-capture from samples, an antibody for OPN was immobilized on the test line for a second specific target identification, and streptavidin-modified gold nanoparticles were sprayed on the conjugation pad for color detection. This LFB achieved as low as 0.1 ng mL^{-1} OPN

sensitivity with a good dynamic detection between 10-500 ng mL^{-1} within 5 minutes. Intriguingly, the LFB allowed a qualitative and semi-quantitative detection of OPN in serum at clinically cut-off levels as in cancer patients, and can discriminate OPN from interfering proteins with high specificity. Thus, it is a promising alterative approach for point-of-care OPN screening and detection.

Keywords: CRISPR/Cas12a/b, Nucleic acid Amplification, Lateral flow biosensor**,** Diseases prognosis**,** Aptamer

Table of Contents

Chapter 1: General introduction and literature review

1.1 Introduction

Clustered Regularly Interspaced Short Palindromic Repeats (CRISPR)/CRISPR-associated (CRISPR/Cas) systems endow bacteria and archaea the adaptive immunity against invading nucleic acids (Barrangou et al., 2007; Jinek et al., 2012). These systems mainly work under the guidance of a guide-RNA (gRNA) that navigates Cas effector proteins to target and cleave an invader DNA sequence (Jinek et al., 2014). Over the last few years, CRISPR/Cas systems such as Type II CRISPR/Cas9 have become a prominent tool in transcription regulation, genome editing, and in situ DNA/RNA detection. Similar to CRISPR/Cas9, Type V CRISPR-Cas effectors such as Cas12 and Cas13 have also been used for gene editing (Tang and Fu, 2018; Ishino et al., 2018; Makarova et al., 2011; Strecker et al., 2019).

Beyond genome editing ability, Cas12 and Cas13 effectors have recently demonstrated remarkable potentials in developing novel biosensing technologies for nucleic acid detection based on their unique property of collateral cleavage of target nucleic acids and non-specific single stranded nucleic acids (used as reporters) to provide fluorescence signal readout (Chen et al., 2018a; Gootenberg et al., 2018; Li et al., 2018a). For example, a Cas13-based RNA targeting method called SHERLOCK (Specific High Enzymatic Reporter UnLOCKing) has been used for the detection of pathogens and SNPs (Gootenberg et al., 2018; Myhrvold et al., 2018). Similarly, LbCas12a-based DETECTR (DNA Endonuclease Targeted CRISPR *Trans* Reporter) (Chen et al., 2018a) and HOLMES (One-Hour-Low cost Multipurpose highly Efficient System) (Li et al., 2018b) have been reported for the diagnosis of human papillomavirus and SNPs, respectively. In general, these biosensing platforms require several critical reaction components, including ssDNA activators, crRNAs, buffer, DNA amplification mixture, reverse transcription system (for SHERLOCK), and the single stranded nucleic acids. Besides, SHERLOCK approach requires dual nucleases (Csm6 and LwaCas13), reverse transcriptase RPA, lateral flow assay with an anti-FAM antibody, streptavidin (SA), protein A, and fluorescence readout of bi-labeled reporters (Chen et al., 2018a). Although sensitive, all these CRISPR biosensing methods rely on target nucleic acid amplification through recombinase polymerase amplification (RPA) and PCR pre-amplification, and fluorescence readers to improve sensitivity (Gootenberg et al., 2018;

Myhrvold et al., 2018). Therefore, they require sophisticated systems and tedious sample/reagent treatment steps, which further rely on expensive fluorescence reader instruments and well-trained technicians. This can cause practical inconvenience and make the system less robust.

LAMP (Notomi et al., 2000a; Huang et al., 2014a) has improved this drawback and allows the entire amplification at a single temperature, higher specificity and sensitivity, and low cost. Recently, Li et al.'s paper in press employed LAMP with thermophilic Cas12b to develop a fluorescence based nucleic acid diagnostic termed HOLMESv2 (Li et al., 2018a). Herein, we integrated *Lachnospiraceae bacterium* Cas12a (LbaCas12a) and *Alicyclobacillus acidoterrestris* Cas12b (AaCas12b) effectors with LAMP to develop an ultrasensitive lateral flow biosensor (LFB) for the detection of *Pseudomonas aeruginosa* (*P. aeruginosa*), characterized with CRISPR/Cas and loop-mediated Isothermal Amplification (termed CIALFB) in a one pot reaction system. *P. aeruginosa* is an opportunistic human pathogen with a large and complex genome and is a critical infectious bacterium classified as a multidrug-resistant pathogen (E. Tacconelli, 2017; Tacconelli et al., 2018). It is widely used as a model for CRISPR/Cas system studies (Gootenberg et al., 2018; Xu et al., 2018a; Pawluk et al., 2016; van Belkum et al., 2015).

The principle of CIALFB method is based on the LFB detection of a biotinylated ssDNA reporter. By targeting the *P. aeruginosa* acyltransferase specific gene and Human papilloma virus conserved L1 gene's hypervariable loop V of HPV16/18, we leveraged the CRISPR-Cas12 reaction conditions (buffer, crRNA, ssDNA reporter, and activator) to enhance the collateral cleavage of the target gene and the ssDNA reporter. The ssDNA reporter cleavage was monitored on the DNA probe based LFB. A DNA probe sequence complementary to the ssDNA reporter was fixed on the test line of the LFB to capture the biotinylated ssDNA reporter sequence; while an inexpensive biotinylated rabbit polyclonal anti-IgG antibody (the antibody was used to fix biotin on the control line) was immobilized on the control line to capture the excessive gold nanoparticle-streptavidin (AuNP-SA) complex that was previously sprayed and dried on the conjugate pad. The AuNP-SA conjugate reacts with biotinylated ssDNA reporters and forms an AuNP-SA-biotin ssDNA reporter complex, which is captured by the capture probe at the test line. The excess complex subsequently reacts with the biotinylated rabbit polyclonal anti-IgG antibody on the control line to spot the biosensor performance (Figure 1.1). In the presence of the target gene, both

the amplified target gene and the ssDNA reporter were cleaved; therefore, the cleaved ssDNA reporters were undetectable at the LFB test line, providing a novel approach for visual detection of target gene on LFB with CRISPR/Cas mediated *trans*-cleavage. We also tested the system with fluorescence detection using a fluorophore (FAM) at one end and a fluorescence quencher (TAMRA) at the other end of the ssDNA reporter, and the results confirmed the single copy sensitivity of this system. Moreover, our CIALFB can discriminate HPV16, HPV18 and *P. aeruginosa* from non-target bacteria (*Escherichia coli* O157:H7, *Staphylococcus aureus*, *Campylobacter jejuni*, *Salmonella typhimurium*, and *Shigella dysenteriae*), both in pure and complex samples. This technique is fast, accurate, robust, and inexpensive for clinical diagnosis of infectious diseases.

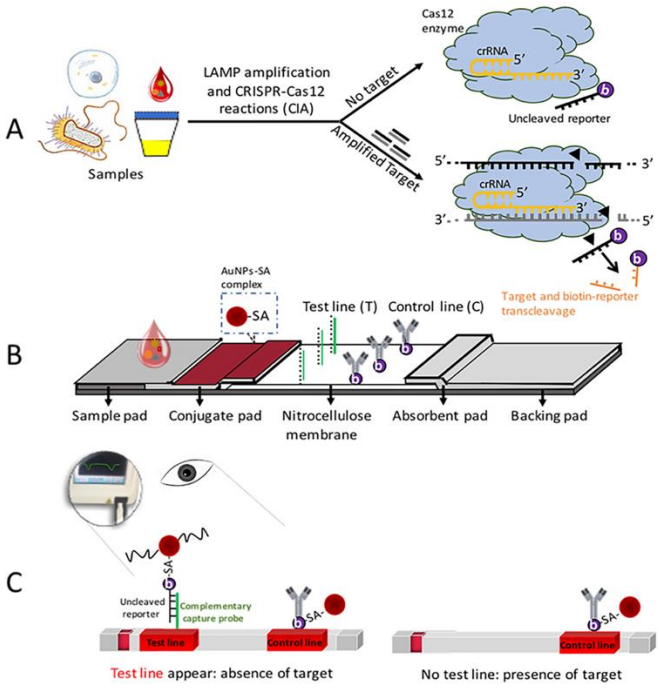

Figure 1. 1 A schematic illustration of the principle of CIALFB.

(A) Samples are heat-treated, LAMP-amplified, and then subjected to Cas12a/b collateral cleavage of the biotinylated ssDNA reporter. (B) The reaction product mixture is directly loaded on the CIALFB. (C) In the absence of the target gene, AuNP-SA-biotin-ssDNA reporter complex is captured by a single strand capture probe that is complementary to the ssDNA reporter, and the test line becomes detectable. The excess of AuNP-SA is then captured at the control line by the biotinylated polyclonal antibody. The amount of uncleaved ssDNA reporter can be detected by naked eye or quantitatively measured using a portable strip reader.

1.1 Diagnostics with Isothermal DNA amplification and LFB

1.1.1 Introduction

Nucleic acid detection techniques are rapidly growing owing to the critical importance in the diagnosis of infections, genetic diseases, and cancers (Yan et al., 2014). PCR has been exploited for nucleic acids detection; however, it is limited for on-site application due to thermocyclers and skilled-personnel demands. Various isothermal amplification methods which amplify nucleic acids isothemally and allow for the detection of various nucleic acid targets have been in use. These include recombinase polymerase amplification (RPA) (Lobato and O'Sullivan, 2018), rolling circle amplification (RCA) (Ali et al., 2014a), loop-mediated isothermal amplification (LAMP) (Notomi et al., 2000a), cross priming amplification (CPA) (Xu et al., 2012a), multiple cross displacement amplification (MCDA) (Wang et al., 2016a), polymerase spiral reaction (PSR) (Liu et al., 2015a), nucleic acid sequence-based amplification (NASBA) (Compton, 1991), and helicase dependent isothermal DNA amplification (HDA) (Vincent et al., 2004a) have been put employed and some their distinct features, advantages, and shortcomings are covered in Table 1. They are an alternative to PCR, which lacks on-site quantitation, fluorescence detection dependency, and is cross-contamination susceptible. Different methods including colorimetric (Geng et al., 2014; Hamidi and Ghourchian, 2015; Oh et al., 2016; Hu et al., 2017a; Baek et al., 2018; Ding et al., 2019), fluorescence (Yang et al., 2015; Jiang et al., 2016; Li et al., 2017a; Shirato et al., 2018; Lin et al., 2019), chemiluminescence (Wang et al., 2016b; Kober et al., 2018), electrochemistry (Cheng et al., 2014; Barreda-Garcia et al., 2015; Del Rio et al., 2016; Tabata et al., 2017; Islam et al., 2018; Kampeera et al., 2019), and surface-enhanced Raman spectroscopy (Draz and Lu, 2016; Yao et al., 2017) have been developed for the analysis of isothermal nucleic acid amplification products. However, most of these methods are apparatus based, which could hinder their on-site application. So, the development of potential approaches for on-site deployment is therefore essential.

Lateral flow biosensor (LFB), one of the foremost commonly exploited methods, owing to its rapidity, simplicity, stability, low cost, visual, and user-friendly characteristics (Gervais et al., 2011), has been widely used in the designing of detection assays. When integrated with one or more of the previous isothermal amplification techniques, they offer a high effective sensing and read-out tool, apparatus-free, affordable in multitude, and user-friendly, that enables the visual detection of nucleic acids by the naked eye of the

operator. Nanoparticles such as quantum dots (Chen et al., 2018b), silver nanoparticles (Rodríguez et al., 2016), and carbon nano-materials (Zhang et al., 2017) have been employed for development of lateral flow biosensor. A huge number of reported LFBs has focused on gold-nanoparticles (AuNPs) as common colorimetric markers due to their easily modified surface and macroscopic optical properties (Xu et al., 2014). LFB consists of five main sections: a sample pad, a section on which the sample is introduced; conjugate pad, a section on which labeled tags reacts with the biological element; nitrocellulose membrane which houses a test line and a control line to capture a target; an absorbent pad to retain wastes; and lastly a backing pad which works as a protective support of the whole system (Elif Burcu and Mustafa Kemal, 2016) (Figure 1.1). It is easy to construct, and the results are observable by naked eye.

Most recently, CRISPR-Cas system, a genome editing tool (Sander and Joung, 2014), has been applied in biosensing. Cas12 and Cas13 effectors have shown to exhibit collateral cleavage of pre-amplified target nucleic acids and non-specific single-stranded sequences (Tang and Fu, 2018; Gootenberg et al., 2018; Li et al., 2018a; Myhrvold et al., 2018; Li et al., 2018b; Chen et al., 2018c). When the latter are fluorophore-quencher labeled and in presence of the target sequence (s), they can provide readable signal after trans-cleavage. Herein, we presented the most used isothermal amplification methods as well as post-amplification product analysis using the currently developed methods that combine isothermal amplification, CRISPR-Cas system, and LFB towards the on-site deployment.

Table 1. 1 Summary of nucleic acid isothermal amplification methods.

Tech nique	Target	Initial heating	Primers needed	Enzyme involved	Incubation temperature (ºC)	Reaction Time (min)	Limit of detection (copies)
RPA	DNA/RNA	No	2	Recombinase polymerase	37-42	20-40	1
SDA	DNA	Yes	4	Polymerase restriction enzyme	30-55	60-120	10
LAMP	DNA	Yes/No	4-6	Polymerase	60-65	60	~5
RCA	DNA/RNA	Yes	1	Polymerase	30-65	60-240	10
NASBA	RNA	No	2	Transcriptase RNA polymerase RNase H	41	60-180	1
HDA	DNA	No	2	Helicase polymerase	65	30-120	1

MDA	DNA	Yes	Random	Ø29 DNA polymerase	30	960-1080	1-10
LCA	DNA	No	2	Ligase & Taq polymerase	60	1	-
NEAR	DNA	No		DNA polymerase	55	120	10

1.1.2 LAMP based lateral flow biosensor

LAMP is a fascinating simple, rapid and cost-effective isothermal nucleic acid amplification technique having close similarity, power, and performance with PCR. Due to its use of two primer sets complementary to six different sequences of the target, the LAMP also realizes high target specificity. The principle of LAMP is illustrated in Figure 1.2. In the forward primer set, a couple of primers are named inner primer (FIP, F1c+F2) and out primer (F3). At 60-65 ℃, the F2 region of FIP first binds to the target and is extended by a DNA polymerase. After the completion of F3 annealing to F3c target strand, a new strand is synthesized by the extension of F3 using a specific enzyme polymerase. The newly formed strand shapes into a stem-loop structure at the 5' end as a result of the interaction between F1c and F1 site. By the action of polymerase, the reverse outer primer (B3) and inner primers (BIP, B1c+B2) anneals to the 3' end and generates a new strand having a stem-loop structure. The dumbbell structured DNA enters the exponential amplification cycle, and strands with several inverted repeats of the target DNA can be made by repeated extension and strand displacement. Different from PCR, there are multiple primer pairs (4-6 pairs) used to amplify a target gene, and numerous amplification products of various lengths are produced. LAMP can generate about 10^9 target DNAs and a large number of by-products within 60 minutes (Mori and Notomi, 2009; Notomi et al., 2000b; Nagamine et al., 2002), even when large amounts of non-target DNA are presented (Nagamine et al., 2002). The resulting products of LAMP consists of numerous distinctive sizes of stem-loop DNAs with several altered repeats of the target sequence and cauliflower-like structures with several loops. The major disadvantage of LAMP resides in complications for designing primers since six regions of the target are covered, even though 4 primers can also work. Moreover, LAMP spurious amplification has been reported, which is highly confusing false positive result as seen in either electrophoresis or colorimetric analysis. To resolve this drawback, and owing to its trending favorable advantages and applications, different types of biosensors were developed using various lateral flow approaches. For example, an integrated rotary

microfluidic system was proposed by Park et al. (Byung Hyun et al., 2016), which is capable of DNA extraction, LAMP, and lateral flow strip based detection for *Salmonella Typhimurium*. It achieved a high specificity and a detection limit (LOD) of 50 CFU within 80 minutes. Another LAMP-LFD approach has been developed to detect *Salmonella* strains within food samples (LOD: 13.5 fg/µl of genomic DNA and 6.7 CFU/ml of cell) (Xueran et al., 2019). In this study, all 52 strains of *Salmonella* were positively detected, and no cross-contamination was observed within 37 tested non-*Salmonella* strains. This assay showed demonstrated a sensitivity of 100 to 1000 times compared to the conventional PCR and real-time PCR assays, respectively. The accuracy of this assay was 100 % when compared to the standard culture based method (ISO 6579:2002) after an enrichment step at 37 °C for 6 h.

In another study, LAMP coupling with a lateral flow was applied for the rapid detection of genetically modified crops (soybean and maize with a limit of detection of 0.5%) (Reona et al., 2018). In retrospect, pointing a huge need for developing multiple targets detection based apparatus, LAMP showed multiplexing potentials due to the ability of primers to target different sequences. LAMP has also improved ability for multiplexing detection when coupled with lateral flow assay. For instance, Yin H.Y. et al. (Yin et al., 2016), proposed a LAMP based lateral flow assay for the simultaneous detection of the sea and seb genes of enterotoxin *Staphylococcus aureus*. Within this study, the sea and seb genes were labeled with biotin and separately labeled by digoxigenin and fluorescein isothiocyanate, respectively. The detection of the two amplicons (sea and seb genes) was achieved by incorporating NeutrAvidin-tagged gold nanoparticles with LFD, allowing the quantification and visual detection through competitive sandwich approach. The LOD of 10-fold lower than of a multiplex PCR (102 CFU/ml) was achieved. This assay established the assay's ease-of-use characteristics, high sensitivity and specificity, making it applicable for P-O-C testing.

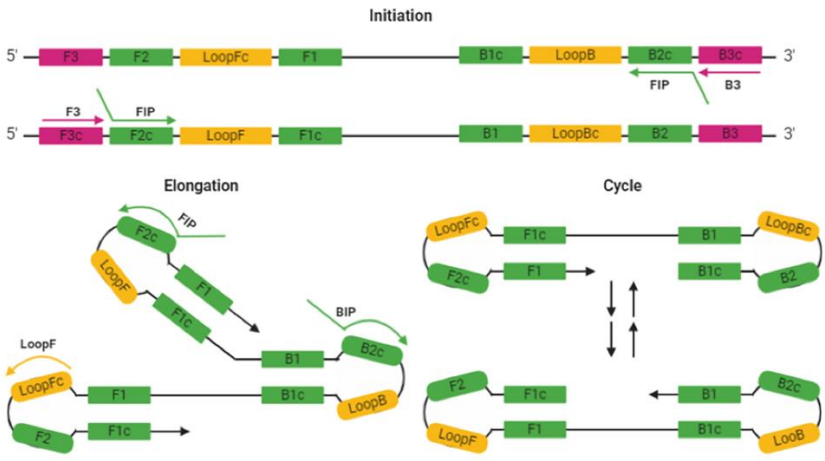

Figure 1. 2 Schematic representation of LAMP.

1.1.3 PSR based lateral flow biosensor

PSR, one of the recently discovered isothermal amplification technique with high efficiency, rapidity and specificity (Liu et al., 2015b). It operates at a constant temperature ranging from 61 to 65 ^{o}C within less than 1 hour by using betaine and Bst DNA polymerase, as a double strand destabilizing agent and unwound single strand extending enzyme, respectively. It is highly effective owing to the simplicity of primers designing using the conventional PCR software. PSR has the advantages of both PCR and LAMP. PSR primers differ from PCR primers in the exogenous sequences (Nr and N) that are extended on the 5' end, while, the remaining bases at the 3' end correspond to the target region (Figure 1.3). Reports demonstrate that PSR is highly sensitive 100 times more than PCR, cost-effective because it uses a water bath for constant temperature monitoring, and convenient with a simple color change to yield results.

The effects of the reaction include a high amount of byproducts of the pyrophosphate ion, which can be clearly visualized by adding an effective pH marker. Increasing numbers of studies have indicated that the PSR method offers a promising isother mal DNA amplification approach that can be employed for fast and minimal resource diagnosis, including the detection of certain clinical pathogens (Ji et al., 2019; He et al., 2020). Unfortunately, PSR based LFB have not been explored at this time. A number of PSR publications have been reported on chromogenic substrate SYBR Green I, which employs fluorescence as a color changing visual detection signal, however, PSR should be considered for future prospects as a potential isothermal amplification method for nucleic acid diagnosis owing to its extremely high sensitivity.

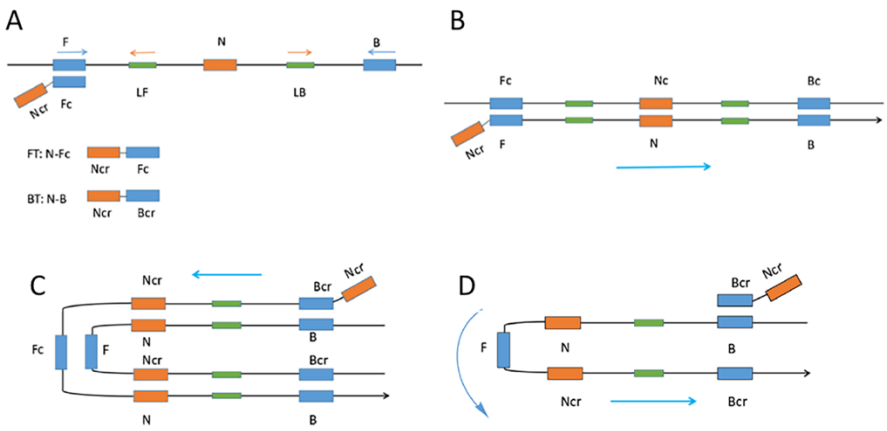

Figure 1. 3 Schematic diagram of PSR amplification.

Adopted with permission from (He et al., 2020) Copyright 2020, Springer.

1.1.4 CPA based lateral flow biosensor

Cross-priming amplification (CPA) is an isothermal amplification process of DNA invented by Ustar Biotechnologies (Hangzhou, China) (Xu et al., 2012b). CPA has proven to be highly specific and sensitive, producing amplicons from as low as four bacteria. This approach uses several cross-linking primers (6-8 primers) to amplify a target DNA sequence at a constant temperature producing hairpin-shaped products with various amounts. The amplification process can be split into three paths: (1) products that are extended with the cross primer and displaced with displacement primers, (2) multiple extensions and displacements with detection probes, and (3) extensions with hairpin-like structure-specific probes.

Xin Huang et al., (Huang et al., 2014b) proposed a CPA based LF strip for nucleic acid detection. As shown in Figure 1.4, the principle of this assay, the priming configuration included: a pair of displacement primers detaching single strand sequences at their 3 ends, one or more cross primers adding an additional priming site at each amplification cycle, a biotinylated primer and a FITC-labeled probe. Dual-labeled CPA products with biotin and FITC could be read easily on a LFB, where the template sequence was immobilized by fixed FITC antibodies to the test line by the help of streptavidin-coated latex particles. This assay had a good detection limit as low as 30 copies, small than that of conventional PCR.

In another study, for on-site detection of African swine fever virus, Yao Gao et al., (Gao et al., 2018) designed a CPA assay to target the p54 gene in combination with immunochromatographic strip (CPA-strip), First, the p54 gene was amplified by CPA using the specified primers and probes, and at the 5-ends, the products were labeled with biotin and FITC to facilitate subsequent interaction and immobilization on the LF strip. The complex of probes and target was allowed to interact with the antibodies fixed at the test and control lines to yield results that could be visualized by the naked eye. It showed a limit of detection of 200 copies with good recoveries.

To sum up, the CPA-LFB assay is accurate, responsive, convenient and low cost, and possesses the potential for effective diseases monitoring.

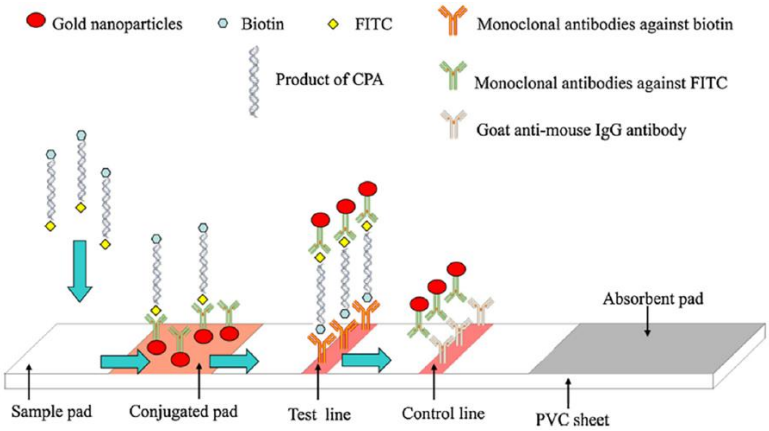

Figure 1. 4 Schematic diagram of the CPA-LF assay.

Reprinted from (Gao et al., 2018) with permission Copyright 2018, Elsevier.

1.1.5 MCDA based lateral flow biosensor

MCDA, a recently established assay by Yi Wang et al., (Wang et al., 2015) has shown potential to achieve extreme sensitivity compared to the previously reported nucleic acid amplification techniques such as PCR, LAMP, and CPA. This method which do not require thermal –regulating equipment, operates at a temperature ranging from 61 to 65 °C and uses a set of 10 specifically designed primers covering ten different target sequence sections, which are known as cross primers (CP1 and CP2), displacement primers (F1 and F2), and amplification primers (D1, C1, R1, D2, C2 and R2) with corresponding different target sites for binding namely P1s, P2s, F1s, F2s, D1s, C1s, R1s, D2s, C2s and R2s, respectively (Figure 1.5).

During the reaction, the 4double-stranded DNAs is fixed at primary-template hybrid dynamic reaction stage, hence the high proportion of primers attach to the target strands without a heat denaturing step to trigger the amplification by the action of *Bst* polymerase. A set of primary binding and extension processes generate multiple single -stranded DNAs and single-stranded single sterm-loop DNA structures for further isothermal amplification stage. Then, these DNA products permit the exponential amplification of the strand-displacement reaction to begin.

When compared to other amplification techniques (like PCR, LAMP, and CPA), MCDA was 16-and 32- times more sensitive than the LAMP and CPA techniques, respectively, and results could be achieved in less than 15 minutes. Recent studies show that MCDA provides a highly-touted approach for nucleic acid amplification that can be used to achieve a desired sensitivity with relatively low diagnosis cost. Shoukui Hu, et al., (Hu et al.,

2019) proposed a duplex MCDA assay that employs disposable LFB for the detection of MCDA amplicons. This assay was successfully applied for the analysis of *Acinetobacter baumannii*, a pathogen that cause nosocomial infections, by targeting the *pgaD* and *blaOXA-23-like* genes. The assay also reports a specificity of 100%, and the practical feasibility in clinical settings. Similarly, Yi Wang et al.,(Wang et al., 2018a) designed a LFB coupled with MCDA (Figure 1.5) for the analysis of nucleic acid and cross-contamination prevention. This method uses the enzyme, uracil-DNA glycosylase (AUDG) and self-avoiding molecular recognition system (SAMRS) components to eliminate cross-contamination, and false-positive results, and enhance MCDA sensitivity, respectively. To demonstrate the functionality for target analysis, Mycobacterium tuberculosis complex (MTC), a condition which causes of human tuberculosis (TB), has been identified by the proposed MCDA assay. MCDA reliability was assessed successfully in detecting MTC from pure culture and clinical specimens.

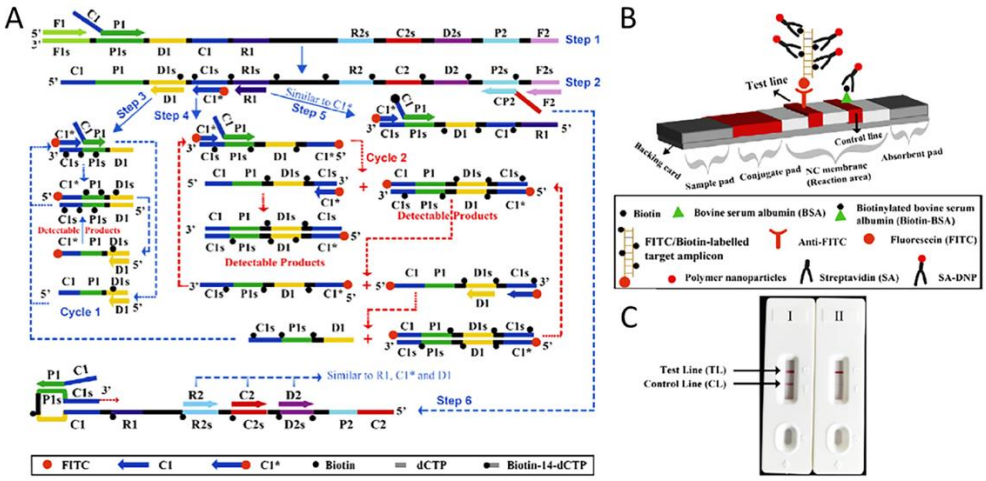

Figure 1. 5 The schematic showing the mechanism of MCDA.

(A) coupled with LFB (B) (Wang et al., 2017a).

1.1.6 RPA based lateral flow biosensor

RPA is a sensitive and specific technique for isothermal nucleic acid amplification that relies on the formation of a complex mainly comprising a recombinase and target-specific primers (Piepenburg et al., 2006). The recombinase first binds to primers, and form a recombinase-primer complex. The complex allows the dsDNA to find the complementary homologous sequence, and thus influence the strand invasion by the primer at the cognate site. Then, the single-stranded DNA (ssDNA) binding protein binds to the displaced DNA to avoid the discharge of the embedded primer. Finally, a strand displacing

DNA polymerase binds the 3’ end of the primer and elongates the primer to form a newly synthesized strand. The latter serve as template for cyclic or exponential amplification (Figure 1.6).

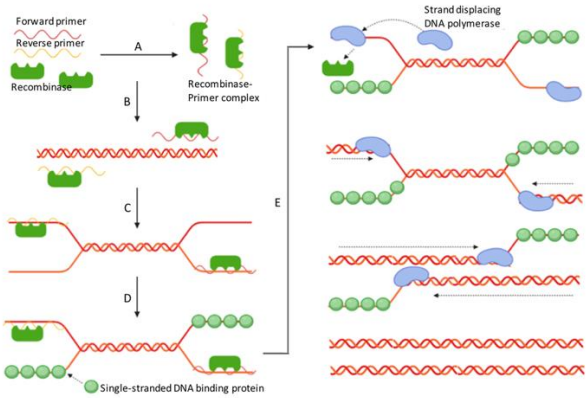

Figure 1. 6 RPA principle.

(A) The forward and reverse primers bind to the recombinase to form primers-recombinase complexes, which recognize only for homologous sequences (B). (C) Strand invasion by the complex at the cognate site. (D) Stabilization of the displaced DNA sequence by single-stranded DNA binding proteins. The recombinase opens the target sequence and a DNA polymerase, which has a strand displacement activity, binds the 3’ end of the primer and elongate it (E). The cyclic continuity of this process leads to the accomplishment of exponential amplification.

The characteristics, focal points, and drawbacks of RPA and other isothermal amplification techniques have been broadly reviewed in Table 1.1 and 1.2. Most importantly, it is an effective approach in terms of sensitivity, specificity, and multiplexing. It operates at the constant and low-temperature range when compared with other isothermal amplification types, which make a positive attribute since there is no requirement for continual temperature control within its operating temperature range. Generally, RPA has proved favorable for widespread use when integrated with LFB to generate robust sensing tools that are affordable, steady, user-friendly, cost-effective, and with low-resource settings for P-O-C (Point-of-Care) testing. To date, RPA combined with LFBs are widely applied in the detection and identification of pathogenic bacteria (Fu et al., 2019; Saxena et al., 2019), viruses (Sun et al., 2019), in food safety, environmental monitoring, and other biomedical fields (Du et al., 2018; Li et al., 2019; Xu et al., 2018b). For example, an RPA-LFB assay for the rapid authentication of mutton products has been developed (Li et al., 2019) (Figure 1.7). In this assay, a pair of specific RPA primers (5' end digoxigenin-modified forward primer and a 5'

end biotin-modified reverse primer) against the mutton cytochrome b (Cyt b) gene. As depicted in Figure 2, the RPA amplicons, and AuNP-mouse anti-digoxigenin conjugates are mixed and then diluted prior to loading on the LFB sample pad. The RPA amplicons are captured by streptavidin immobilized on the test line, hence forming a complex of streptavidin avidin-RPA-antibody conjugated with AuNPs. Excess AuNP-mouse anti-digoxigenin complex is captured by goat anti-mouse antibodies attached to the control line. In the absence of mutton products, there is no RPA amplicons, thus no detactable test line (Li et al., 2019). In another study, a similar system named duplex RPA–LFD (RPA lateral flow dipstick) assay was introduced to detect influenza viruses (Sun et al., 2019). Three different types of antibodies (Anti-fluorescein isothiocyanate, anti-digoxigenin, and biotinylated bovine serum albumin) were immobilized on the two test lines, and a control line, respectively; to capture dual-labelled products (influenza A and B viruses) and SA-Au modified by biotin, respectively. The assay achieved visible test lines with a LOD of 50 and 500 copies for both influenza A and B viruses, respectively (Sun et al., 2019). Recently, Xu Yet al. (Xu et al., 2018b), also developed a promising all-in-one platform based on RPA–LFD combining the strategy of a technique named universal blocking linker recombinase polymerase amplification (UBLRPA) and a peptide nucleic acid (PNA) based lateral flow device (PLFD) for the visual detection of pathogens in food and environmental samples. The DNA products were obtained using the working principle of UBLRPA amplification. Then, the DNA products were converted to a single strand using the UBLRPA amplification system. Therefore, through dual hybridization of the AuNP modified PNA probe and the universal linker, UBLRPA products could detected, producing a characteristic visual red band on the LFB. This approach exhibited high sensitivity and specificity as a result of the strong binding affinity between PNA and DNA. More interestingly, this approach can be used to identify other types of pathogens by only changing the primers.

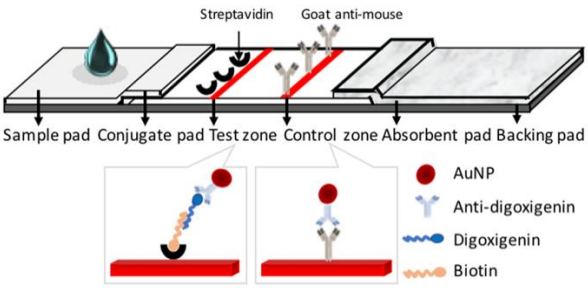

Figure 1. 7 Schematic illustration of RPA-LFD approach.

1.1.7 SDA-based lateral flow biosensor

SDA was first proposed by Walker and his co-worker in 1992. It is an isothermal nucleic acid amplification method that relies on the nicking restriction enzyme that cuts the unmodified strand of a hemiphosphorothioate form at its recognition regions, and the capacity of some polymerases (lacks the 5'–3' exonuclease activity) to extend the 3'-end at the nick and displace the downstream DNA strand (Walker et al., 1992a; Walker et al., 1992b).

As described in Figure 1.8, unlike other amplification systems, SDA consists of 3 phases of amplification, and its main components include 4 primers (B1, B2, S1, S2) and a nicking enzyme. A 5' overhang of the primer bound to the target strand comprises a specific sequence recognized by a restriction enzyme (e.g. HincII). By substituting thiol-modified deoxyadenosine triphosphate (dATP) rather than deoxyadenosine (dATP), the newly synthesized DNA strand is modified with a thiophosphate, which is HincII inactive, resulting in the original primer being cleaved by HincII rather than the synthetic DNA strand.

SDA is based on particular polymerases with more excellent strand displacement capabilities to extend the 3' end and replace the downstream DNA strand, and the restriction enzyme cleaves the unprotected primer strand at its recognition site, leaving the complementary modified strand intact. Since the polymerase lacks 5'-3' exonuclease activity, it can extend at the 3' end of the nick and replace the downstream strand at a temperature ranging from 30 to 55 °C. Thus, a new endonuclease recognition sequence is generated. Consequently, the exponential amplification is accomplished through the hybridization of sense SDA and antisense SDA in which strands are displaced (Walker et al., 1992a).

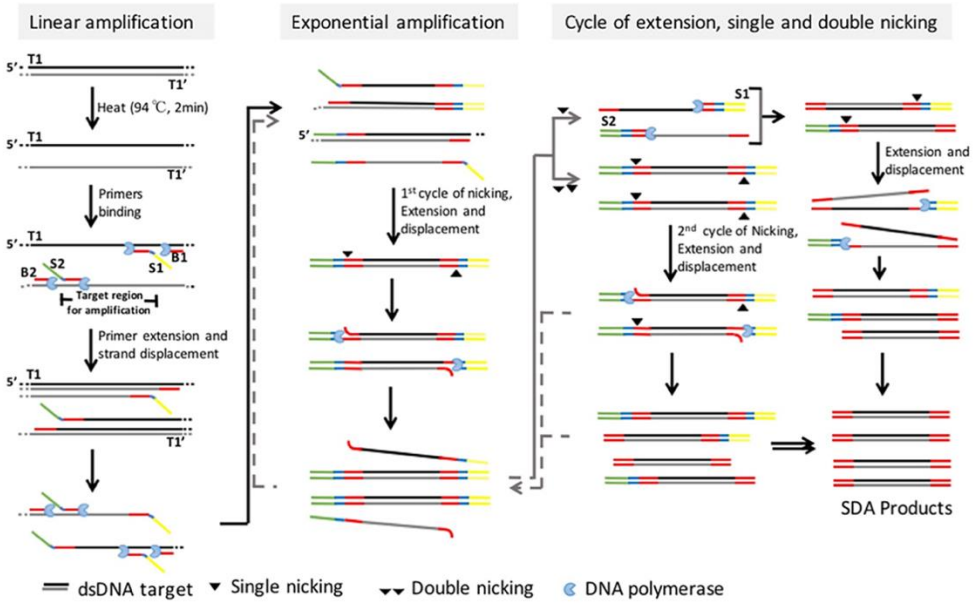

Figure 1. 8 The working principle of SDA.

The first step relies on the denaturation of the DNA double-strand before primer binding. The primers S1 and S2 comprise the recognition sequence regions that nick green and yellow endonucleases, a linker (blue) and a red region which is a sequence complementary to the target sequence. The SDA primers (S1 and S2) contain recognition sequences for nicking endonuclease (green and yellow), a linker (blue), and a sequence complementary to a target sequence (red). Bumper (B1 and B2) primers which complement the sequence of the target are located upstream of the SDA primers (red) respectively (black and grey). After the binding of primers to the sequence of the target, exo− Klenow or Bst which act as specific DNA polymerase, the strand is extended through a strand displacement mechanism. After arrangement of strands harboring a nicking site (linear amplification), the nicking enzyme nicks them, and the DNA polymerase primes a new round of replication (first cycle). Exponential amplification of the target sequence starts with the cycle of single and double nicking, extension, and displacement.

Based on LFB and aptamer mediated SDA, a simple and rapid assay was introduced to detect food-borne pathogens (Fang et al., 2014a; Wu et al., 2015a) and human pluripotent stem cells (hPSCs) (Wu et al., 2015b). In the study, to accomplish the successful detection of harmful bacteria (Figure 1.9), two distinct aptamers specific for the outer membrane of the pathogens were designed. One was a biotin modified capture-aptamer (c-aptamer) which was used for the bacteria enrichment, and the other one was an amplification-aptamer (a-aptamer), which served as a template for SDA amplification. Then, the amplified ssDNA was

subsequently detected via a probe-based lateral flow biosensor, which contains complementary sequence to amplified ssDNA sequences immobilized on the test line. These assays achieved as low as 10 CFU for *S. enteritidis* (Fang et al., 2014a) and *E. coli* O157:H7 (Wu et al., 2015a). Moreover, SDA assay is an excellent amplification method since it does not require DNA extraction, with minimal handling and simple equipment which render this method a fast and steady alternative method to conventional methods in foodborne pathogens detection (Wu et al., 2015b).

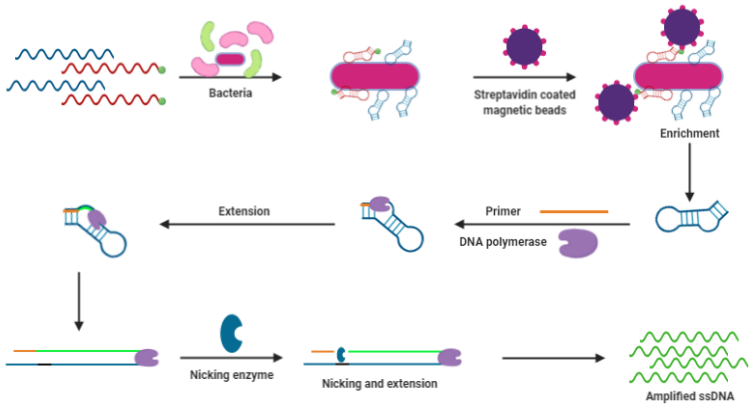

Figure 1. 9 Schematic representation of the aptamer-based nucleic acid isothermal amplification for lateral flow biosensor detection.

1.1.8 RCA based lateral flow biosensor

RCA is an enzyme based isothermal amplification technique that uses circular DNA to amplify target nucleic acids (DNA or RNA) with the help of DNA or RNA polymerase. It has the amplification power as high as PCR, with potential to amplify even a whole viral genome. The product of RCA contains tens to hundreds of repeated segments that are complementary to the circular mother template, which is usually an ssDNA or RNA (polyplex). RCA does not require complicated steps such as continuous temperature regulation using thermal cyclers and thermal stable DNA polymerase. RCA is direct, robust, and versatile for the amplification of circular DNA templates such as plasmids, bacteriophage, and circular RNA using the strand displacement capabilities of polymerases and it does so with both in pure and complex biological samples (Blanco et al., 1989). As described in Figure 1.10, RCA primer anneals to the circular template and the nucleic acid begins to replicate, and simultaneously, the polymerases displace the circular template continuously by adding the nucleotides until it reaches the terminal end of the target, resulting in a complete loop. The polymerase with strand displacement activity then displaces the newly synthesized strand while starting the synthesis of the next loop. The same amplification procedure

continues until the nucleotides are depleted, or the polymerase enzyme loses activity. Therefore, this results in the production of a long ssDNA strand having 10 to 100 of tandem repeats. This technique is very potent and can be used to amplify DNA strands up to 10^5 bp in length (Banér et al., 1998).

In a recent study reporting for the development of biosensor based on RCA technique, Yao and co-workers first developed a simultaneous, fast, sensitive, specific, and selective method based on RCA coupling with LFB strip for sensing miRNA 21 and miRNA let-7a, which achieved the LOD of 20 pM and 40 pM, respectively (Yao et al., 2019a). The padlock probe was designed specifically, whose 5' and 3' end were complementary to the sequence of target miRNA. After the padlock probe binding to the miRNAs and cyclizing in the presence of Splint R ligase, the amplification began under the function of DNA polymerase, and repeated ssDNAs were produced. The amplified products were then detected by AuNPs based lateral flow strip. In the presence of RCA products, the sandwich format of AuNPs-probe complexes and RCA products ran along the nitrocellulose membrane (NC) and captured by two specific probes. A positive signal as a red test line was observed. In contrast, when the RCA products were not present, the AuNPs-probe complexes were not recognized on the test line, leading to the absence of the test line. Moreover, strategies named HRCA-LFD (Chunyun et al., 2019), and E-RCA-LFD (Liu et al., 2019) were designed for the detection of *Karenia mikimotoi* and *Karlodinium veneficum*, respectively. The HRCA-LFD was specific and 100-fold more sensitive than PCR (Chunyun et al., 2019), and the E-RCA-LFD showed excellent sensitivity than the conventional PCR and reached a LOD of 0.01 cell/ml (Liu et al., 2019). RCA-LFD is playing a vital role in increased sensitivity and reduced cost of experimentation, which may contribute to saving detection time and could be selected as a potential tool for the detection and identification of target nucleic acids.

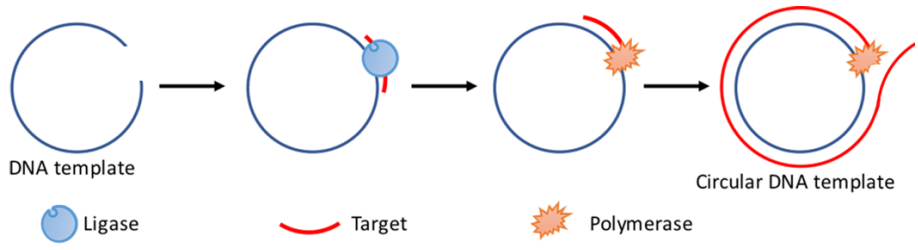

Figure 1. 10 Schematic illustration of RCA.

1.1.9 NASBA based lateral flow biosensor

NASBA was first reported by Clampton in 1991 (Compton, 1991) and later on, Gene-Probe successfully launched a NASBA based product, capable of doing both reverse

transcription and amplification for the detection of RNA (Deiman et al., 2002). A typical NASBA reaction mixture consists of an avian myeloblastosis virus reverse transcriptase (AMV-RT), T7 RNA polymerase, RNase H and a couple of oligonucleotide primers (P1 and P2) (Figure 1.11). NASBA can also produce false positives caused by genomic dsDNA, as it is the case with RT-PCR. In addition, NASBA is still limited by complex reaction mixture such as two primers and three enzymes – AMV-RT, T7 RNA polymerase, and RNase H - are involved in NASBA. Moreover, high temperature treatment (denaturation) can deactivate them. Thus, NASBA is not suitable for amplifying dsDNA targets because there is no initial denaturation step unless cooling and amplification steps are involved (Deiman et al., 2002). Other examples includes FRET (Park et al., 2011) and colorimetry (Niazi et al., 2013) based NASBA to detect 18S rRNA of *Aspergillus* and *Leishmania*, respectively. They achieved ultrasensitive detection of NASBA products (Park et al., 2011; Niazi et al., 2013). Although all those techniques have been developed, a more rapid and straightforward NASBA assay using lateral flow strip is not yet available.

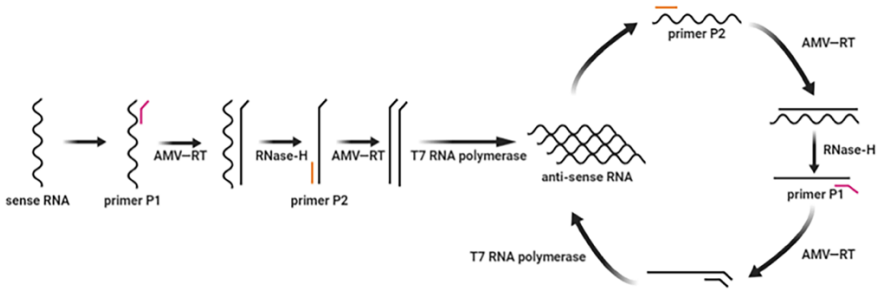

Figure 1. 11 Schematic illustration of NASBA.

P1 is made of a 3'-end target recognition sequence and a 5' end T7 RNA polymerase promoter sequence. Upon addition of the target RNA, P1 anneals to the complementary site at the 3'-end of the target, followed by the initiation of the synthesis of a complementary DNA strand catalyzed by AMV-RT to produce a DNA-RNA hetero-duplex. The RNase H then hydrolyzes the target RNA of the DNA-RNA hetero-duplex, leaving a ssDNA. P2 attaches to the 5' end of the DNA strand, and AMV-RT begins to synthesize another DNA strand starting from P2 using the DNA strand as a template, thereby producing a DNA homologous duplex (dsDNA) containing the T7 RNA polymerase promoter sequence. T7 RNA polymerase continuously transcribes the complementary RNA strand of the dsDNA template. The new formed RNA is used as a secondary RNA target, and the new cycle begins with the binding of P2 to the synthesized RNA, thereby entering the cycle of amplification. Therefore, NASBA starts amplifying the target RNA exponentially and produces an ssRNA product, which

amplifies the target by up to >1000 times within 120 minutes at 41 °C.

1.1.10 HDA based lateral flow biosensor

The working principle of HDA is very similar to the standard PCR procedure (Vincent et al., 2004b), except that for isothermal amplification, HDA does not use DNA denaturation at high temperatures as in PCR, but uses helicase to separate DNA strand (Figure 1.12), using single-stranded binding proteins to prevent the separation of separate DNA strands. It has close similarity to the cellular DNA replication as helicases untie dsDNA during the replication of DNA. The involvement of the helicase helps to eliminate the thermal cycler and allows the reaction to occur at room temperature while maintaining exponential amplification. As shown in Figure 1.12, a dsDNA is first expanded by helicase, then anneals with primer, and is extended by polymerase (exo$^-$Klenow fragment). The critical trait for HDA resides in no requirement for an initial heat denaturation step to generate ssDNA from the dsDNA target while many other isothermal amplification methods require an initial specific denaturation temperature before the target gets amplified at lower temperatures (Vincent et al., 2004b). Nevertheless, before performing HDA, it is often desirable to optimize experimental conditions, including buffer compositions and primer sequences. Unfavorably, the optimization process usually involves the use of PCR, which causes a significant amount of extra cost to HDA. Consequently, additional work is required to attain the potentiality of HDA including identification of the rate-limiting steps. One possible rate-limiting step is the interaction between the ssDNA binding protein and the target DNA strand since this interaction considerably prevents re-hybridization of the DNA strands separated by helicase. The efficiency of the helicase-catalyzed target dsDNA separation is another possible rate-limiting step as tests for many polymerases have not shown any significant differences between them (Vincent et al., 2004b). HDA is a fascinating alternative method to PCR because of its simplicity, limited complicated steps, and its excellent compatibility with various nucleic acid detection. Claudia and co-workers introduced a BacR HDA-strip assay for detecting ruminant faecal pollution sources, which can yield qualitative results paving the way for future simple-to-use microbial source tracking (MST) screening tools (Kolm et al., 2019). The entire process only took two hours, and no extensive practical training was required.

Alternatively, a more advanced HDA named thermophilic HDA (tHDA), was put in place for improved performance of the conventional HDA. The tHDA

uses a thermostable UvrD enzyme to separate the dsDNA and produce ssDNA templates used for subsequent amplification by the DNA polymerase. The dsDNA unwinding and amplification is conducted at isothermal temperature, between 60 and 65 °C that renders this method better suited for the construction of microbial point-of-need detection systems, because a thermocycler is not mandated for DNA denaturation at 95 °C to initiate the amplification. When combined with LFB, tHDA provides potentials for the visualization of amplified products. For example, Xin-jun Du et al., established a lateral flow read-out assay that could visualized the positive control of tHDA amplification products without the use of any sophisticated equipment. Amplicons-conjugated and non-conjugated gold nanoparticles were used for signal read-out, as they could be captured by the streptavidin and anti-mouse antibody immobilized at the test line and control lines, respectively. This assay was able to detect salmonella within real sample such as milk, chicken, and infant nutritional cereals, in limited time, with high sensitivity, and specificity and could be suited for the application in resource-limited areas.

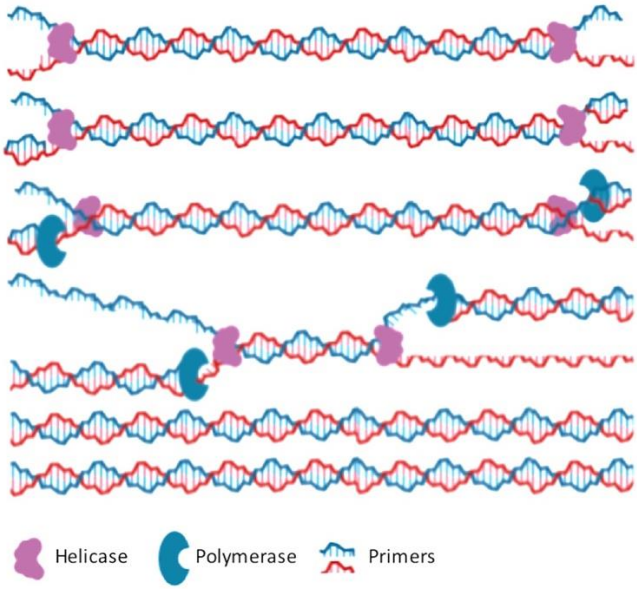

Figure 1. 12 Schematic Illustration of HDA.

1.1.11 Carryover contamination monitoring

Inhibition of carryover contamination has been a subject since two decades ago within all the fields concerned with nucleic acids manipulation. The amplification of by-products, handling, and exposure of reaction tubes, including sampling, capping, and uncapping operations are the main sources that are linked with cross-contamination. A number of strategies were recommended to eliminate and monitor carryover contamination. For

subsequent amplification, carryover of previously amplified amplicons is the most influential source of contamination. Many approaches were used to prevent contamination of the carryover, such as physical or mechanical, and chemical treatment. physical or mechanical treatment to avoid amplification products carryover requires strict isolation of laboratory zones where samples, materials, and reagents, are handled from the environments where amplification is conducted and amplification products are tested. Each laboratory zone must be fitted with the appropriate equipment, disposable tools, lab clothing, aerosol-free tubes and pipettes, and ventilation

systems. All materials and disposables used for each zone must all be delivered directly to that area (Aslanzadeh, 2004; Qian et al., 2017). Chemical treatment involves the usage of techniques such as Ultra-violet light irradiation, Inactivation of nucleic acids with furocoumarins (which is based on amplicon sterilization and the prevention and blockage of Taq polymerase to extend or amplify primers during amplification reaction), primer hydrolysis (post PCR hydrolysis of RNA residues of the amplicons by NaOH), Hydroxylamine chemically modifies C interfere C+G pairing), and enzymatic inactivation with uracil-N-glycosylase (Hsieh et al., 2014; Ma et al., 2017; Wang et al., 2017b). The latter one is most efficient techniques that include dUTP and uracil DNA glycosylase (UDG) in amplification reaction. Cheng Qian et al., (Qian et al., 2019) developed UDG-mediated CRIPSPR/Cas12a combined with LAMP for visual detection and carryover contamination monitoring. In the amplification experiment, dUTP is used in this method to substitute TTP, so that all amplicons contain dUTP. Until starting each amplification, fully loaded reactions are treated using UDG, that cleaves the uracil base in dUTP carrying DNA (amplicon) but will not interact with dUTP and has no effect on original DNA templates comprising thymidine groups or RNA. UDG could be inactivated after initial treatment by thermal denaturation before the PCR. New PCR product, amplified from genuine DNA template, is not destroyed, although it contains dUTP. The destroyed DNA is not appropriate to be used as a guide for hybridization or as a template for DNA polymerases, thus in subsequent reactions, it cannot be re-amplified or used as contaminant.

Table 1. 2 General remarks, advantages, and disadvantages of commonly used nucleic acid isothermal amplification techniques.

Technique	Merits	Demerits	General comments	Ref.
RPA	• Uses exponential amplification • Operates at the low-temperature range (37 and 42^{o}C) compared with other isothermal amplification types, which make a positive attribute since there is no requirement for continual temperature control • does not require initial denaturation steps to generate ssDNA from the dsDNA target • Provides a fast response compared to other isothermal amplification types (15-30 min) • RPA reagents are supplied in stable lyophilized form and can last up to six months while other isothermal reagents require refrigeration	• RPA kits are costly • Prior to amplification, RPA requires protein digestion, and purification to prevent the impairment of flow • Real-time RPA amplification requires highly skilled personnel because it is not straightforward • It has not been yet validated by FDA to be used for no-site testing applications	• RPA is used to amplify a wide variety of target nucleic acids (RNA, miRNA, ssDNA, and dsDNA) from diverse samples. It is highly selective and sensitive as it can reach as low as 1-10 copies of amplified target. More importantly, it does not require continuous temperature regulation. However, its future applications need to address on-site exploitation for commercial devices	(Lobato and O'Sullivan, 2018; Singh et al., 2019)

LAMP	• Displays an amplification power close to that of PCR • exhibits high sensitivity and specificity due to its two sets of primers with the ability to compliment six different target sequences • LAMP amplified target products can be indirectly detected by other methods such as turbidity or non-specific dyes • Improved ability for multiplex detection • Test kits available for both RNA and DNA detection	• Sometimes requires initial denaturation support to yield ssDNA from the dsDNA target • Presents extreme challenges in designing multiple primers, which may also result in contamination • Difficult to use for multiplex detection since designing primers requires skills • Requires careful calibration and accurate temperature monitoring	• LAMP is a fascinating simple, rapid (30-60 min), cost-effective and sensitive (1-5 copies) isothermal nucleic acid amplification technique having close similarity and performance with PCR. However, LAMP is carried out isothermally at moderately low temperature through the strand displacing technique	(Li et al., 2017b; Qi et al., 2018; Dong et al., 2019)
RCA	• Works on circular DNA such as plasmids, bacteriophage, and circular RNA • Suitable for amplification at high temperatures • Can amplify as low as 10 copies/reaction	• Requires an initial denaturation step to generate ssDNA from the ds DNA target • requires a thermal cycler and a thermostable DNA polymerase • Restricted to amplification of circular nucleic acids • Limited application since test kits are only available for virus detection	• RCA is an enzyme based isothermal amplification technique that uses circular DNA to amplify target nucleic acids (DNA or RNA). It has excellent amplification power as high as it was even used for the amplification of the whole viral genome	(Gao et al., 2019; Yao et al., 2019b)

NASBA	• Amplification occurs at a constant temperature of 41 °C • Does not require an initial denaturation step to generate ssDNA from the dsDNA target • Does not need additional reverse transcription step like PCR, preventing contamination • Can selectively amplify RNA even in the presence of genomic DNA	• Is designed for the specific detection of RNA targets • Is not completely isothermal since some heat denaturation steps are required, enzymes are also separately added due to their differences in temperature stability • Can only amplify only short nucleotides ranging from 120-250 base pairs	• NASBA is also known as self-sustained sequence replication (3SR), is a sensitive, and transcription-dependent isothermal amplification technique that is mostly applied for the identification of RNA targets. It is highly sensitive since it can even amplify RNA in the presence of genomic DNA	(Deng and Gao, 2015; Dunbar and Das, 2019)
HDA	• Does not require an initial heat denaturation temperature to generate ssDNA from the dsDNA target • The entire amplification reaction can take place at a constant temperature • It is a good alternative to PCR because of its simplicity, procedure, and fair compatibility to various nucleic acids detection methods • Can be easily miniaturized due to its simple protocols	• Requires optimization of primers which is mostly accomplished through PCR • The efficiency of helicase is highly doubtful since it does not provide functional dissimilarities with other polymerases during the unwinding of dsDNA	• HDA amplification is similar to PCR procedure. However, HDA uses helicase to recognize and unwind the double structure of DNA. It also uses other specific strand-binding proteins to prevent reannealing of separated strands	(Mayboroda et al., 2018; Zhao et al., 2015a)
MDA	• Less-prone to non-specific	• Requires an initial	• MDA is an advanced	(Shen et

	binding since it can be preferred to amplify the whole genome in preference to PCR • Can rapidly amplify the minute amount of target nucleic acid without further nucleic acid isolation or purification.	denaturation step to generate ssDNA from the dsDNA target • When hexamer primers are used during amplification, they slow down the initial priming because of its high concentration	version of SDA because both share the same amplification working principle. It presents an outstanding efficiency because it can even amplify the small concentration of the target	al., 2019; Wang et al., 2018b)
LCA	• Applies unique hybridization procedure by using a single DNA strand and its complementary synthetic oligonucleotide • Uses highly thermostable DNA ligase • Is highly sensitive, specific, easy to perform, and can be readily automated	• May generate false-positive results due to high background signal while free ligations occur in the absence of target DNA • Presents difficulties in inactivating post-amplification products • Contamination quickly arises when coupled with other methods	• LCA is an exponential isothermal amplification technique which is somehow similar to PCR. The generated LCA target products can be selectively detected by other techniques like fluorescent label detection, polyacrylamide gel electrophoresis, and auto-radiography.	(Chen et al., 2013)
NEAR	• Can be used to identify both DNA and RNA	• Generates many non-specific products that not only interfere with the progression of the forward reaction but also limit the sensitivity, which may require more specific and accurate amplification analysis techniques to prevent detection errors	• Is applied for the detection of small DNA or RNA fragments that are directly generated from the target nucleic acid. It relies on primers, nicking endonucleases, and a strand displacing DNA polymerase	(Deng and Gao, 2015)

1.1.12 CRISPR/Cas-isothermal amplification based lateral flow biosensor

Clustered Regularly Interspaced Short Palindromic Repeats (CRISPR) and CRISPR-associated (Cas) system endow bacteria and archaea adaptive immunity against foreign nucleic acids (Barrangou et al., 2007; Jinek et al., 2012). For effective targeting, this system utilizes a guide-RNA and Cas proteins to target an invading DNA, generating a protospacer sequence that integrates into the genome near PAM (protospacer adjacent motif) region for recognition and cleavage of future similar invader (Sander and Joung, 2014). The CRISPR-Cas9 has been extensively used for gene editing, typing and mutant detection. It requires a CRISPR RNA (crRNA) and trans-activating or a chimeric single guide RNA (Sander and Joung, 2014; Zhang et al., 2018; Jia et al., 2018; Liang et al., 2015) for targeting and cleavage. The RNA-guided cleavage is mediated by RuvC (a member of RNase H family) and HNH catalytic domains at the gRNA-target base-pairing site. When Cas9-gRNA complex recognizes a G-rich PAM region of the target sequence, it becomes activated followed by blunt-end cleavage (Sternberg et al., 2014). Similar to Type II CRISPR-Cas9, Type V CRISPR-Cas effectors such as Cas12 and Cas13 have also been used for gene editing (Tang and Fu, 2018; Ishino et al., 2018; Makarova et al., 2011; Strecker et al., 2019). However, these enzymes require a single mature crRNA for self-assembly and processing, and ribonucleoprotein surveillance-dependent nuclease for interference activity (Swarts et al., 2017; Gao et al., 2016) but not a dual functional crRNA-tracrRNA as for Cas9 (Brouns et al., 2008; Deltcheva et al., 2011). Unlike Cas9 and Cas13, CRISPR-Cas12a system uses only a RuvC catalytic domain to guide gRNA and cut the cognate dsDNA by recognizing a T-rich PAM region that leaves a staggered 5’ and 3’ ends (Samai et al., 2015; Sogo et al., 2002).

Based on this targeting, it has been recently discovered that Cas12a/b and Cas13a/b enzymes exhibit collateral cleavage of target nucleic acids and non-specific single-stranded nucleic acids (Chen et al., 2018a; Gootenberg et al., 2018; Li et al., 2018a) (Figure 1.13). For example, an RNA detection method called Specific High Enzymatic Reporter UnLOCKing (SHERLOCK) harnessed Cas13 enzymes for the diagnosis of bacteria and single nucleotide polymorphisms (SNPs) (Gootenberg et al., 2018), while DNA Endonuclease Targeted CRISPR *Trans* Reporter (DETECTR) uses LbCas12a for human papillomavirus detection (Chen et al., 2018a). These methods depend on several critical reaction components such as ssDNA activators, crRNAs, buffer and signaling single-strand nucleic acids (hereafter referred as reporters), DNA amplification mixture, and reverse transcription system (for SHERLOCK) to provide fluorescence signal readout. To enhance the sensitivity and

fluorescence readout, these diagnostics and another method called One-Hour-Low Cost Multipurpose highly Efficient System (HOLMES) (Li et al., 2018b) required pre-amplification of target nucleic acids using recombinase polymerase amplification (RPA) and PCR, respectively. RPA has currently shown potential when combined with CRISPR-Cas system (Gootenberg et al., 2018; Myhrvold et al., 2018; Chen et al., 2018c). Although RPA is formidable isothermal amplification of nucleic acids, it is still limited by target sequence length, complex reaction premix, low sensitivity and specificity, and cost compared to Loop-mediated isothermal amplification (LAMP) (Notomi et al., 2000a; Huang et al., 2014a); while PCR depends on expensive machinery such as thermocyclers. LAMP amplification allows the entire amplification at a single temperature, making it rapid, cost and time-effective but with difficulty in recognition of target bands and is more prone to cross-contamination. Moreover, HOMESv2 combined LAMP and RT-LAMP with Cas12b for the detection of DNA and RNA, respectively (Li et al., 2018a). Although the approach has improved sensitivity, overall, the fluorescence-based result readout remains a concern.

To overcome machinery limitations towards on-site deployment, an RNA-targeting method called SHERLOCK applied fluorescence reader and lateral flow biosensor, and combined RPA with Cas13, Cas12a, and Csm6 to detect nucleic acids (Gootenberg et al., 2018). The principle of this lateral flow is that cleaved FAM-biotin labelled reporters are not accumulated by the Anti-FAM antibody-gold nanoparticle immobilized at the test line(Gootenberg et al., 2018; Tsou et al., 2019). The technique is advantageous compared to assays such as DETECTR (Chen et al., 2018a) and HOLMES, which employed fluorescence readouts only (Gootenberg et al., 2018; Myhrvold et al., 2018). However, SHERLOCK lateral flow biosensor is likely to be expensive owing that it requires complicated reaction with an anti-FAM antibody, streptavidin (SA), protein A, and fluorescence based detection of bi-labelled reporters. Our recent paper in press reported a low-cost lateral flow biosensor, which consists of a test line DNA probe that cannot bind trans-cleaved biotinylated ssDNA reporter upon target recognition, paving the way towards developing sensitive, inexpensive devices for monitoring CRISPR/Cas reporter trans-cleavage (Mukama et al., 2020).

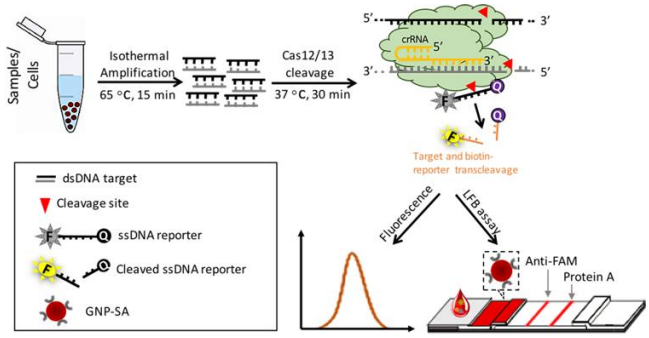

Figure 1. 13 Illustration of CRISPR/Cas-isothermal amplification detection principle.

Clinical samples are subjected to nucleic acid extraction (heat treatment, genomic DNA extraction) for isothermal amplification such as RPA (37 ºC, 15 min) or applied to LAMP amplification (65 ºC, 15 min). The product of amplification is applied to Cas12 (for DNA target) or Cas13 (for RNA target) cleavage system, which collaterally cleaves the amplicons and the FAM-labeled reporter. The product of reporter targeting can be detected using fluorescence or lateral flow biosensor.

1.1.13 Perspective isothermal amplification method for this research

The most effective isothermal amplification methods for nucleic acids detection include, LAMP, RPA, MCDA, PSA, etc. They require combination with several techniques for result readout. This is due to the fact that isothermal amplification methods exhibit short-comings of result readout and stringent experimentation. Moreover, they have hardly shown the multiplexing abilities (Notomi et al., 2000a; Fukuma et al., 2011; Blomstrom et al., 2008) and have also shown to depend on the dye for colorimetric based detection and quantification experiments, which could be prone to cross-contamination. To resolve this issue, we hypothesized herein that the use of LAMP –a highly sensitive isothermal amplification method- with CRISPR/Cas based enzymes can be advantageous. The Cas effectors collateral cleavage of target and non-target nucleic acids; and 2) its substantial reduction of LAMP amplicons. Moreover, CRISPR-Cas based analysis of isothermal amplicons is rapid, sensitive and specific, and can be integrated into colorimetric or fluorescence-based portable devices, allowing their on-site implementation. They can also be multiplexed when specific reporter nucleic acids are labelled with different fluorescence molecules. However, the use of multiple enzymes and long reaction and steps complicates the methods thus requires rigorous optimization. Moreover, fluorescence-based techniques generate backgrounds; thus, it is still of great importance to developing robust techniques. The use of miniature Cas enzymes such as Cas14 could speed up the reactions. Besides, the

discovery of new polymerases possessing both strand displacement and reverse transcription propensity -as in the case of RT-LAMP- could reduce the complexity of the trans-cleavage reaction in both DNA/RNA detection. Notwithstanding that CRISPR-based techniques have shown some promiscuous trans-cleavage; thus, thorough buffer and activator optimization are of great importance. Furthermore, one can replace antibodies with DNA probe-based lateral flow biosensor, which can likely boost up specificity, sensitivity and improve cost for its use in low-resource settings P-O-C testing.

1.2 Targets used in this study (Human Papilloma Virus and *Pseudomonas aeruginosa*)

1.2.1 Human Papilloma Virus

Human Papilloma Virus (HPV) represents the main etiologic factor behind more than 90% of cervical cancer cases in women. Cervical cancer is the fourth most commonly reported fatal disease in women worldwide, causing around 90 % of deaths in developing countries. All HPV types are associated with vaginal warts, but, of all types, HPV16 and HPV18 cause 75 % of cervical cancer (Ferlay J, 2018; Lowy and Schiller, 2012). Patients with both types of viruses are mostly asymptomatic; however, the onset of infection can cause pruritus vulvae, rare delicacy, and mild vaginal bleeding. Advanced signs and symptoms of cervical cancer include fatigue, pain (leg, pelvis, and back), heavy vaginal bleeding, swollen legs, weight loss, bone fractures, and (rarely) leakage of urine or feces from the vagina (Burd, 2003). Fortunately, cervical cancer is one of the most common types of tumor with clear etiology and high treatment efficiency. Thus, it can be prevented by a timely and accurate prognosis. For example, in developed countries, HPV has reduced its incident rate by 70% (Lowy and Schiller, 2012; Gustafsson et al., 1997; Dickinson et al., 2012). However, nearly 90% in developing countries are still significantly exposed due to the lack of proper measures of vaccination, screening, detection, and treatment of precancerous lesions (Ferdous et al., 2018; Cuzick et al., 2008). This urges to develop diagnostics that meet the World Health Organization's ASSURED criteria (Affordable, Sensitive, Specific, User-friendly, Rapid, Equipment-free, and Delivered) for use in rural places, where high-risk population live (Kumar et al., 2015; Halliday et al., 2017).

Culture methods cannot detect HPV; thus techniques such as imaging (Corey and Hudgins, 2012) and various molecular testing including polymerase chain reaction (PCR) (Abreu et al., 2012), immunochromatographic assay (Mariano et al., 2016), and *in-situ*

hybridization (Siti-Aishah et al., 2000) have been developed for its sensitive and specific detection. But, these methods are time-consuming, expensive, and laborious, and are still limited to be adopted in poor-resource settings. Advances in isothermal amplification methods, such as strand displacement amplification (SDA) (Lu et al., 2017), loop-mediated isothermal amplification (LAMP) (Notomi et al., 2000a), recombinase polymerase amplification (RPA) (Ma et al., 2019), rolling circle amplification (RCA) (Ali et al., 2014b), have promised the on-site application. These techniques, however, also have certain limitations, particularly the complicated post-amplification analyses of DNA products, which may lead to false-positive results.

The current integration of LFB for the detection of isothermal amplification products has simplified results readout and is promising to the development of self-testing and surveillance diagnostics for various pathogens and diseases. These LFBs can be readily harnessed to capture labeled amplicons specifically, but their general utilization is scarce. Thus, the development of inexpensive, rapid and accurate platforms is a prerequisite.

Recently, apart from genome editing (Strecker et al., 2019), CRISPR/Cas system has been expanded to the development of diagnostics. For example, Cas12 and Cas13 enzymes have been found to trans-cleave target nucleic acid and non-specific single-stranded nucleic acids in the vicinity (Strecker et al., 2019; Gootenberg et al., 2018; Li et al., 2018a; Myhrvold et al., 2018). When the ssDNA/ssRNA is bi-labeled with fluorescent and a quencher, it provides a signal upon collateral cleavage of a cognate target. Most of the diagnostics with CRISPR/Cas system employ fluorescent-based approaches (Chen et al., 2018a; Gootenberg et al., 2018; Li et al., 2018a; Myhrvold et al., 2018), although an antibody-based LFB has also been reported (Gootenberg et al., 2018). These platforms are ultrasensitive and specific. However, their reliance on fluorescent apparatus or antibodies may cause false-positive results with increased cost (Kim et al., 2016a; Kleinstiver et al., 2016a). The development of DNA-probe based LFBs could be an alternative approach for sensitive, specific, and inexpensive on-site detection (Strecker et al., 2019; Fang et al., 2014b).

1.2.2 *Pseudomonas aeruginosa*

P. aeruginosa is an opportunistic human pathogen with a large and complex genome and is a critical infectious bacterium classified as a multidrug-resistant pathogen (E. Tacconelli, 2017; Tacconelli et al., 2018). It is widely used as a model for CRISPR/Cas system studies (Gootenberg et al., 2018; Xu et al., 2018a; Pawluk et al., 2016; van Belkum et

al., 2015). Selective culture methods based on Mac-conkey and cetrimide agar can detect *P. aeruginosa* (Kodaka et al., 2003). However, these methods are hampered by non-specificity towards different species of the target and tediousness. Various molecular methods such as PCR and isothermal methods (LAMP, RPA, etc.) have been used for the detection of *P. aeruginosa* specific genes (OprI/OprL, exotoxin A (ETA)), which improved rapidity and accuracy. For example, the PCR approach targeting ETA achieved a sensitivity of 0.1 pg of DNA and 5-10 cells with ~96-100% specificity (Jami Al-Ahmadi and Zahmatkesh Roodsari, 2016). The drawback of PCR is machinery requirement, DNA extraction and operation time. Unlike PCR, isothermal amplification such as LAMP can work at single temperature (65) in an expensive heat block without genomic DNA extraction. We presumed that the advantages of LAMP can be exploited and be combined with CRISPR collateral cleavage to achieve an ultransensitive and ultraspecific approach.

1.3 Hypothesis and aims

The use of biosensor will facilitate the detection of different nucleic acid targets. The actual role of excellent specific genes, CRISPR/Cas diagnostic systems and amplification methods will enable us to discover quick and accurate diagnostics. This will help to drastically reduce time, errors, effort, and costs. Subsequently, this study will act as a beacon in guiding the development and application of universal portable diagnostics.

1.4 Objective

1.4.1 Main objectives

- ✓ To establish efficient CRISPR-Cas effectors in combination with appropriate nucleic acid isothermal amplification of specific sequences towards developing a cheap, faster and accurate on-site deployable Lateral flow biosensor.

1.4.2 Specific objectives

1. To find out sequence specific genes for efficient detection of different infectious diseases.
2. To use CRISPR-Cas effectors such as Cas12a, Cas12b for collateral cleavage activity.
3. To find out proper isothermal amplification of target for Cas effectors collateral cleavage activity.

4. To verify the CRISPR-Cas effectors collateral cleavage by lateral flow biosensors.
5. To validate the developed approach for clinical diagnostic

Chapter 2: CRISPR/Cas12a based Lateral flow biosensor for the detection of HPV16 and HPV18

2.1 Introduction

Abnormal growth of uterine cervix cells may eventually lead to cervical cancer, which is mainly associated with the two most prevalent types of Human Papilloma Virus (HPV), namely HPV16 and HPV18. Cervical cancer can be prevented or treated owing to its slow progression. Therefore, it's early, fast, and sensitive diagnosis is crucial. For this purpose, we developed an ultrasensitive approach for HPV16 and HPV18 detection based on a combination of loop-mediated isothermal amplification (LAMP), CRISPR-Cas12a trans-cleavage propensity and lateral flow biosensor (LFB), collectively termed CIALFB (CRISPR/Cas-Isothermal Amplification based LFB). CIALFB is characterized by Cas12a-mediated trans-cleavage of the reporter ssDNA upon target recognition, which results in undetectable LFB test line signal (Figure 2.1). This method was sensitive to detect 3.1 attomoles (~1.8 copies) of the target, as well as specific to detect both virus types from clinical samples with various HPV strains. Our system possesses the potential to detect other infectious diseases without tedious DNA extraction and handling, and expensive apparatuses.

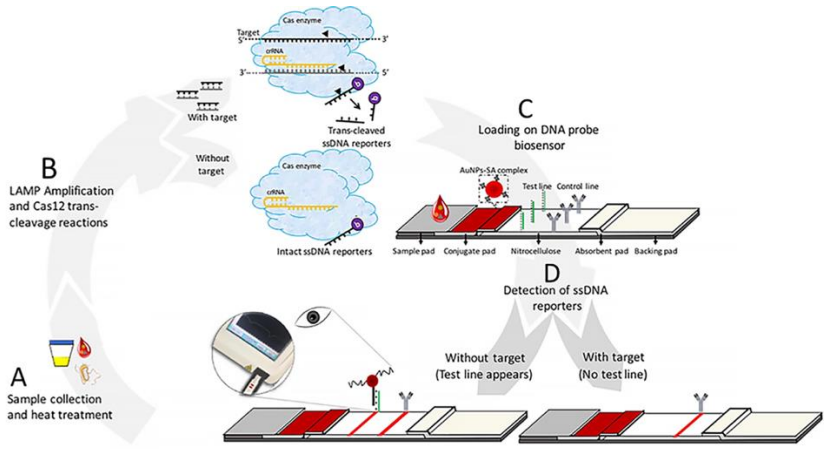

Figure 2. 1 The working principle of CIALFB approach.

It comprises three main steps: sample collection (A), isothermal amplification of samples and Cas effectors cleavage reaction (B), and the detection of (B) reaction products on the LFB (C, D). (A) Clinical samples can be heat-treated at 98 ℃ for 5 min to generate a crude genomic DNA template. (B) The template is LAMP-amplified and then used as a substrate for Cas12a (drawn in off-blue color) cleavage reaction. In the presence of the target, Cas12a collaterally cleaves the LAMP product as well as a biotinylated ssDNA reporter. (C) AuNP-SA complex

and ssDNA probe complementary to the complete ssDNA reporter are immobilized on the conjugate pad and test line, respectively. The biotinylated goat anti-mouse polyclonal IgG is fixed on the control line to capture excessive SA-AuNP from the conjugate pad (the inexpensive IgG was used to fix biotin on the control line). (D) In the presence of the target, the cleaved reporter cannot bind to its corresponding ssDNA probe (no test line), and vice versa (test line appears).

2.2 Material and methods

2.2.1 Reagents and chemicals

All oligonucleotides, including HPV16 and HPV18 specific target sequences, primers, crRNAs (designed using benchling), reporters, and lateral flow capture probes were synthesized by Sangon Biotech (Shanghai, China). *Bst* 2.0 WarmStart polymerase and LbaCas12a enzymes were purchased from New England Biolabs (NEB) (New England, USA) (Figure S1). Biotinylated goat anti-mouse polyclonal IgG was purchased from Beyotime Biotechnology (Shanghai, China), Deoxynucleoside triphosphates (dNTPs) and Taq polymerase premix were purchased from Takara (Beijing, China). Genome and plasmid extraction kits were purchased from Qiagen (Hilden, Germany) and Tiangen Biotech (Beijing, China), respectively.

$HAuCl_4.3H_2O$, trisodium citrate, and streptavidin (SA) were purchased from Sigma–Aldrich (Steinheim, Germany). Absorbent CH37 (ABP-S370) and fiberglass papers SB-08 and nitrocellulose membranes CN140 (1UN14ER100025NT) were purchased from Sartorius AG (Gottingen, Germany). A dispenser HM3030 for antibody, DNA probes and conjugates; and nitrocellulose membrane cutter ZQ2002 were obtained from Shanghai Kinbio (Shanghai, China). A portable strip reader was obtained from Goldbio Technology Co. (Shanghai, China). Genome and plasmid extraction kits were purchased from Qiagen (Hilden, Germany) and Tiangen Biotech (Beijing, China). Unless indicated otherwise, all buffer used in this study were prepared in our laboratory with ultrapure double distilled water (18.2 MΩ.cm).

2.2.2 Preparation of AuNP and its conjugate

AuNP with 15 nm diameter was synthesized as described previously (Zeng et al., 2013) with slight modifications. Briefly, 350 ml (1 mM) gold chloride solution (HAuCl4) was boiled, stirred in a flask, and subsequently added 3.5 ml of 1% sodium citrate solution. The

mixture resulted in a colorless solution that turns to wine red after 10 min boiling, which was cooled at room temperature for use (Figure 2.2A). The AuNP size measured using UV-Vis spectrometry had single absorption peak at 518 nM after scanning between 400-700 nM, which confirmed uniformity and the expected particle size (Figure 2.2B).

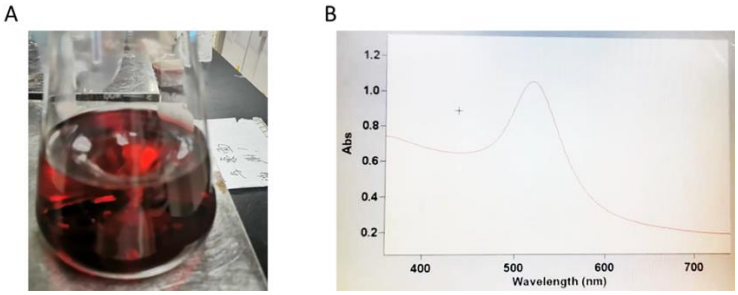

Figure 2. 2 AuNP synthesis (A) and spectral absorbance analysis (B).

To prepare AuNP–SA conjugate, 1 ml of the prepared AuNP solution was collected by centrifugation (21,100 ×g, 25 min), concentrated 4 times, and subsequently mixed with 100 µl of suspension buffer (10% sucrose, 0.1% NaN_3, 5% BSA, 0.25% Tween-20, 20 mM Na_3PO_4). Then, 0.5 mg/ml of SA was added, gently shaken for 3 hours at 4 ◦C, centrifuged (21,100 ×g, 25 min), and then rinsed three times with suspension buffer to eliminate free SA. The red pellet was resuspended in 100 µl of suspension buffer before dispensing on the conjugate pad.

2.2.3 SDS-PAGE detection of Cas enzymes, osteopontin protein and anti-osteopontin

3 µl of the commercial LbaCas12a/AaCas12b or different concentrations of osteopontin recombinant protein and anti-osteopontin were loaded on 10% acrylamide gel. After the electrophoresis, the gel was stained and directly photographed using a phone camera.

2.2.4 Construction of the LFB

As shown in the Figure 1 scheme, the LFB is composed of three main components: the sample pad, nitrocellulose membrane, and absorbent pad. The 38 base capture probe (5'–AATAAAAAAAAAAAAAAAAATAAAAAAAAAAAAAAAA-3') (100 µM) and biotinylated rabbit polyclonal anti-IgG antibody (0.7 mg/ml) were dispensed on the LFB nitrocellulose membrane strip (25 mm in width) to form a test and control zones, respectively. The membrane was dried at room temperature for 12 h and stored in a desiccant container at room temperature until use. To assemble the LFB, a fiberglass sample pad (16 mm in width) was immersed in sample pad buffer (2% glucose, 1% Triton, 1% BSA, 50 mM boric acid, pH

8.0), dried and stored. The conjugate (6 mm) and absorbent pads (17 mm) were used without buffer treatment. Then, all pads were sequentially assembled along the adhesive part of the nitrocellulose membrane with an overlap of 2 mm and then cut into 0.4 cm-wide strips.

2.2.5 Target DNA design, cloning, and amplification

HPV16 and HPV18 L1 gene's hypervariable loop V was used as a specific sequence for target DNA amplification (Seaman et al., 2010). LAMP amplification specific primers for HPV16 and HPV18 target viruses were designed using Premier Biosoft designer and confirmed by NCBI-Blast. The target was cloned into a customized pUC57 plasmid. The recombinant plasmid was used as a model for PCR/LAMP amplification and CRISPR/Cas12a reaction. LAMP amplification was performed according to NEB instruction. Briefly, 25 µl LAMP premix was composed of primers F3, B3 (0.2 µM) and FIB, FIP (1.6 µM), 1.4 mM dNTP, 6 mM $MgSO_4$, 1× isothermal amplification buffer, 320 U/ml *Bst* 2.0 WarmStart DNA polymerase, 2 µl target DNA template, 1 M betaine and added ddH_2O up to the final volume. The mixture was then LAMP-amplified at 65 ◦C for an hour prior to gel electrophoresis, or 15 min for Cas12a cleavage reaction.

For PCR amplification, 25 µl PCR premix was composed of 12.5 µl 1× rTaq Premix, 1 µl forward and reverse primers (0.3 µM), 1-2 µl of extracted genomic DNA (200 ng) and ddH_2O to the final reaction volume. The reaction mixture was incubated in a thermocycler using 3 steps PCR protocol: 95 ◦C, 5 min for denaturation; 95 ◦C, 10 sec for each cycle; 55 ◦C (for HPV16)/ 62 ◦C (HPV18), 10 sec for annealing; 72 ◦C, 30 sec for elongation; 35 cycles.

2.2.6 Target cleavage assay

Cas12a cleavage assay was carried out according to the previous method (Chen et al., 2018a), with slight modifications. Briefly, a 25 µl reaction mixture of the Cas12a cleavage reaction consisted of 3 µl NEB 3.1 buffer, crRNA (40 nM), LbaCas12a (40 nM), activator (32 nM), biotinylated ssDNA reporter (60 nM), and 2-3 µl target DNA or heated clinical samples, and added nuclease-free water to make up the final volume. Finally, the Cas12a reaction was incubated at 37 ◦C for 30 min with intermittent mixing every 10 min and analyzed using LFB after adding 35 µl ddH_2O prior to sample pad loading.

For fluorescence analysis of trans-cleavage reaction, the Cas12a reaction set up was prepared as mentioned above with 5'-FAM and 3'-TAMRA labeled ssDNA reporter instead

of biotinylated ssDNA reporter. The reaction mixture was incubated at 37 ◦C in a 96-well microplate and then read using the Mithras^2 LB 943 plate reader (Berthold Tech, Germany). The fluorescence from the cleavage of the reporter was measured from 0 to 1 hour (excitation at 495 nm and emission at 520 nm). All measurements were conducted in triplicate.

2.2.7 LFB detection of reporter sequences

From the probe-based LFB optimization, 11 bases biotinylated reporter (5'–biotin-TTTTTTTTATT-3') was found to successfully hybridize with 38 base capture probe (5'–AATAAAAAAAAAAAAAAAAATAAAAAAAAAAAAAAAA-3') immobilized on the LFB test line. The bold sequence was repeated twice to increase the sensitivity of the LFB test line. For the LFB detection of reporter cleavage after CIALFB reaction, 25 µl of the reaction was mixed with 35 µl of ddH_2O and then loaded on the sample pad. After 5 min, the biosensor was read using a portable LFB reader. Excellent performance of CIALFB was considered positive when the reporter sequence was entirely trans-cleaved by Cas12a (no test line signal), and appearance of the control line via biotinylated rabbit polyclonal anti-IgG antibody capture of the excess of AuNP-SA complex from the conjugate pad (Figure 1). After 5 minutes, the LFB was read using a portable LFB reader and peak intensities were analyzed using ImageJ (NIH Research Services, US), which provided peak areas for plotting and sensitivity calculation determination. Reproducibility of the approach was confirmed by testing each sample three times and the biosensor can be used for real sample determination.

2.2.8 Clinical sample preparation and analysis

A total of 21 clinical cervical exfoliated cell samples of both healthy and HPV16 or HPV18-suspected patients were collected and confirmed using conventional PCR/LAMP (Figure 2). For PCR amplification, 200 µl of each sample was used to extract genomic DNA templates to confirm the presence of the target viruses. Prior to the LAMP amplification and CIALFB assay, each specimen was 10 times diluted, heat-treated at 98 ◦C for 5 min, followed by centrifugation at 11,000 ×g for 10 min. Two-four µl of each sample was used in the CIALFB assay, as mentioned above.

2.3. Results and discussion

2.3.1 Establishment of CIALFB for *HPV16*/*HPV18* detection

CIALFB is orchestrated by two main components: i) ssDNA reporter, that is trans-cleaved by Cas12a to provide a signal upon target recognition, and ii) LFB probes immobilized on the LFB test line to capture and monitor reporter trans-cleavage. Therefore, we optimized reporters and probes of different lengths and bases (Table S1). The biotinylated reporters bind with the AuNP (Fig. 2) combined with SA at the conjugate pad and migrate to hybridize with their complimentary test-line probes. As shown in Figure 2.3A, no test line was detected when 5-11 base reporters (100 nM) were applied to LFB on which probes with similar lengths were fixed. However, 12 and 13 bases displayed a faint detectable test line. The increase of the test line probe to 13 bases resulted in strong test lines as long as the length of the reporter is longer or equal to 11 bases (Figure 2.3B). Therefore, 11 base reporters were used as Cas12a substrate to obtain no test line upon trans-cleavage, while the full-length ssDNA reporters hybridized with test-line probes in the absence of trans-cleavage, i.e. the absence of either target (Table S1). Furthermore, different concentrations of the optimized reporter (1, 5, 10, 20, 30, 40, 50, 60, 100 nM) were tested on the LFB (Figure 2.3C). A test line was detected at a reporter concentration above 10 nM, which became prominent with a subsequent increase in concentration (Figure 2.3C). Sixty nM concentration was used in the following experiments to provide strong test lines in the absence of the target, and non-detectable test line signal in the presence of the target. Accordingly, the concentration of 60 nM and the reporter length 11 bases were further selected for subsequent Cas12a cleavage experiments.

Figure 2. 2 AuNP synthesis (A) and spectral absorbance analysis (B). Test line AuNP signal intensity depends on the length and concentration of reporters and capture probes.

(C) 100 nM of different poly-thymine reporters (in red) suspended in water and then loaded on the LFB to hybridize the corresponding poly-adenine capture probes (in blue) immobilized on the test line. (D) LFB showing various reporters (in red-black) binding to capture probes (in blue-black) with an efficient binding of 8Ts to 16 As. (E) Determination of the optimum concentration of 8Ts reporters on 16As capture probes.

2.3.2 Design and validation of CIALFB method

Buffer, crRNA, activator, and Cas enzymes are crucial components of diagnostics with CRISPR/Cas system (Chen et al., 2018a; Gootenberg et al., 2018; Gootenberg et al., 2017). Preliminary experiments were performed using recombinant plasmid with HPV16 and HPV18 L1 gene's hypervariable loop V as a specific target sequence, its specific crRNA, and activator- a sequence complementary to the crRNA (Table 2.1 and S2, Figure 2.4A). Firstly, the recombinant plasmid and 21 clinical exfoliated cell samples were verified by PCR and LAMP amplification (with 3 samples of HPV presented). Figure 2.4B and C show the specific amplified bands of PCR and LAMP amplification, respectively. Secondly, both amplified and non-amplified recombinant plasmid (30 nM) were applied to Cas12a cleavage. No test line was observed in the presence of either plasmid as a result of reporter trans-cleavage, while a visible test line was only observed in the absence of the target plasmid (data not shown).

Table 2. 1 Oligonucleotide sequences used in this study.

Oligonucleotide	Sequence (5'-3')	Reference
ssDNA Reporters	B-TTTTTTTTATT, FAM-TTTTTTTTATT-TAMRA	This study
Test line capture probe	AATAAAAAAAAAAAAAAAAAATAAAAAAAAAAAAAAAA	This study
Forward primer	GTATCAGGATTACAATACAGG / GTGCTTCACCTGGCAGCT GTGTGTATTCTC	(Chen et al., 2018a)
Reverse primer	GTGAAGTTCCACTGGATATTTGTACATCTA / GATGACACTGA AAGTTCCCATGCCGCCACG	(Chen et al., 2018a)
F3	TTATAATCCAGATACACAGCG / TGCCGCCACGTCT AA	This study
B3	TTATAATCCAGATACACAGCG / GCTGCCAGGT GAAGC	This study
FIP	ACATTCTCTATTATCCACACCTGCAGGTCGTGGTCAGCC / AA TCGCCCTGTGATAAAGGACGAGA TTATAAGCAGACACAGTTATGT	This study

BIP	CCATGTACCAATGTTGCAGTAACACCATCCTGAATAACTGT GT / CTTACGGCGTGAGCAGCATATAAGGATTGAGGCACAG TG	This study
LoopF	GCTGCATAAGCACTAGCATT / GTGCCTTTAGCCC AGTGT	This study
LoopB	GTGATTGTCCACCATTAGAGTTAA / TTGGAATAGAGCAGG TACTATGG	This study
CrRNA	UAAUUUCUACUAAGUGUAGAU**CUACAUUACAGGCUAA CAAA** / UAAUUUCUACUAAGUGUAGAU**GUACAUUGCAAG AUACUAAA**	This study
Activators	**TGTAATGTAG**TAAAGTCCATAGCAC/**TGCAATGTAC**TAAA GTCCATGGCAC	This study

B stands for 5'biotinylation, FAM and TAMRA are fluorescence and quencher labeled at 5'-3' ends, respectively.
Underline represents reporter capture probe sequence (repeated twice).
Bold represents crRNA targeting sequence
Slash separates HPV16 and HPV18 sequences, respectively.

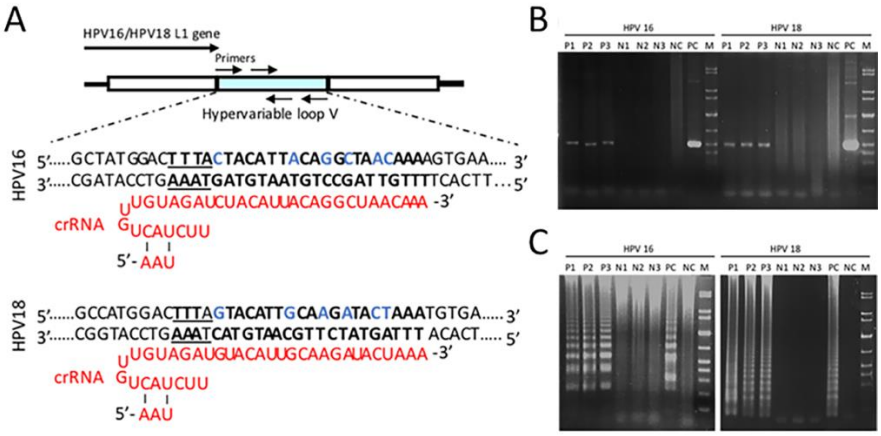

Figure 2. 3 CIALFB experimental design and verification.

(A) HPV16 and HPV18 L1 gene's hypervariable loop V specific target sequence cloned in pUC57 plasmid. Gel electrophoresis of PCR (B) and LAMP (C) amplification of clinical samples and the recombinant plasmid, with 2 µl of 50 ng/µl template inputs for HPV16 and HPV18 plasmid, respectively. P: positive sample, N: negative sample, NC: negative control (water), PC: positive control, M: 1kb DNA marker.

2.3.3 Sensitivity of CIALFB for *HPV16* and *HPV18* detection

The sensitivity of CIALFB was assessed using different concentrations of serially diluted HPV16 and HPV18 recombinant plasmid (3.1×10^{-9}, 3.1×10^{-12}, 3.1×10^{-15}, 3.1×10^{-18}, 3.1×10^{-21} M), tested by two different protocols: one with Cas12a reaction alone, while the other was subjected to LAMP pre-amplification combined with Cas12a reaction

(CIALFB) (Figure 2.5A). Cas12a alone was only sensitive in the presence of 3.1×10^{-9} M and higher concentrations, depicted through reporter trans-cleavage (data not shown). To improve the sensitivity, the recombinant plasmid containing samples were subjected to CIALFB. As low as 3.1×10^{-18} M (~1.8 copies in 2 µl) and above concentrations showed no test line within an hour, which is evident from the reporter trans-cleavage (Figure 2.5B). A detectable test line was observed at 3.1×10^{-21} M (< 1 copies) and in control (Figure 2.4B). These results suggested that the developed biosensor could achieve a single-copy sensitivity for HPV16/HPV18. The same set of samples were also tested using FAM-TAMRA labeled reporters, which demonstrated similar sensitivity as achieved with CIALFB (Figure S1), which is comparable to the previously reported CRISPR/Cas12 and Cas13 based methods (Chen et al., 2018a; Gootenberg et al., 2018). However, our assay exhibited more convenience and reduced cost. Thus, CIALFB holds potentials for point-of-care deployment without fluorescence readers and expensive set-ups.

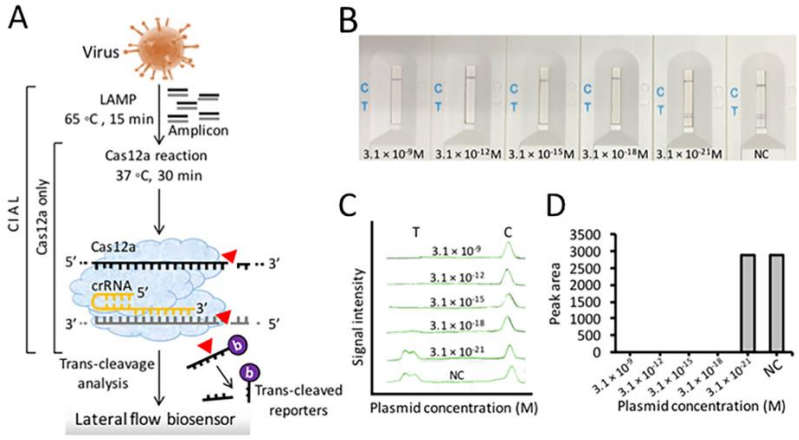

Figure 2. 4 CIALFB sensitivity.

(A) Schematic illustration of CIALFB and Cas12a alone reactions. (B) LFB detection of different concentrations of HPV16/HPV18 recombinant plasmid with CIALFB. (C) Corresponding peak intensities and (D) corresponding peak areas.

2.3.4 Validation of CIALFB for *HPV16/HPV18* detection in clinical samples

A total of 21 clinically obtained exfoliated cell samples were first confirmed HPV16, HPV18 positive or HPV-negative (Figure 2.3). Prior to CIALFB detection, 1 ml of each sample was heated (98 °C, 5 min), followed by centrifugation at 11,000 ×g for 10 minutes. Four µl of the supernatant was separately applied to CIALFB. As shown in Figure 2.6, none of the 7 HPV16 or HPV18 positive samples displayed a detectable test line as result of

reporter trans-cleavage, while 7 HPV16 or HPV18 negative samples (with 1 LFB presented) showed visible test lines within an hour for LAMP and ~2 hours for PCR based Cas12a assays. As shown in Figure 2.4B, C, the PCR/LAMP amplification also corroborated with the CIALFB assay results. Overall, our assay was fast with inexpensive readout on AuNP based LFB comparing with previously reported methods, like stand-alone PCR and LAMP, and other CRISPR based approaches, which require expensive materials such as electrophoretic, fluorescence apparatus, and monoclonal antibodies (Chen et al., 2018a; Gootenberg et al., 2018; Myhrvold et al., 2018; Li et al., 2018b). Thus, it is applicable for on-site analysis of nucleic acids in samples with significantly enhanced detection efficiency and convenience.

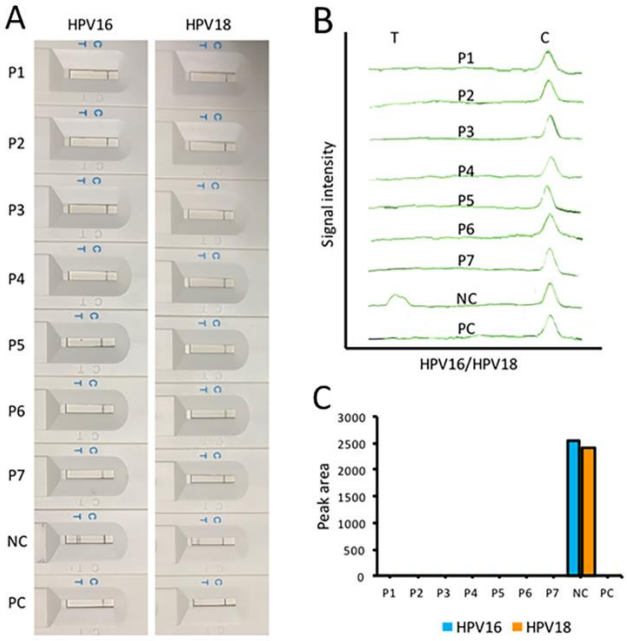

Figure 2. 5 Validation of CIALFB using HPV16 and HPV18 clinical samples.

(A) Photographic images of the CIALFB biosensors loaded with different HPV16 and HPV18 patient samples. (B) Representative peaks of the test lines corresponding to samples from different HPV patients. (C) The calculated peak areas corresponding to the test line peak intensities in (B). P1-P7 corresponds to the 7 HPV16 and 7 HPV18 positive samples; NC corresponds to the 7 HPV16 and 7 HPV18 negative samples, and PC corresponds to the positive control (recombinant plasmid).

2.3.5 CIALFB specificity for *HPV16/HPV18* detection

To evaluate the specificity of CIALFB assay, different intermediate and high-risk HPV types (52, 56, 89, 33, 39, 59, 66, 52, 58, 68, 31, 51, 45), and three separate mixtures (52/56, 33/39/59, 52/31) were used in the presence of HPV16 or HPV18 CIALFB set-up.

Three µl of heat-treated samples with non-target and target viruses were separately applied to CIALFB. For the non-target virus samples, a strong signal was observed at the LFB test lines, indicating no cleavage of the reporter; whereas, in the presence of either target virus, the test line was not detected, highlighting complete trans-cleavage of the reporter (Figure 2.7A, B). Similarly, the co-incubation of non-target viruses in the absence of either target virus showed a detectable test line, while in the presence of either target virus displayed no test line. These results were confirmed by signal intensities (Figure 2.7C) and peak areas of the LFB test lines (Figure 2.7D).

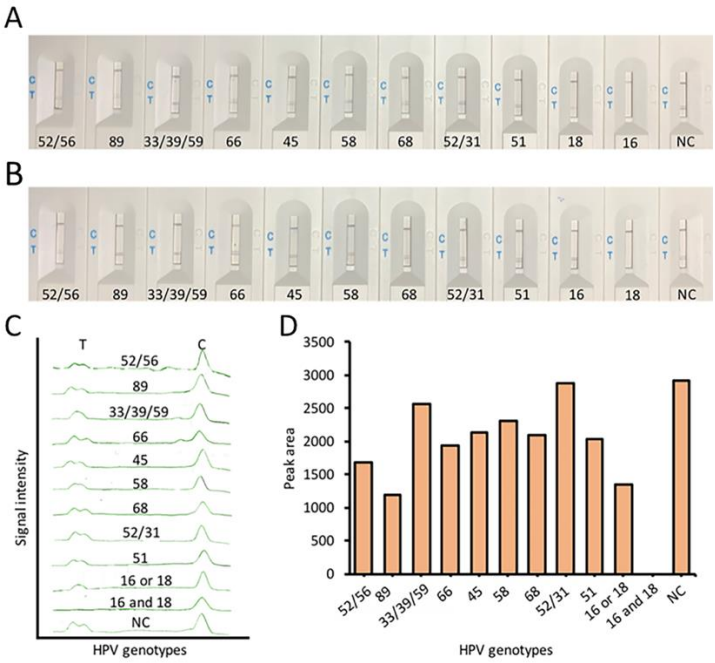

Figure 2. 6 CIALFB differentiates HPV16 or HPV18 from other HPV genotypes.

(A) CIALFB detection of HPV genotypes using HPV16 set-up (LAMP primers, crRNA, and activator). (B) CIALFB detection of HPV genotypes using HPV18 set-up (LAMP primers, crRNA, and activator). (C) Similar test line peaks generated by LFB reader corresponding to the test lines in (A) and (B). (D) Calculated test line peak areas corresponding to the test line peak intensities in (B).

CIALFB specificity was also examined using different recombinant plasmids of HPV16 (with the PAM sequence, without the PAM sequence, and with a single nucleotide mutation in 20 bases downstream the PAM region) (Table S2.1). As shown in Figure 2.8, the test line was not detected when the assay was performed with PAM containing the full-length target. Except for the 1st and 19th base mutations, all the mutated target sequences exhibited no trans-cleavage or reduced trans-cleavage. Thus, CIALFB assay confirmed the role of

PAM-mediated dsDNA target complementarity between the crRNA and target strand that activates reporter *trans*-cleavage (Kim et al., 2016b; Kleinstiver et al., 2016b).

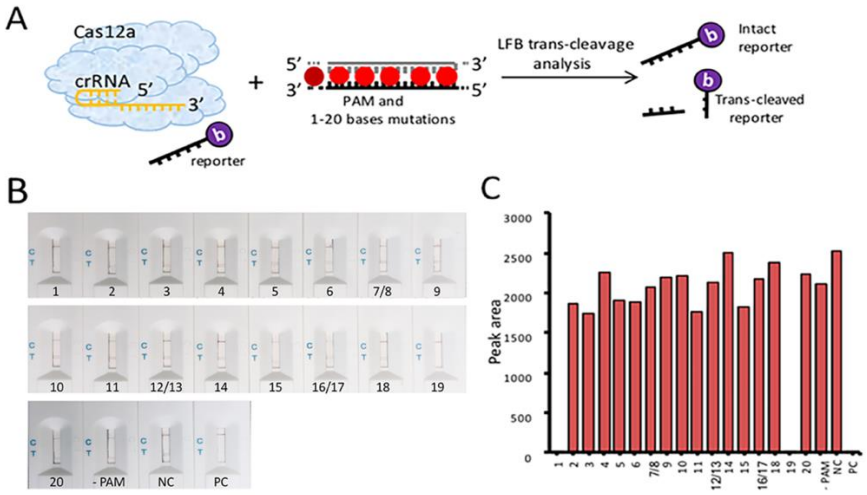

Figure 2. 7 High specificity of CIALFB is PAM- and proximal-PAM nucleotide (s)-dependent.

(A) Schematic illustration of CIALFB reaction using pUC57 plasmid-harboring intact or mutated target sequence of HPV16. (B) CIALFB and semi-quantitation of reporters' trans-cleavage in the presence or absence of PAM, and mutation near PAM-region of the target sequence. (C) Calculated peak areas of the LFB test line signal intensities in (B).

In summary, we have developed an ultrasensitive and specific Cas12a based biosensor for simple detection of HPV16 and HPV18 by combining CRISPR-Cas12a trans-cleavage propensity, LAMP isothermal amplification and lateral flow biosensor (LFB) termed "CIALFB". This method has several advantages. Firstly, LAMP enhanced the sensitivity of the assay without expensive and tedious genomic DNA extraction, while the CRISPR/Cas12a system allowed specificity and results readout on the probe-based LFB through reporter trans-cleavage detection. From the best of our knowledge, CIALFB is cost-effective compared to the use of expensive fluorescence readers or antibody-based LFB as required in all previously reported CRISPR/Cas based techniques (Chen et al., 2018a; Gootenberg et al., 2018; Li et al., 2018a; Myhrvold et al., 2018; Gootenberg et al., 2017). Secondly, without more handling and time-consuming process, our method provided a simple and rapid alternative to traditional methods, i.e., results can be obtained in within an hour. Finally, this biosensor ambiguously distinguished both HPV16 and HPV18 from other closely related virus types. Intriguingly, this technique can be easily applied for the diagnosis of other pathogens by changing the respective crRNAs and target nucleic acid pre-amplification primers.

Chapter 3: CRISPR/Cas12a based Lateral flow biosensor for the detection of *Pseudomonas aeruginosa*

3.1 Introduction

Herein, we present an ultrasensitive DNA probe based lateral flow biosensor (LFB) based on CRISPR/Cas and loop-mediated Isothermal Amplification (namely CIALFB) with remarkable potential in developing novel biosensing applications for the detection of *Pseudomonas aeruginosa.* The concept behind this approach is also a non-detectable test line on the LFB when the Cas effector protein collaterally cleaves the cognate target and a single stranded DNA (ssDNA) reporter sequence (Figure 2.1). The CIALFB can detect as low as a single copy cloned *Pseudomonas aeruginosa* acyltransferase gene, 1 cfu/ml plasmid containing *E. coli* DH5α pure cultures, as well as clinical samples without DNA extraction/purification or advanced apparatuses. No cross-reactivity with other non-target bacteria was observed. The naked eye result readout was obtained in 15 min of LAMP amplification, 30 min of Cas12 reaction, and 5 min of LFB readout. This platform is robust and of low cost for on-site testing.

3.2 Material and Methods

3.2.1 Reagents, chemicals and apparatuses

P. aeruginosa specific target sequence, primers, crRNAs (designed using benchling), reporters, and lateral flow capture probes were also synthesized by Sangon Biotech (Shanghai, China) (Table S2). All required material and reagents were similar to the previous ones except pET28a-AaCas12b plasmids gifted from Tolo Biotech (Shanghai, China) was expressed in BLD21 and purified accordingly using Nickel column and gel filtration (Li et al., 2018a) (Figure S1).

3.2.2 Bacteria culture and crude genomic DNA extraction

P. aeruginosa acyltransferase DNA target was cloned into pUC57 vector and transformed into *E. coli* DH5α. Bacteria strains used in this study were *P. aeruginosa* and negative controls such as *S. aureus*, *E. coli*, *C. jejuni*, *S. typhimurium*, *S. dysenteriae* (ATCC,

Manassas, VA). Bacteria were cultured in Luria-Bertani medium at 37 ◦C to > 2 OD. Then, the culture was collected, washed and adjusted to 2, 1, 0.8, 0.6, 0.4, 0.2, 0.1 OD. Serial dilutions were made from the culture plate with 0.1 OD for the preparation of 10^8, 10^7, 10^6, 10^5, 10^2, 10, 1 colony forming units (cfu/ml).

To obtain a crude genomic DNA for subsequent amplification, bacterial cultures were heat-treated (95 ◦C, 5 min), centrifuged (6500 rpm, 10 min), followed by 10-fold serial dilutions, and measuring using nanodrop at $A_{260/280}$.

3.2.3 LAMP and PCR amplification

LAMP amplification was performed according to NEB instruction. Primers were designed using Premier Biosoft LAMP designer and NCBI-BLAST for template sequence specificity check. Briefly, 25 µl LAMP reaction mixture was composed of primers F3, B3 (0.2 µM) and FIB, FIP (1.6 µM), 1.4 mM dNTP, 1.0 M betaine, 6 mM $MgSO_4$, 1× isothermal amplification buffer, various target DNA template concentrations, and 320 U/ml *Bst* 2.0 WarmStart DNA polymerase, which allows the reaction mixture set up at room temperature. The mixture was then LAMP amplified at 65 ◦C for 15-30 min and then terminated at 80 ◦C for 10 min.

For PCR amplification, 25 µl PCR reaction mixture was composed of 1 µl forward and reverse primers (0.3 µM), 12.5 µl 1× rTaq premix, 1-2 µl template (200 ng) and ddH_2O to final reaction volume. The reaction mixture was incubated in a thermocycler using 3 steps PCR protocol: 95 ◦C, 10 min for denaturation; 95 ◦C, 10 sec for denaturation; 62 ◦C, 10 sec for annealing; 72 ◦C, 30 sec for elongation; 35 cycles.

3.2.4 Target cleavage assays

For CIALFB analysis of trans-cleaved reporters, the cleavage assay (Chen et al., 2018c) was carried out with slight modifications. A 25 µl set up of Cas12a/b cleavage assay consisted of 6 µl of cleavage buffer (150 mM KCl, 10 mM $MgCl_2$, 1 % glycerol, 0.5 mM DTT, 20 mM HEPES (pH 7.5)), 3 µl crRNA (300 nM), 1 µl Cas12a/b (1 µM), 3 µl activator (400 nM) and 2 µl reporter (250 nM). Unless indicated otherwise, 1-2 µl target DNA and nuclease free water were added up to the final volume prior to incubation at 37 ◦C at different time intervals. For one-pot reaction, a 50 µl reaction was made of Cas12a/b premix as described above and double concentration of the LAMP amplification components. Then, the mixture was incubated at different temperature and time intervals prior to analyzing using

LFB after adding ddH_2O up to 60 µl final volume.

For fluorescence analysis of trans-cleavage reaction, 25 µl set up was prepared as mentioned above with 5'FAM and 3'TAMRA labeled ssDNA reporter instead of biotinylated ssDNA reporter. The reaction was incubated at 37 ◦C in 96-well microplate and then read using the Mithras^2 LB 943 plate reader (Berthold Tech, Germany). The fluorescence from the cleavage reaction was measured at different time course with excitation at 495 nm and emission at 520 nm.

3.2.5 Construction of LFB and LFB detection of reporter sequences

AuNP synthesis/characterization, conjugation, and LFB assembling is similar to as pre-mentioned material and methods (Figure 2.2).

3.2.6 Spiked and clinical isolates analysis

Clinical human serum and milk samples were confirmed *P. aeruginosa* negative using PCR. Twenty-five µl of each sample was 10 times diluted, spiked separately with different concentrations of *P. aeruginosa* crude genomic DNA or recombinant plasmid, and then subjected to CIALFB assay in a total volume of 50 µl.

For clinical sample test, 40 clinical sputa from *P. aeruginosa* suspected patients were collected. The samples were heated at 56 ◦C for 30 min for enzymatic inhibition. The heat-treated samples were either used for DNA extraction for PCR amplification or 10 times diluted and heated at 95 ◦C for 5 minutes and centrifuged (6500 rpm, 10 min) prior to LAMP amplification. Two µl of the heat extracted DNA was used in the CIALFB assay as mentioned above.

3.2 Results

3.3.1 Optimization of the length and concentration of the reporters and their complementary ssDNA capture probes on the LFB test line

Reporters with a certain nucleotide composition and length are crucial to provide optimal signal readout upon Cas effector mediated collateral cleavage (Gootenberg et al., 2018; Li et al., 2018b; Chen et al., 2018c). Therefore, we adopted a 5'-TTATT-3' ssDNA reporter (Chen et al., 2018c) with slight modifications. The reporter was extended at the 5'-end with 1 to 9

thymines and biotinylated, and its complementary capture probes were immobilized on the LFB test line to achieve a detectable signal through hybridization (Table S2). The test lines were detected when the reporters and the capture probes were longer than 9 bases (Figure S3.1A, B). As shown in Figure S3.1C, D, strong hybridization was obtained with the combination of 11 bases reporter (5'-Bio-TTTTTTTTATT-3') and 38 bases capture probe (3'-16ATAA-5'): 5'-**AATAAAAAAAAAAAAAAA**AATAAAAAAAAAAAAAAA-3', respectively. The highlighted sequence is repeated twice to increase the binding force with the reporter.

We subsequently tested different concentrations of the 11 bases reporter (5, 10, 15, 20, 25, 30, 50, 70, 100 nM) on the LFB (Figure S3.1E). The test line was detected at a reporter concentration above 10 nM, which became prominent with a subsequent increase in concentration (Figure S3.1E). However, 20 nM was found to be the optimum concentration to obtain a strong test line in the absence of the target, and non-detectable test line signal in the presence of the target (data not shown). The concentration of 20 nM and the reporter length 11 bases were then used for subsequent Cas12 cleavage experiments.

3.3.2 Sensitivity of CIALFB

Cas12a exhibits a PAM-depended collateral cleavage property and target pre-amplification increases its sensitivity (Gootenberg et al., 2018; Li et al., 2018b; Chen et al., 2018c). The sensitivity of the CIALFB was evaluated using a cloned *P. aeruginosa* acetyltransferase gene with a conserved PAM (TTT) region cloned in pUC57 plasmid (Figure 3.1A, Table S1) and verified with LAMP and PCR amplification (Figure 3.1B)**.** The cloned plasmid DNA was serially diluted to different concentrations (1×10^{-10}, 1×10^{-11}, 1×10^{-14}, 1×10^{-17}, 1×10^{-18}, 1×10^{-21} M). Two µl of each diluted sample was LAMP amplified and 1 µl of the amplified product was applied to Cas12a cleavage reaction. The product of the LAMP-Cas12a (CIA) reaction was directly loaded to the LFB. As shown in Figure 3.1C and D, samples with concentrations of 1×10^{-18} M or higher target plasmid DNA showed no test line as a result of reporter trans-cleavage. However, samples with the concentration of 1×10^{-21} M target plasmid DNA showed a test line indicating no cleavage of the reporter sequence. This sensitivity was achieved with 15 min of LAMP amplification, 15 min of Cas12a cleavage (Figure 3.1E, F) and 5 min of LFB readout. One aM (1×10^{-18} M) plasmid DNA in 2 µl contains 1.2 copies, depicting that the sensitivity of the CIA system reached single copy level. The sensitivity of the CIALFB was also tested using different amounts of

pre-heated *E. coli* DH5α containing target recombinant plasmid DNA (1×10^8, 1×10^7, 1×10^6, 1×10^5, 1×10^2, 1×10, 1, 0 cfu/ml). None of the samples, except the control (0 cfu/ml), showed a test line on the LFB (data not shown). A sensitivity of 1 cfu/ml was achieved within 30 min of the CIA reaction and 5 min LFB readout (Figure S4A). The same set of samples was also tested using FAM-TAMRA labeled reporters, and the same sensitivity was also achieved (Figure S4B). The CIALFB reached single copy level sensitivity for plasmid DNA and 1 cfu/ml sensitivity for plasmid containing *E. coli*.

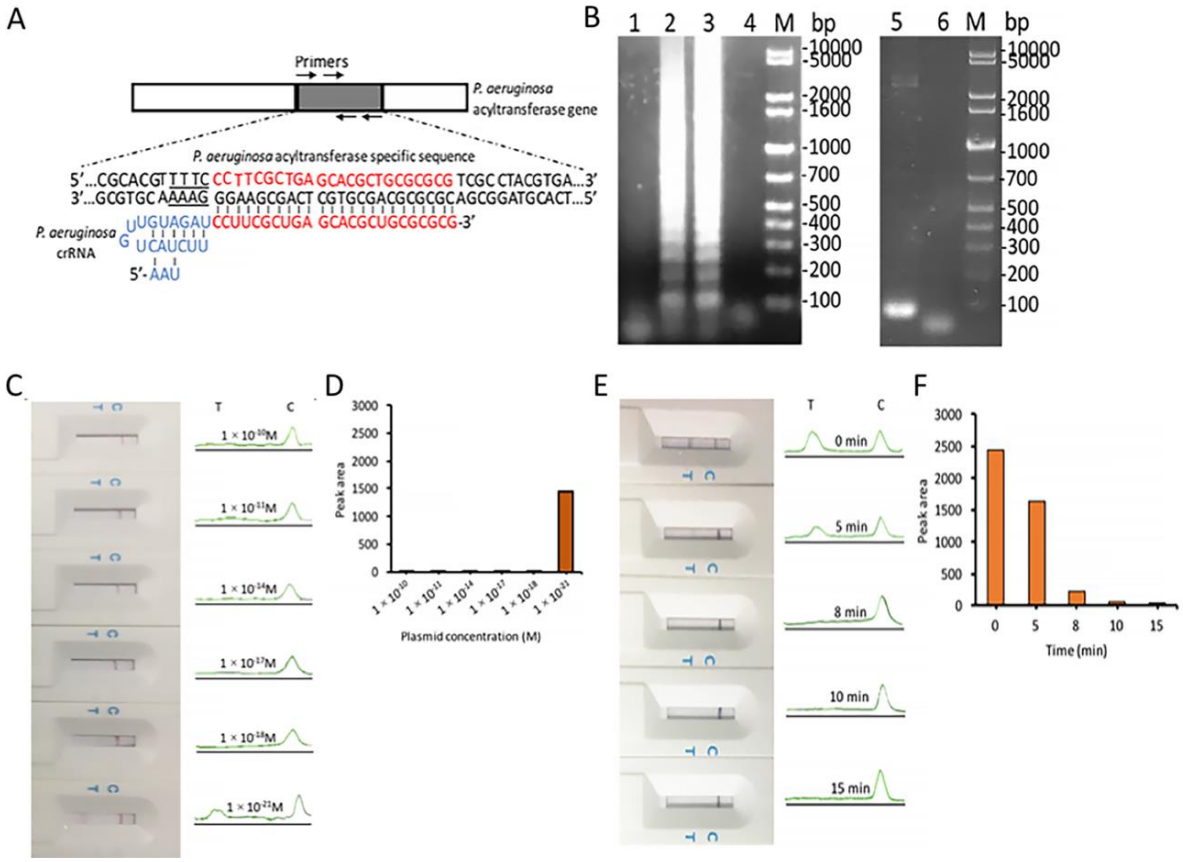

Figure 3. 1 Condition optimization and sensitivity of CIALFB using recombinant plasmid. (A) Design of P. aeruginosa cognate template and crRNA sequence. (B) Amplification of 2 µl P. aeruginosa acyltransferase gene (40 ng/µl). Lanes 1-3 correspond to LAMP amplification at 55, 60, and 65 ◦C; lanes 4 and M correspond to negative control and 1-kb marker, respectively; lanes 5 and 6 correspond to PCR amplification of the gene, its negative control, and M is 1-kb marker, respectively. (C) CIALFB Sensitivity using different concentrations of recombinant plasmid DNA and (D) corresponding peak areas. (C) The CIALFB results for the detection of 1cfu/ml plasmid containing E. Coli for different Cas12a trans-cleavage reaction time and corresponding peak areas (F).

We further validated the CIALFB detection of target DNA from *P. aeruginosa* culture.

P. aeruginosa culture was heat-treated at 95 ◦C for 5 minutes to release the genomic DNA for CIA reaction (Figure 3.2). The genomic DNA was serially diluted to different concentrations (3.4×10^{-12}, 3.4×10^{-13}, 3.4×10^{-14}, 3.4×10^{-15}, 3.4×10^{-18}, 3.4×10^{-19}, 3.4×10^{-20}, 3.4×10^{-21}, 3.4×10^{-22} M) and then applied to CIALFB reaction. As shown in Figure 3.2B and C, samples with crude genomic DNA of 3.4×10^{-18} M or higher didn't show any test line, the sample with 3.4×10^{-19} M showed faint test line and samples with lower input target DNA showed strong test lines indicating that attomolar crude genomic DNA from cultured *P. aeruginosa* was detected with the CIALFB. Two µl of crude genomic DNA sample with the concentration of 3.4×10^{-18} M contains 4 copies. This sensitivity was also obtained in plasmid DNA detection assay (1.2 copies in 2 µl) and Cas12a/b-based one-pot reaction (Figure S5A-F). However, Cas12a could not withstand the LAMP reaction temperature higher than 55 ◦C and thus resulted in reduced reporter shearing (Figure S6). This sensitivity is comparable to previously reported CRISPR/Cas based diagnostics (Gootenberg et al., 2018; Li et al., 2018a; Li et al., 2018b; Chen et al., 2018c).

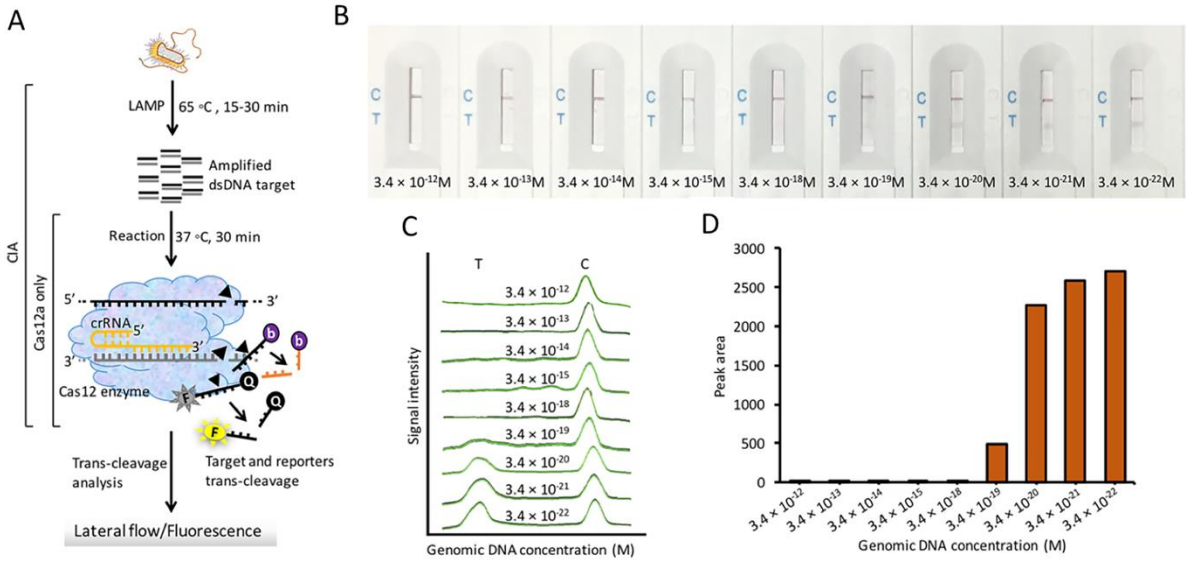

Figure 3. 2 Detection of P. aeruginosa crude genomic DNA.

(A) Scheme illustration of LAMP coupled with Cas12 detection (CIA). (B) CIALFB detection of different concentrations of P. aeruginosa crude genomic DNA, corresponding signal intensities of the LFB (C) and calculated peak areas (D).

3.3.3 Detection of *P. aeruginosa* in spiked and clinical samples with CIALFB

Milk and serum were spiked with serially diluted *P. aeruginosa* crude genomic DNA (3.4×10^{-12}, 3.4×10^{-13}, 3.4×10^{-14}, 3.4×10^{-15}, 3.4×10^{-18}, 3.4×10^{-19}, 3.4×10^{-20}, 3.4×10^{-21},

3.4×10^{-22} M) and then subjected to CIALFB reaction. As shown in Figure 3.3A-C, the LFB for the spiked samples with 3.4×10^{-18} M or higher crude genomic DNA showed invisible test lines as a result of cleavage of the reporter, samples with lower concentrations exhibited visible bands and high signal intensities on the test lines as a result of uncleaved reporters. Although the spiked sample with the concentration of 3.4×10^{-18} showed weak signal when a strip reader was used (Figure 3.3C), the sensitivity results obtained here for complex samples (milk and serum) is similar as that for heat released crude genomic DNA from bacteria culture (Figure 3.2). This sensitivity for target cleavage in complex samples (milk and serum) was also confirmed using the fluorescence assay (data not shown).

Moreover, we tested our CIALFB on 40 clinical samples that were previously confirmed *P. aeruginosa* sputa positive or negative by conventional culture and PCR (Figure S4C). All samples were tested using CIALFB. The biosensor corroborated 100 % with the conventional PCR method and conventional culture (Figure 3.3D). The assay showed a fast response in 30 min and required no expensive materials such as electrophoretic, fluorescence apparatus, or monoclonal antibodies as in previous platforms (Gootenberg et al., 2018; Li et al., 2018a; Myhrvold et al., 2018; Li et al., 2018b; Chen et al., 2018c). Furthermore, apart from the fluorescent dyes, the usage of AuNPs based LFB enabled the visualization of results with naked eye. Thus, our method is applicable for on-site detection of nucleic acids in clinical samples.

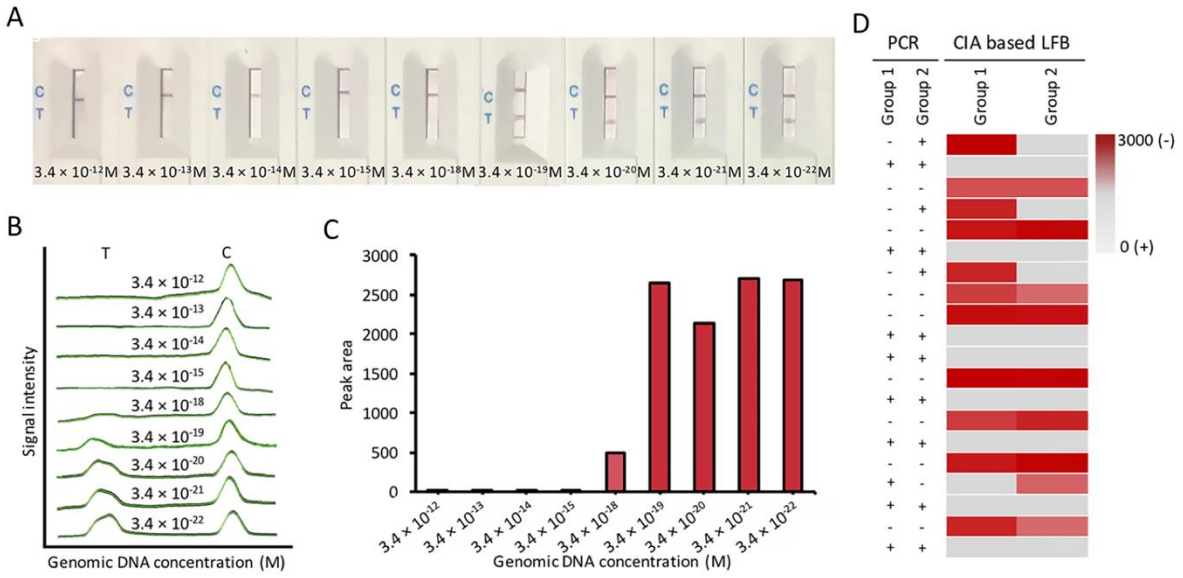

Figure. 3. 3 Sensitivity of the CIALFB for the detection of P. aeruginosa from spiked and clinical samples.

(A) CIALFB results for different concentrations of spiked genomic DNA and the

corresponding signal intensities (B) and calculated peak areas (C). (D) Heatmap validating the detection of P. aeruginosa in 40 clinical sputa samples that were separated into two groups. The calculated peak areas of the LFB test line intensity is represented by red color (red cells: negative, gray cells: positive).

3.3.4 Specificity of the CIALFB assay

The specificity of the CIALFB assay was tested with non-target bacteria species such as *E. coli* O157:H7, *S. aureus*, *C. jejuni*, *S. typhimurium*, *S. dysenteriae*. Two µl of heat-treated non-target bacteria (10^4 cfu/ml) and target bacteria (1 cfu/ml) were separately applied to CIA reaction. For the non-target bacteria samples, a strong signal was observed at the LFB test lines indicating no cleavage of the reporter, whereas in the presence of as low as 1 cfu/ml *P. aeruginosa*, the test line was not detected indicating complete cleavage of the reporter (Figure 3.4A, B). The specificity of the assay was also tested using a mixture of different number of non-target bacteria species (10^4 cfu/ml) in the presence or absence of *P. aeruginosa* (1 cfu/ml). As shown in Figure 3.4C, a detectable test line was observed only in the absence of the target bacteria, the test line was not observed as long as the target bacteria is present, even though the target bacteria were at a very low concentration (1 cfu/ml). These results were confirmed by signal intensities (Figure 3.4D) and peak areas (Figure 3.4E) of the test lines. The high specificity could also be attributed to the crRNA targeting since target sequences without PAM or 15 bases truncation near the PAM region exhibited no trans-cleavage or reduced trans-cleavage, respectively (Table S1, Figure S7).

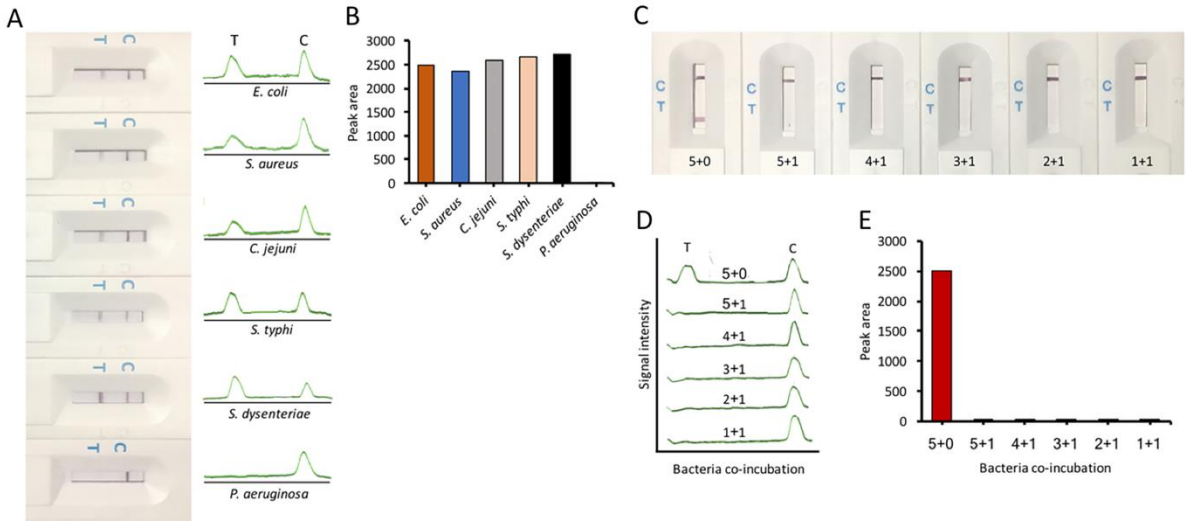

Figure 3. 4 Specificity assay.

(A) CIALFB tests of the target *P. aeruginosa* (1 cfu/ml) and non-target bacteria (10^4 cfu/ml).

(B) Test line signal peak areas of the CIALFB. (C) LFB detection of *P. aeruginosa* samples mixed with different non-target bacteria. The first number is the number of different types of non-target bacteria, and the second number indicates the presence (1) or absence (0) of the target bacteria. (D and E) Test line signal intensity plot (D) and bar chart (E) of the LFB detection results of mixed samples with and without *P. aeruginosa*.

To decipher the high specificity of the CIALFB assay, we modified the crRNA binding site of the target sequence (Table 3). Different target sequences (with the PAM sequence, without the PAM sequence, and with 15 bases truncation near the PAM region) were constructed and cloned into the plasmid pUC57 and tested by the CIALFB (Figure 3.5A). As shown in Figure 3.5B and C, the test line was not detected when the assay was performed with PAM containing the full-length target. The target sequence without the PAM region or with 15 bases truncation exhibited no trans-cleavage or reduced trans-cleavage, respectively. This experiment further confirmed the specificity of the CIALFB assay at a molecular level.

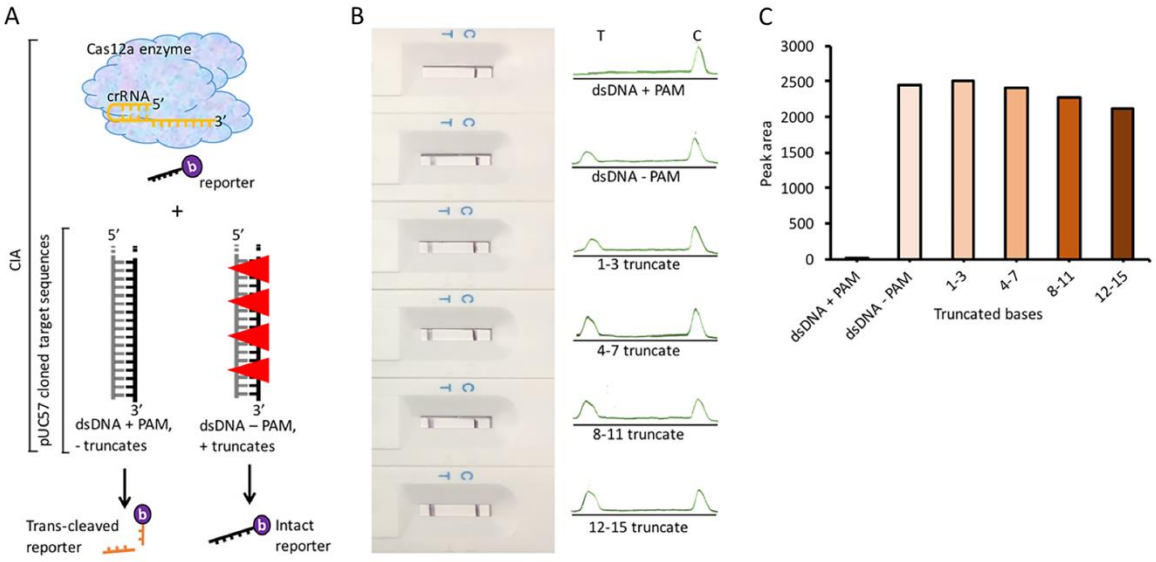

Figure 3. 5 High specificity is PAM- and proximal-PAM nucleotide (s)-dependent.

(A) CIALFB and semi-quantitation of reporters' trans-cleavage in the presence or absence of PAM, and truncation near PAM-region of the target sequence. (B**)** Calculated peak areas of the test line signal intensity.

3.3.5 One-pot reaction

We further exploited the possibility of combining LAMP isothermal amplification and Cas cleavage to achieve a one-pot CIALFB reaction system. To begin with, a 50 μl volume

system comprising the pre-heated crude genomic DNA (3.4 aM) from *P. aeruginosa* culture, LAMP and Cas12a premix, were incubated at different temperature (45, 50, 52, 55, 60, 65 ◦C) and different time intervals. As shown in Figure 3.6A-C, by using Cas12a in the reaction, the attomolar range input template was successfully detected between 52-55 ◦C within an hour of LAMP-Cas12a reaction and 5 min of LFB readout. However, Cas12a could not withstand the LAMP reaction temperature higher than 55 ◦C and thus resulted in reduced reporter shearing (Figure S5).

To enhance the efficiency of one-pot reaction, we sought to integrate thermophilic Cas12b (Figure S2b) (Strecker et al., 2019; Li et al., 2018a) with LAMP at a higher temperature. As shown in Figure 6e, the pre-heated crude genomic DNA (3.4 aM) was detected by the Cas12b based LFB in less than 45 minutes, which is also evident from the signal intensities (Figure 3.6F), and calculated peak areas of the LFB test lines (Figure 3.6G). No test line signal was detected at 45 minutes or longer reaction time.

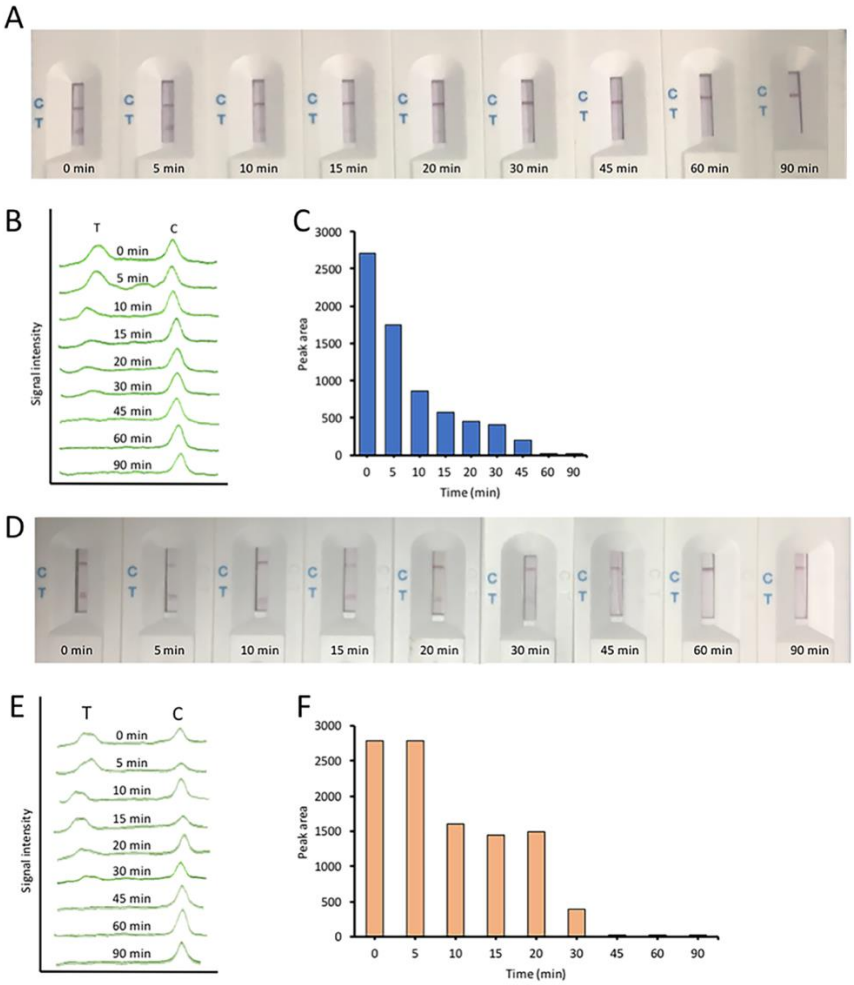

Figure 3. 6 One-pot CIA reaction for the detection of 3.4 aM P. aeruginosa genomic DNA. (A) The CIA based biosensors at different Cas 12a reaction time, with a corresponding

decrease in test line intensities (B) and the calculated peak areas (C). The disappearance of the test line indicates the complete cleavage of the reporter. (D) CIA based biosensors at different Cas 12b reaction time, with the corresponding test line intensities (E) and calculated peak areas (F). The disappearance of the test line indicates the complete cleavage of the reporter.

Chapter 4: A CRISPR-Cas12a based universal lateral flow biosensor for the sensitive and specific detection of African swine-fever viruses

4.1 Introduction

African swine fever (ASF) is a highly contagious, fatal infectious disease caused by African Swine Fever Virus (ASFV) in domestic and wild pigs (Kleiboeker et al., 1999). It can be expressed in 3 main forms: acute, subacute and chronic (Parker et al., 1969; Gomez-Villamandos et al., 2013). ASFV has a morbidity and mortality rate of up to 100% and is widely prevalent in 13 different countries and regions around the world since its discovery in Kenya in 1921 (Gallardo et al., 2014; Ruiz-Fons et al., 2008). ASFV is still a major problem in countries worldwide for both developing and developed countries such as Russia and western Europe (Gogin et al., 2013; Śmietanka et al., 2016; Sanchez-Vizcaino et al., 2013). According to China Center for Animal Health and Epidemiology, ASFV epidemics has currently caused serious loss to the livestock industry in China (Liu et al.).

At present, the detection of ASFV can be divided into two categories according to different diagnostic tests: one is the detection of antibodies; the other is the detection of viral DNA. Conventional detection methods are serological enzyme-linked immunosorbent assay (ELISA) (Cubillos et al., 2013) and DNA based like polymerase chain reaction (PCR) (Agüero et al., 2003). These methods are robust, but they are still hindered by cost, reproducibility, convenience, and are prone to false-positive results. These disadvantages have hindered their in-depth application in the on-site testing. Therefore, it is particularly important to develop rapid, accurate, and non-cross-contamination detection technologies.

Recently, CRISPR-Cas12/Cas13/Cas14 systems have been exploited in analytical method field and have been found to be very suitable for the detection of various targets, including bacteria, drug resistance genes, human DNA genotypes and cancer mutations based on its unique transcleavage property of target nucleic acids and non-specific single-stranded DNA (ssDNA) (refered hereafter as a reporter) in vicinity (Chen et al., 2018a; Li et al., 2018a; Myhrvold et al., 2018; Gootenberg et al., 2017; Harrington et al., 2018). For example, DETECTR (Chen et al., 2018c) and HOLMES (Li et al., 2018a; Li et al., 2018b) detection systems used crRNA-guided Cas12a enzymes for ultra-sensitive and rapid detection of target DNA, and SHERLOCK (Gootenberg et al., 2018) for target RNA. To increase the sensitivity, CRISPR-systems are combined pre-amplification methods such as PCR (Li et al., 2018b),

recombinase polymerase amplification (RPA) (Chen et al., 2018a; Gootenberg et al., 2018), which also reduce the possibility of false results. The high specificity of CRISPR-Cas12a relies on the fact that it doesn't initiate cleavage of the reporter nucleic acid if there is a mismatch (es) between the target DNA sequence and the gRNA. Though this method is expected to bring a revolutionary breakthrough in the field of molecular diagnostics, however, all the existing methods use expensive fluorescence-based instruments and antibody-based lateral flows, which are still costly and prone to false-positive results. Thus, further efforts are advocated to develop cost-effective detectors with reduced background, contamination, bench-work, and expertise.

Here, we present CRISPR/Cas-LFB assay, which is an ultrasensitive and specific LFB that can respond to cleaved ssDNA reporter from crRNA-guided Cas12a cleavage of ASFV DNA target. The principle is that ASFV containing sample was pre-amplified by PCR to enhance sensitivity. Then, the amplified product was added to the Cas12a detection system (inacluding crRNA, Cas12a protein, biotinylated ssDNA reporter). The Cas12a and crRNA complex recognize and cleave the target DNA and subsequently trigger the trans-cleavage of the biotinylated ssDNA reporter, which cannot hybridize to its complementary DNA immobilized at the LFB test line (Figure 4.1). The CRISPR/Cas-LFB assay achieved a good sensitivity and could identify ASFV in complex samples such as blood. Thus, unveiling a new CRISPR-based lateral flow biosensor for rapid and cost-effective identification of infectious diseases.

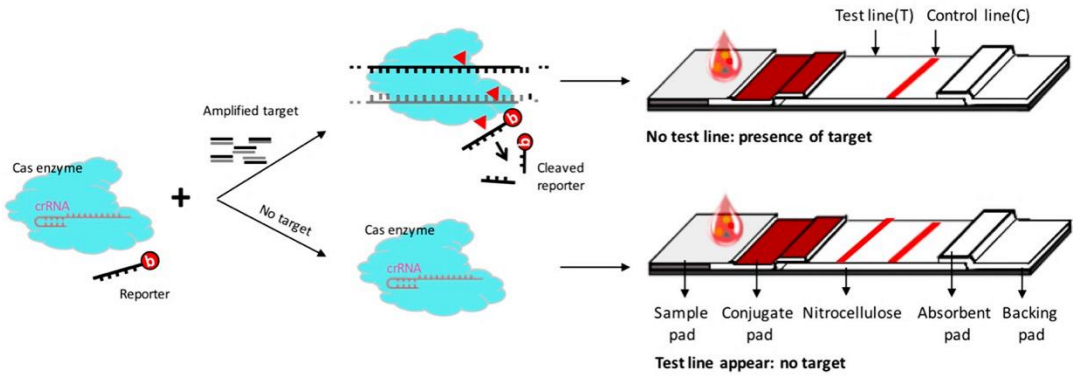

Figure 4. 1 Illustrative principle of CRISPR/Cas-LFB assay.

Target DNA from pre-extracted real samples is PCR pre-amplified. The amplicons are applied to Cas12a reaction, which contains specific crRNA, activator and biotinylated ssDNA reporter. In the presence of the target, Cas12a transcleave the biotinylated ssDNA reporter, resulting in an undetectable test line on the LFB.

4.2 Materials and methods

4.2.1. Materials, chemicals, reagents and methodology

P. aeruginosa specific target sequence, primers, crRNAs (designed using benchling), reporters, and lateral flow capture probes were also synthesized by Sangon Biotech (Shanghai, China) (Table S2). All required material and reagents were similar to the previous ones except pET28a-AaCas12b plasmids gifted from Tolo Biotech (Shanghai, China) was expressed in BLD21 and purified accordingly using Nickel column and gel filtration (Li et al., 2018a) (Figure S1).

4.2.2 Target DNA design, virus collection and DNA extraction

In this study, two types of ASFV target DNA were used: 1) a 270 bp ASFV specific sequence targeting VP73 genes of 7 types of ASFV (Agüero et al., 2003) synthesized and cloned in pUC57 vector was used for study design and positive control; and 2) ASFV positive and negative samples identified using PCR. We furthermore reconfirmed these samples by PCR using previously published method (Agüero et al., 2003) after DNA extraction using Qiagen Blood Kit (Beijing, China) (Figure S4.1, cloning and verification of real samples). For CRISPR/Cas-LFB assay, extracted DNAs were used.

4.2.3 PCR amplification

For PCR amplification, 25 µl PCR premix was composed of 1 µl forward and reverse primers (0.3 µM), 12.5 µl 1× rTaq Premix, 2 µl of extracted genomic DNA (200 ng) and ddH_2O to final reaction volume. The reaction mixture was incubated in a thermocycler using 3 steps PCR protocol for 45 min: 95 ◦C, 5 min for denaturation; 95 ◦C, 10 sec for each cycle; 55 ◦C, 10 sec for annealing; 72 ◦C, 30 sec for elongation; 35 cycles. PCR products were analyzed using 2.5 % agarose gel electrophoresis.

Table 4. 1 Nucleic acids to be used in this study.

Name	Sequence (5'-3')
Target dsDNA for ASFV	TGTGAACAAAAGTTATGGGAAACCCGACCCCGAACCCAC TTTGAGTCAAATCGAAGAAACACATTTGGTTCATTTTA**AT GCGCATTTTAAGCCTTATGTTC**CAGTAGGGTTTGAATAC AATAAAGTACGCCCGCATACGGGTACCCCCACCTTGGGA AACAAGCTTACCTTTGGTATTCCCCAGTACGGAGACTTTT TCCATGATATGGTGGGCCACCATATATTGGGTGCATGTCA

	TTCGTCCTGGCAGGATGCTCCGATTCAGGGCAC
PCR primers (Agüero et al., 2003)	
Forward	AGTTATGGGAAACCCGACCC
Reverse	CCCTGAATCGGAGCATCCT
crRNA	UAAUUUCUACUAAGUGUAGAU**ATGCGCATTTTAAGCCT TATGTTC**
Activator (24 bp)	TTTGGTTCATTTTA**ATGCGCATTTT**
Reporter	Biotin-TTTTTTTTATT
Test-line probe (38 bases)	AATAAAAAAAAAAAAAAAAAATAAAAAAAAAAAAAAAA

Underline represents PAM region
Bold represents crRNA binding sequence

4.2.4 Target cleavage assays

For CRISPR/Cas-LFB assay analysis of trans-cleaved reporters was also analysed by lateral flow and fluorescence measurement as previously methioned with slight modifications. Briefly, the cleavage assay was carried out according to (Chen et al., 2018c) with slight modifications. The LbaCas12a complex was preassembled as follows: 12 µl of cleavage buffer (150 mM KCl, 10 mM $MgCl_2$, 1 % glycerol, 0.5 mM DTT, 20 nM HEPES (pH 7.5)) or 3 µl NEB buffer 3.1, 3 µl crRNA (300 nM), 1 µl LbaCas12a (36 nM) and 5 µl activator (40 nM) incubated at 37 ◦C for 15 min. Then, a LbaCas12a detection was prepared using 21 µl LbaCas12a-crRNA-activator complex, 2 µl biotinylated ssDNA reporter (20 nM), and 2 µl extracted target DNAs. Finally, the reaction was incubated at 37 ◦C and analyzed using LFB after adding ddH_2O up to 60 µl.

For fluorescence analysis of trans-cleavage reaction, 50 µL reaction set up was prepared as mentioned above with 5'FAM and 3'TAMRA labeled ssDNA reporter instead of biotinylated ssDNA reporter. The reaction was incubated and proceeded at 37 ◦C in a 96-wells microplate reader Mithras^2 LB 943 (Berthold Tech, Germany). The fluorescence from reporter sequence cleavage was measured every 5 minutes from 0 to 1 hour with detection at λ excitation = 495 and λ emission = 520.

4.2.5 Construction of the LFB

AuNP synthesis/characterization, conjugation, and LFB assembling is similar to as pre-mentioned material and methods (Figure 2.2).

4.2.6 Statistical analysis

Each result presented is the mean ± standard error of the mean (SEM) of triplicate samples from three independent experiments. However, the standard errors were intentionally omitted due to non-significant differences between LFB peak areas readings.

4.3 Results

4.3.1 Overview of the CRISPR/Cas-LFB detection system

As illustrated in Figure 1, the principle of CRISPR/Cas-LFB approach is based on PCR pre-amplification to improve the sensitivity through target DNA pre-amplification, and the detection of trans-cleaved biotinylated ssDNA reporter upon target recognition by Cas12a effector. As previously reported (Mukama et al., 2020), from a wide range of screened reporter sequences length, the 5'biotin-TTTTTTTTATT-3' reporter (11 bases) successfully hybridized with its complementary test line where the capture probe (38 bases) immobilized on the LFB test line, allowing it to be detectable by the naked eye (Table 4.1, Figure 4.2A). The test line was not observed when ddH_2O and shorter reporter sequences were applied (Figure 4.2A). The test line intensity depended also on the concentration of the repoter, of which 50 nM was chosen for all downstream experiments (Figure 4.2A). In the presence of the target, trans-cleaved reporters were not detected on the test line as a result of length reduction. The appearance of the control line indicated that the LFB works perfectly through capturing the excess of AuNPs-SA conjugate complex by the biotinylated immunoglobulin immobilized thereof.

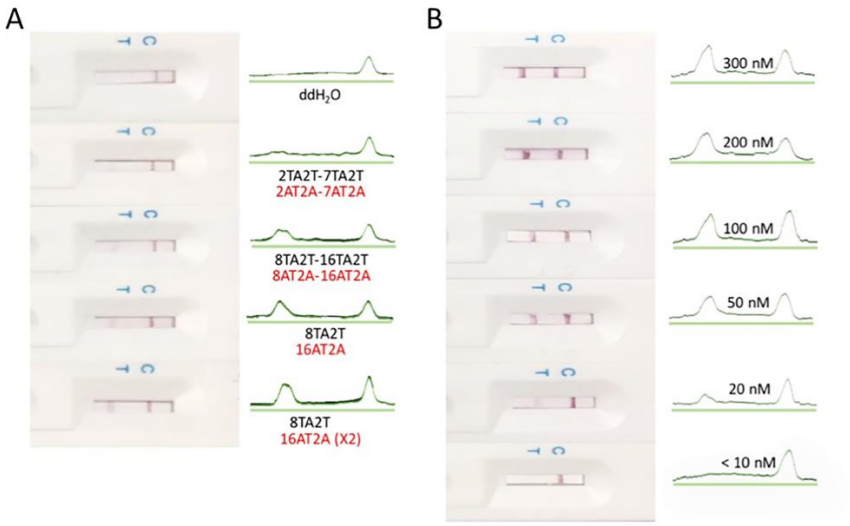

Figure 4. 2 Optimization of reporter length and concentration.

(A) Different length of 100 nM water-dissolved reporter sequences (in black) applied on the LFB test line complementary probe (in red). (B) Different concentrations of 8TA2T reporter applied on the 16AT2A (X2) LFB complementary probe.

4.3.2 The feasibility and sensitivity evaluation of CRISPR/Cas-LFB assay using recombinant plasmid

The system was firstly studied using pUC57-ASFV recombinant plasmid DNA target (Figure 4.3A). The conserved region of ASFV target genes (VP73) (Table 4.1) was selected due to its potential in the simultaneous distinction of 7 different ASFV types (Agüero et al., 2003). PCR pre-amplification of ASFV target was performed for 45 min (Figure 4.3A) and applied to Cas12a reaction specific components (crRNA, activators and biotinylated ssDNA reporter). The CRISPR/Cas12a-LFB assay identified accurately and easily the presence of the target plasmid through undetectable LFB test line. In contrast, in the absence of the critical reaction components a visible LFB test line was observed (Figure 4.3B,C).

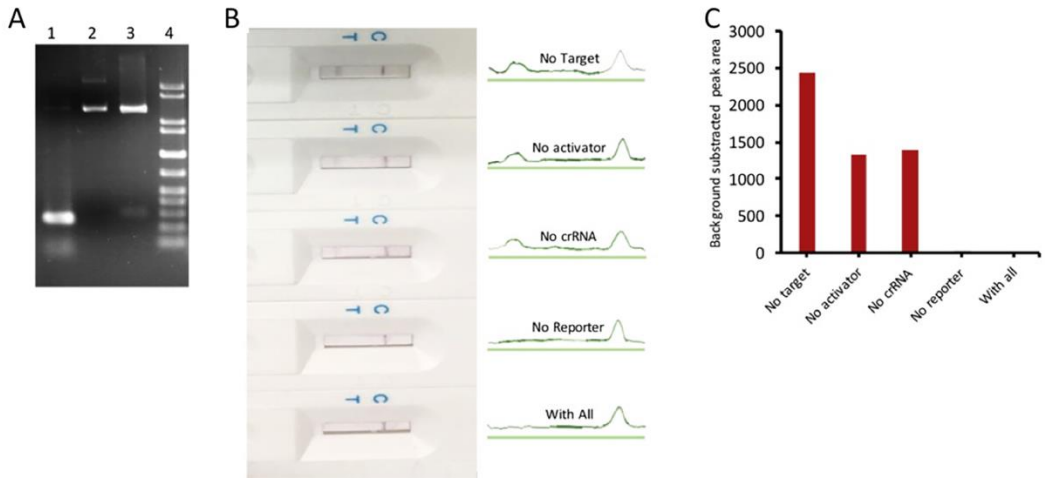

Figure 4. 3 The feasibility assay of CRISPR/Cas-LFB assay using a recombinant plasmid. (A) Gel electrophoresis of the PCR-amplified 270 bp of ASFV specific sequence (1), cloning in pUC57 (2), and double digestion verification at *BamHI*/*EcoRI* enzyme site (3). (B) CRISPR/Cas-LFB reaction in the presence/absence of different reaction components. (B) Test and control line signal intensities. (C) bar chart of the LFB test lines in (A,B).

In order to evaluate the sensitivity, different concentrations of the serially diluted recombinant plasmid (2.5×10^{-8} - 0.5×10^{-15} M) were tested using both PCR and CRISPR/Cas-LFB. PCR alone achieved sensitivities > 25×10^{-15} M (Figure S4.1). However, for PCR combined CRISPR/Cas-LFB, except for the samples with $\leq1\times10^{-15}$ M, no detectable test line was observed as result of the reporter trans-cleavage (Figure 4.4). As low as 2.5×10^{-15} M (~1554.46 copies/µl) was detected, which is comparable to fluorescence assay (data not shown) and previously reported CRISPR diagnostics (Li et al., 2018a; Li et al., 2018b). Distinct from the previous assays, our CRISPR/Cas-LFB can be combined with isothermal amplification to reduce cross-contamination, cost and can be readily deployed.

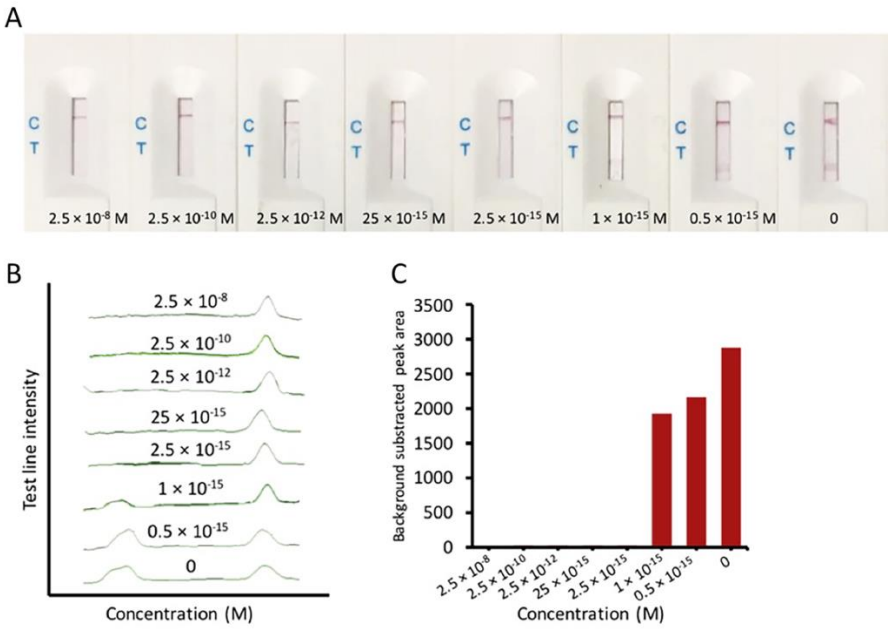

Figure 4. 4 The sensitivity using different concentrations of the recombinant plasmid. (A) LFB responses for the different concentrations. (B) Test and control line signal intensities. (C) bar chart of the LFB test lines in (A,B). 0 stands for negative control.

4.3.3 Selectivity of the biosensor for ASFV detection.

The selectivity assay consisted of various bacteria strains (*E. coli*, *P. aeruginosa*, *S. aureus*), viruses (Iridovirus, ASFV), and co-incubation in the presence of ASFV. Except for the absence of ASFV, which showed similar detectable test lines, the distinctive cleavage was only be observed in the presence of ASFV (Figure 4.5A). These results were confirmed by detectable peak intensities and areas (Figure 5BC). The co-incubation of the prementioned strains with ASFV showed no test lines as a result of reporter trans-cleavage (Figure S4.3).

Figure 4. 5 Selectivity assay using different strains.

Biosensor images with test and control lines responses corresponding to the subjected 10^4 cfu/ml strains.

4.3.4 The application of CRISPR/Cas-LFB assay in real samples

A total of 6 available blood samples with 4 ASFV-positive and 2 ASFV-negative were confirmed by PCR (Figure S4.2) and examined blindly using CRISPR/Cas-LFB assay (Figure 4.5). As shown in Figure 4.5, no detectable test line was observed from the positive samples, while a clear test line was detected in negative samples (Figure 4.6a), indicating the high specificity of our biosensor. This activity was also confirmed using PCR amplification, which corroborated with our assay (Figure S4.2).

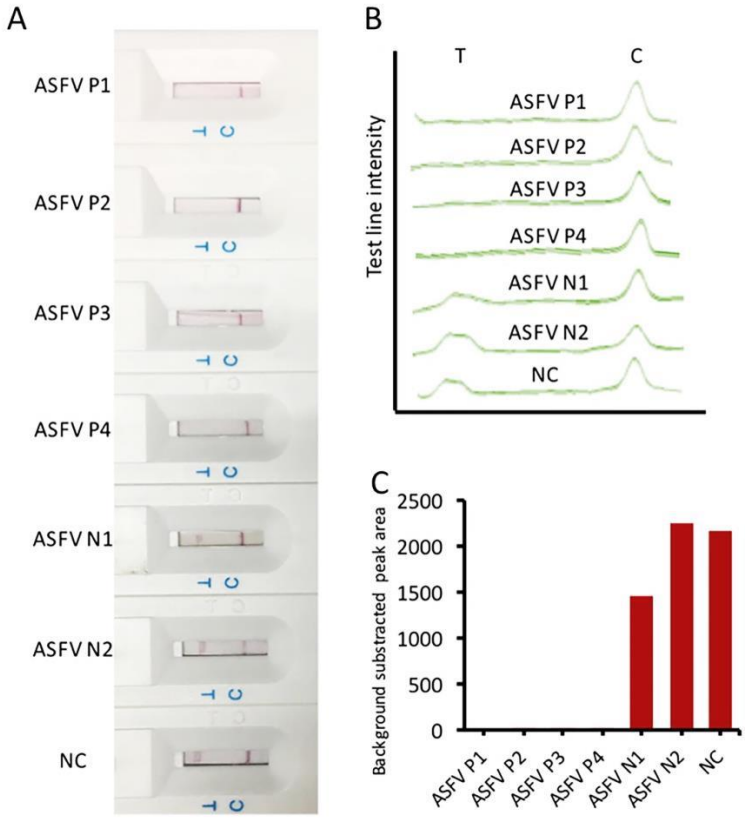

Figure 4. 6 Clinical samples testing.

(A) LFB responses for the positive (ASFV P1-P4) and negative (ASFV N1-N2) clinical samples. (B) Test and control line signal intensities. (C) bar chart of the LFB test lines in (A,B). NC stands for negative control (water).

In conclusion, we have shown **t**he early detection of ASFV as is crucial for early control, monitoring and treatment. Traditional detection methods such as ELISA and PCR based

methods have been utilized, but they are still laborious, costly, and non-deployable. Nucleic acids isothermal amplification methods are currently promising in the rapid detection of ASFV. Nevertheless, carry-over cross-contamination, tedious gel electrophoresis analysis and toxic dyes still pose difficulties. The currently developed CRISPR-Cas based detection systems promised potential diagnosis of broad range nucleic acids (Chen et al., 2018a; Gootenberg et al., 2018; Li et al., 2018a; Myhrvold et al., 2018; Li et al., 2018b; Gootenberg et al., 2017). However, all these approaches employed expensive fluorescence based apparatuses or monoclonal antibody-based lateral flow biosensors. Our developed approach is a readily, inexpensive and universal lateral flow biosensor for the detection of ASFV and other infectious diseases. By targeting the conserved region of VP73 genes in 7 different ASFV strains (Agüero et al., 2003) with PCR amplification specific primers and Cas12a based biosensor, we unambiguously identified ASFV in blood samples with no false positive results or expensive apparatuses, indicating the applicability of our technique. Our CRISPR/Cas-LFB method can detect around a thousand copies per µl in less than 2 hours, which is comparable to the existing traditional methods and CRISPR-Cas diagnostics (Chen et al., 2018a; Gootenberg et al., 2018; Li et al., 2018b). Most importantly, our designed probe-based biosensor is universal for any singleplex CRISPR-Cas detection. Although PCR is mature and commonly used, it could hinder the on-site application of this assay in resource-limited areas; thus, isothemal amplification can be integrated. Besides, a multiplexing biosensor can also be designed to detect more targets simultaneously by using their specific reaction components.

Chapter 5: A rapid and sensitive CRISPR/Cas12a based Lateral flow biosensor for the accurate detection of Epstein-Barr virus

5.1 Introduction

EBV, also known as human herpesvirus IV belongs to a lymphofollicular virus of Herpesviridae family. EBV is the first oncovirus discovered, and its infection rate remains high, with serological positives up to 90% of the population. serological positives up to 90% of the population.(Smatti et al., 2018) EBV infection is associated with NPC, Hodgkin's lymphoma, Burkitts, lymphoma, gastric cancer, and other malignant tumors.(Chou et al., 2008) According to the International Agency for Research on cancer, EBV is a class 1 carcinogen.(Niedobitek et al., 2001) It is closely related to NPC, which is one of the most common multiple malignant tumors with high incidence worldwide.(Wu et al., 2018) Early-stage NPC is more sensitive to radiotherapy up to 91%.(Hu et al., 2017b) However, due to the hidden location of NPC, the symptoms are difficult to distinguish from other benign diseases; thus, most middle and late-stage NPC can be diagnosed. Therefore, early detection of the causative agent is an effective way to improve the treatment of NPC and other EBV related diseases.

The most common methods for detection EBV are enzyme-linked immunosorbent assay (ELISA) (Cai et al., 2018) and polymerase chain reaction (PCR).(van Beek et al., 2002) ELISA is labor-intensive and time-consuming because of multiple steps and long incubation time. Moreover, though it detects EBV-antibodies in the blood, sometimes false-positive may occur. While, PCR provides high specificity, sensitivity, efficiency, however often requires more steps of laborious gel electrophoresis and analysis, and remains susceptible to cross-contamination.

To overcome these drawbacks, most currently, diagnostics with CRISPR/Cas system have been developed. For example, DETECTR,(Chen et al., 2018c) SHERLOCK,(Gootenberg et al., 2018; Gootenberg et al., 2017) and HOLMES (Li et al., 2018a; Li et al., 2018b) detection systems rely on collateral cleavage of target and any single nucleic acid (reporter). In the presence of the target, fluorescence signals were detected upon CRISPR/Cas system trans-cleavage of the fluorophore-quencher labeled reporter. To increase the sensitivity, the target gene sequence was amplified by the specific amplification method,

where HOLMES used PCR, while the rest employed RPA. Although these approaches were sensitive and specific, their reliance on fluorescent apparatus increases cost and time, and are inconvenient for resource-limited areas. Therefore, the development of DNA-probe based LFBs could be an alternative approach for sensitive, specific, and inexpensive detection.

Lateral flow biosensor (LFB) is a biosensor that can analyze the results with naked eyes. (Wu et al., 2015c; Fang et al., 2014c) Its structure mainly includes five parts: sample pad, conjugate pad, nitrocellulose membrane, and absorb pad assembled on a plastic backing pad. It has the advantages of simple operation, high sensitivity and specificity and low cost. Hence, it has been widely used in clinical diagnosis, virus detection and environmental monitoring.

In this study, we present a CRISPR/Cas system based universal LFB for the detection of EBV-DNA. The LFB principle is that, in the presence of EBV-DNA target, the *lachnospiraceae bacterium* Cas12a (LbaCas12a) cleaves an ssDNA reporter and the target collaterally, and the trans-cleaved ssDNA reporter cannot bind to a complementary DNA immobilized to the LFB test line; while the presence of test line indicates the absence of target (Figure 5.1). Based on the PCR pre-amplification and specific crRNA design, the LFB detected EBV-DNA successfully with high sensitivity and uncompromised specificity, respectively. This assay displays great promise in practical applications for the detection of infectious diseases.

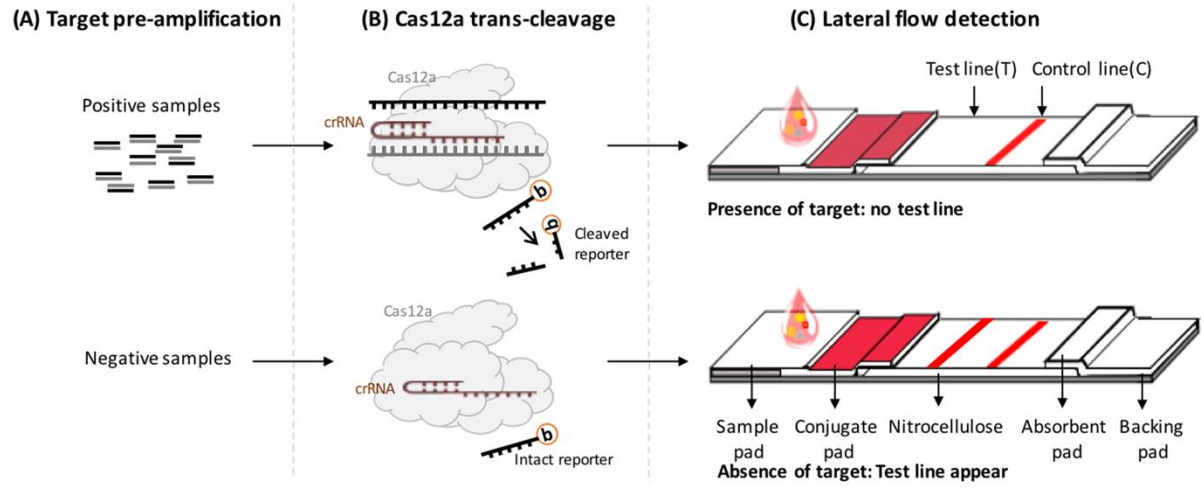

Figure 5. 1 Schematic representation of the CRISPR based LFB for EBV detection**.**

(A) Genomic DNA extraction from samples and PCR pre-amplification. (B) Cas12a reaction using the PCR product. (C) The product in (B) is loaded to LFB, where the positive samples exhibit no test line as a result of reporter transcleavage, while negative ones display a test line.

5.2 Material and methods

5.2.1 Reagents and chemicals

All oligonucleotides, including EBV specific target sequence, primers, crRNAs (designed using benching), reporters, and LFB capture probes were synthesized by Sangon Biotech (Shanghai, China) (Table 5.1). Other materials were from the same source as mentioned in previous chapters.

5.2.2 Construction of LFB and LFB detection of reporter sequences

AuNP synthesis/characterization, conjugation, and LFB assembling is similar to as pre-mentioned material and methods (Figure 2.2).

5.2.3 Target DNA design, cloning and amplification

EBV-DNA sequence was cloned into a customized pUC57 vector, and the recombinant plasmid was used as a model for PCR amplification, and CRISPR/Cas12a reaction. For PCR amplification, 25 µl PCR premix was composed of 0.3 µM forward and reversed primers, 12.5 µl 1× rTaq Premix, 1-2 µl of extracted genomic DNA (200 ng) and ddH_2O was added to final reaction volume. The reaction mixture was run in a thermocycler for 45 min with 95 ◦C, 5 min for denaturation; 95 ◦C, 10 sec for each cycle; 62 ◦C, 10 sec for annealing; 72 ◦C, 30 sec for elongation; 35 cycles. PCR products were analyzed using 2.5 % agarose gel electrophoresis.

5.2.4 Target cleavage assay

Cas12a cleavage assay was carried out according to the previous method with slight modifications. Briefly, Cas12a-crRNA complex was preassembled as in previous sections, and added 2 µl EBV target DNA/spiked or DNA extacted clinical samples, and then added nuclease-free water to final reaction volume of 25 µl. Finally, the reaction was incubated at 37 ◦C and analyzed using LFB after adding 35 µl ddH_2O water prior to sample pad loading. For fluorescence analysis of trans-cleavage reaction was perfoemed as prementioned.

5.2.5 LFB detection of reporter sequences

Prior to sample analysis, 11 bases biotinylated reporter (5'–biotin-TTTTTTTTATT-3') were used in the Cas12a cleavage assay, which in absence of cleavage can hybridize with 38 bases capture probe (AATAAAAAAAAAAAAAAAAATAAAAAAAAAAAAAA) immobilized on the LFB test line. For the LFB analysis of reporter cleavage after Cas12a reaction, 25 µl of the reaction was mixed with 35 µl of ddH_2O then loaded to the sample pad. After 5 min, the biosensor was read using a portable LFB reader. The peak area intensities of the test lines were plotted after LFB photo-analysis using Image J (NIH Research Services, US), which provided similar intensities between each analyzed triplicate. Excellent performance of Cas12a cleavage was considered positive when the reporter sequence was entirely *trans*-cleaved by Cas12a (no test line signal), and the control line containing the biotinylated rabbit polyclonal anti-IgG antibody captured the excess of AuNP-SA complex from the conjugate pad (Fig. 5.1).

5.2.6 EBV plasmid spiked and clinical samples preparation and analysis

EBV-negative/positive serum samples were used in our assay. Two hundred µl of each negative sample was spiked with different concentrations of EBV-DNA containing plasmid then subjected to using the whole blood genome extraction kit. The EBV-DNA from frozen clinical serum samples were similary extracted without pretreatment. Two µl of each extracted DNA was subjected to PCR and then applied to Cas12a cleavage assay, as mentioned above.

Table 5. 1 Oligonucleotide sequences used in this study [a, b]

Oligonucleotide	**Sequence (5'-3')**
Reporter (8TATT)	B-TTTTTTTTATT
Test line capture probe	AATAAAAAAAAAAAAAAAAATAAAAAAAAAAAAAAA
EBV DNA	TGGAAACCCGTCACTCTCAGTAATTCCCTCGAATCCCTACC AGGAACAACTGTCAGACACTCCATTAATTCCACTAACAATC TTTGTTGGGGAAAACACGGGGGTGCCCCCACCACTCCCACC ACCCCCCCCACCACCACCCCCACCACCCCCACCACCCCCAC

	CACCCCCACCACCCCCACCACCTCCACCACCTTCACCACCA
	CCCCCGCCCCCACCACCCCCACCACCTCAGCGCAGGGATGC
	CTGGACACAAGAGCCATCACCTCTTGATAGGGATCCGCTA
	GGATATGATGTCGGGCATGGACCTCTAGCATCTGCTATGCG
	AATGCTTTGGATGGCTAATTATATTGTAAGACAATCACGGG
	GTGACCGGGGCCTTATGTTGCCACAAGGCCCACAAACAGC
	CCCTCAGGCCAGGTTGGTACAGCCACATGTCCCCCCTCTAC
	GCCCGACAGCACCCACCATTTT**GTCACCTCTGTCACGACC**
	GAGGCTTACCCCTCCACAACCACTCACGA
Forward primer	CCACCTCCACCACCTT
Reverse primer	TCGTGAGTGGTTGTGGA
crRNA	UAAUUUCUACUAAGUGUAGAU**GUCACCUCUGUCACGAC**
	CGAGGCU
Activator	AGCACCCACCATTTT**GTCACCTCTG**

B stands for 5'biotinylation.

[a] Underline represents reporter capture probe sequence (repeated twice).

[b] Bold represents crRNA targeting sequence

5.3. Results and discussion

5.3.1 Establishment of CRISPR based LFB biosensor for EBV detection

The CRISPR/Cas12a based LFB is orchestrated by two main components: i) ssDNA reporter, that is trans-cleaved by Cas12a and provide a signal upon target recognition, and ii) LFB probes immobilized on the LFB test line to capture reporter. Therefore, as previously repoted(Mukama et al., 2020), reporters and probes of different lengths of bases were used to monitor reporter trans-cleavage (Table 5.1). On the LFB, the biotinylated reporter binds to AuNPs-SA complex at the conjugate pad and migrates to hybridize with its complimentary test-line probes. As shown in Figure 5.2A, weak test lines were detected when 100 nM of 11 bases reporter (8TATT) dissolved in double distilled water was applied to LFB with a similar length probe on the test line. The increase of test line probe to 38 bases detected strongly 11 bases reporter. Therefore, 11 base reporters were used as Cas12a substrate to obtain no test line upon transcleavage, while the full-length ssDNA reporters hybridized with test-line

probes in the absence of transcleavage. We furthermore tested different concentrations of the optimized reporter (25, 50, 100 nM) on the LFB (Figure S1). The test line was detected at a reporter concentration above 10 nM, which became prominent with a subsequent increase in concentration (Figure S1). Fifty nM concentration provided a strong test line in the absence of the target, and non-detectable test line signal in the presence of the target (Figure 2B). The concentration of 50 nM and the reporter length 11 bases were then used for subsequent Cas12a cleavage experiments.

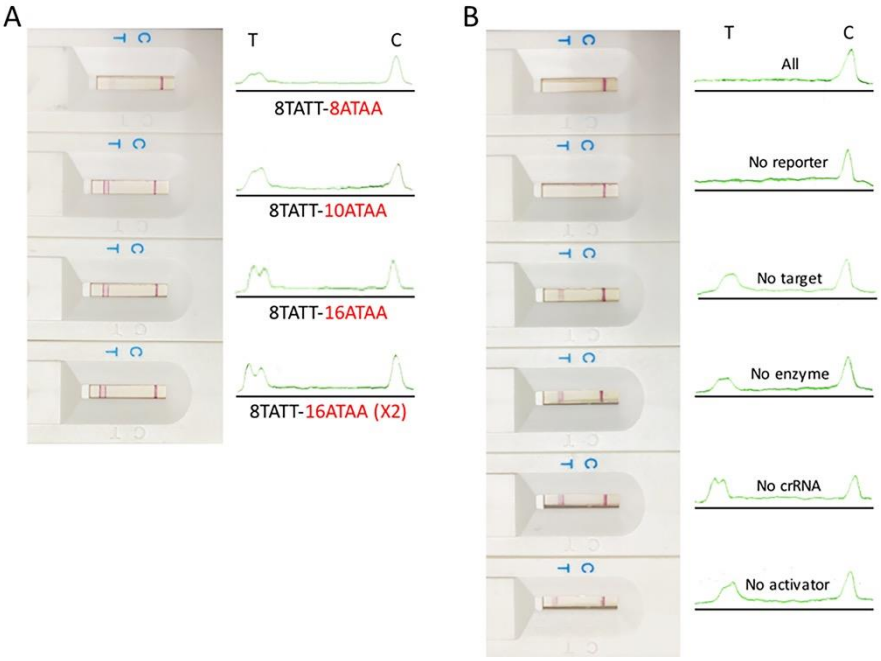

Figure 5. 2 Reporter length optimization and controls for CRISPR based LFB.

(A) LFB images (left) and intensity chromatograms (right) corresponding to 100 nM reporter (8TATT, in black) subjected to different lengths of test line probes immobilized on the test line (in red). (B) LFB images of the CRISPR based LFB for EB detection in the presence of its all reaction components (All) or absence of one component.

5.3.2 Sensitivity of the biosensor for EBV detection

The sensitivity of the biosensor was assessed using different concentrations of serially diluted EBV recombinant plasmid (7.1×10^{-9}, 7.1×10^{-10}, 7.1×10^{-11}, 7.1×10^{-12}, 7.1×10^{-13}, 7.1×10^{-14}, 7.1×10^{-15}, 7.1×10^{-16} M) applied to CRISPR based LFB with and without PCR pre-amplification. There was no detectable test line at 7.1×10^{-14} M, and above for PCR pre-amplified target plasmid (45 min), while strong test lines were observable at $\leq 7.1\times10^{-15}$

M (Fig. 5.3, S2). Without PCR pre-amplification, our assay detected 7.1×10^{-9} M alone (Fig. S3). The result suggested that the developed LFB had high sensitivity for EBV testing. Although this sensitivity is less than previously reported isothermal amplification-based CRISPR diagnostics(Gootenberg et al., 2018; Chen et al., 2018c) and nested PCR(Chan et al., 2001), it is still comparable to PCR based CRISPR approaches.(Li et al., 2018a; Li et al., 2018b; Ai et al., 2019). However, our assay was accomplished without tedious gel electrophoresis, sophisticated PCR, or fluorescence reader apparatuses, reducing susceptibility to false positive that can be generated from fluorescence background. Not withstanding that in future one can combine our LFB with other pre-amplification methods such as RPA, LAMP etc. to enhance the sensitivity to single copy of EBV DNA.

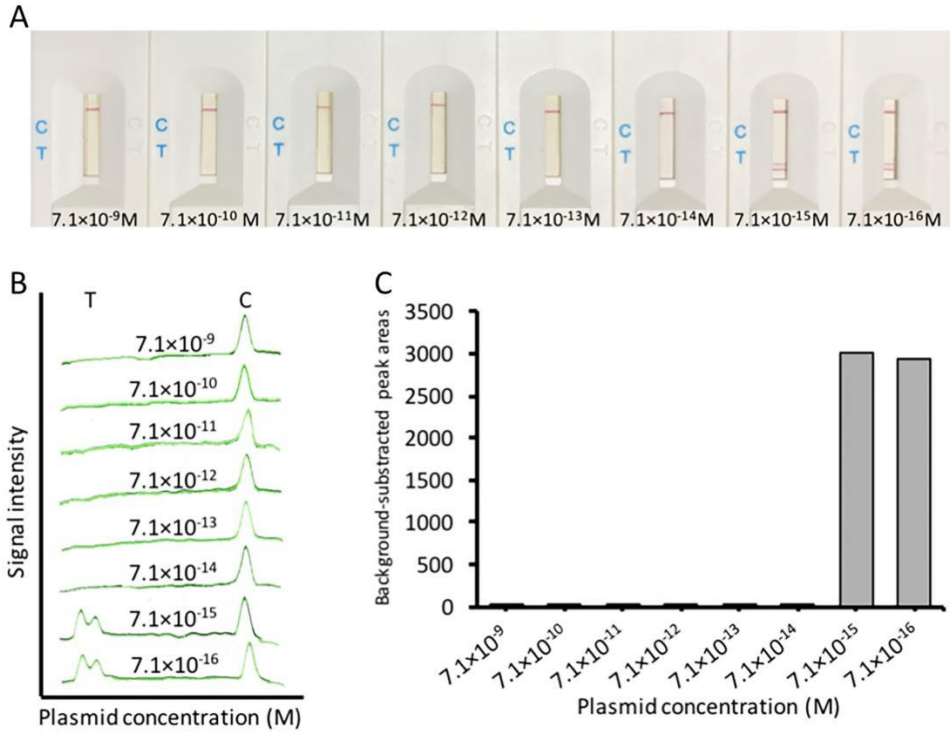

Figure 5. 3 Sensitivity of the CRISPR based LFB assay.

(A) From left to right, the concentration of EBV recombinant plasmid subjected to PCR and then to CRISPR based LFB. (B) Peak intensities corresponding to the LFB in (A). (C) Calculated peak areas corresponding to the LFB test lines in (A).

5.3.3 Clinical sample and selectivity of the biosensor for EBV detection.

EBV can cohabits with other microbiome both in the bloodstream, other body fluids such as saliva, and even can spread via objects or human interaction(Limeres Posse et al., 2017). Thus, the selectivity of the sensor was tested using various bacteria strains (*Streptococcus sp.*,

P. aeruginosa, *S. typhi*, *E. coli*, *S. aureus*), 10 EBV negative serum, 1 available EBV positive serum and EBV recombinant plasmid as a positive control (EBV). Fig. 4A shows the typical photo images of the biosensor. Except for the absence of EBV, which showed similar detectable test lines, the distinctive cleavage was only be observed in the presence of EBV (Fig. 4A). These results were confirmed by detected peak intensities and areas (Fig. 4BC).

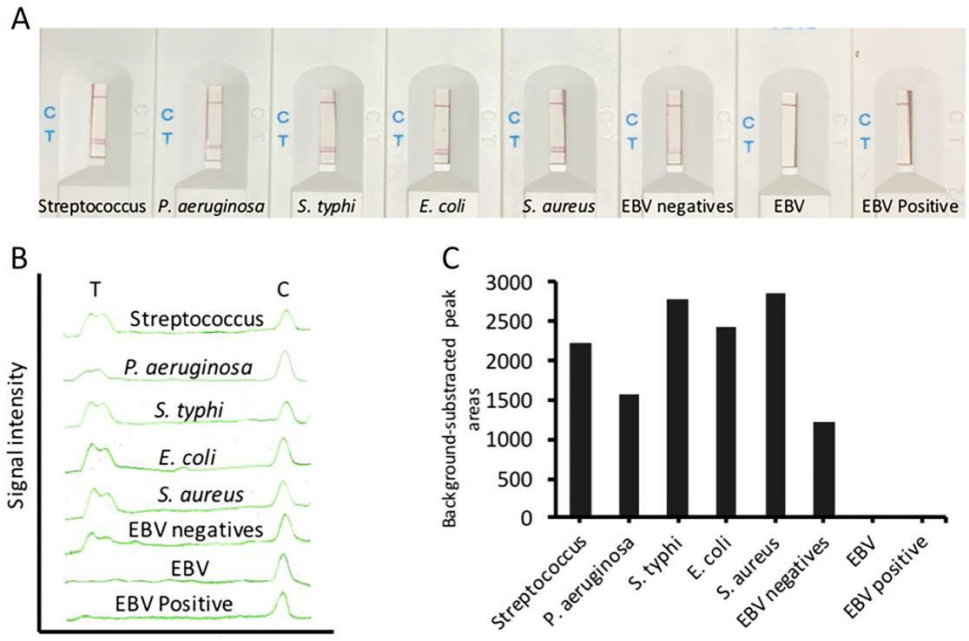

Figure 5. 4 Specificity of the CRISPR based LFB.

(A) LFB images (left) and intensity chromatograms (right) corresponding to human DNA, different bacteria strains (10^4 cfu/ml), EBV recombinant plasmid (EBV), and clinical samples. (B) Peak intensities corresponding to the LFB in (A). (C) Calculated peak areas corresponding to the LFB test lines in (A).

In summary, a lateral flow biosensor based on CRISPR-Cas12a combined with PCR was successfully constructed for the detection of EBV. CRISPR-Cas12a provided high specificity derived from its crRNA, while the use of LFB made the assay fast, simple and inexpensive in avoiding gel electrophoresis processes, which reduced in part cross-contamination. The short period of PCR pre-amplification enriched the target and improved the LFB sensitivity, which is higher than the stand-alone PCR. The high corroboration of PCR and CRISPR based LFB demonstrated also a high specificity as shown in both EBV recombinant plasmid, clinical samples, and various bacteria. Our established CRISPR based LFB could be applied to the on-site diagnosis of infectious diseases by using their specific gRNAs and the introduction of isothermal amplification approaches.

Chapter 6: Lateral flow aptasensor for the sensitive and specific detection of human osteopontin

6.1 Introduction

OPN protein is considered as a bridge between bones and blood owing to its localization in tissues and biological fluids (Haylock and Nilsson, 2006). As one of the matricellular proteins, OPN has multiple functional domains regulating various physiological and pathological mechanisms (Das et al., 2003). OPN is involved in several cellular and extracellular processes such as cell adhesion (Reinholt et al., 1990), apoptosis, inflammation (Takahashi et al., 2004), and diseases (Strom et al., 2004; Bautista et al., 1996) especially cancer (Das et al., 2003; Teramoto et al., 2005; Wai and Kuo, 2004). Extensive studies have associated OPN with tumor progression, metastasis and aggravation due to its overexpression in the lung (Hu et al., 2005), breast (Bramwell et al., 2014a), colon (He et al., 2012; Zhao et al., 2015b), liver (Gotoh et al., 2002; Lorena et al., 2006), oral cavity and solid organ (Zhao et al., 2018). As a potential cancer biomarker, its targeted suppression has also gained significant attention in prevention and alternation of tumor growth as well as metastasis (Lorena et al., 2006; Rittling et al., 2014; Mi et al., 2009). Therefore, the rapid determination of OPN level is crucial in biomedicine researches, cancer prognosis, and sepsis (Vaschetto et al., 2008).

Aptamer-based approaches can target OPN for cancer diagnosis (Meirinho et al., 2017) and therapy (Mi et al., 2009). Currently, detection methods such as electrochemical aptasensors (Meirinho et al., 2017, 2014) and Enzyme-linked immunosorbent assay (ELISA) (Chakraborty et al., 2018a) are alternatives to high-performance liquid chromatography (HPLC) (Saad et al., 2008; Lenton et al., 2017), surface plasmon resonance (SPR), and spectrometry analytical methods (Christensen et al., 2010; Chen et al., 2014), etc. and they are sensitive. However, these assays remain tedious and require complicated procedures and apparatuses. For instance, the electrochemical aptasensor can achieve a good quantification and detection limit of 1.3 ± 0.1 nM for OPN (Meirinho et al., 2017); however, its aptamer immobilization on the electrodes is time-consuming and could be susceptible to interference with other proteins (El-Din Bessa et al., 2010). Moreover, available ELISA-based detection methods are highly sensitive for OPN but are still apparatus-dependent and tedious

(Chakraborty et al., 2018a; Bramwell et al., 2014b). Thus, these bottlenecks impede their on-site applications.

LFB is an ideal platform for the rapid detection of various targets, including cancer biomarkers (Baryeh et al., 2017; Huang et al., 2017; Mukama et al., 2017). LFB integrates four main parts: sample, conjugate, and absorbent pads, and a nitrocellulose membrane, which can detect analytes in one-step, rapidly and inexpensively (Sajid et al., 2015) (Figure 1). In recent years, various methods such as SPR, LFB, electrochemical assays have been combined with nanoparticles and streptavidin (SA)-biotin chemistry to achieve ultrasensitive detection of different targets (Guo et al., 2015; Kim et al., 2017; Oh et al., 2017). Besides, based on nanoparticle conjugated to DNA probes and antibody, we have previously developed highly sensitive and specific LFBs for the detection of proteins (Fang et al., 2011), stem cells and bacteria (Wu et al., 2015c; Fang et al., 2014c). However, the direct linkage of aptamers to nanoparticles such as gold nanoparticles (AuNPs) could suffer from steric hindrance, complex fractal aggregation, nucleotide preference, and longer reaction time (Kalra et al., 2018a; D'Agata et al., 2017).

In this chapter, we show a highly sensitive and specific LFB for rapid detection of OPN that relies on a unique property of the combination of single anti-OPN antibody and aptamer. A biotinylated aptamer was used to capture OPN and react rapidly and strongly with AuNPs-SA complex on the conjugate pad. The resulting complex was subsequently captured at the test line by OPN-specific antibody within 5 minutes (Figure 6.1). Thus, this developed biosensor for OPN determination provides a great promise in cancer prognosis.

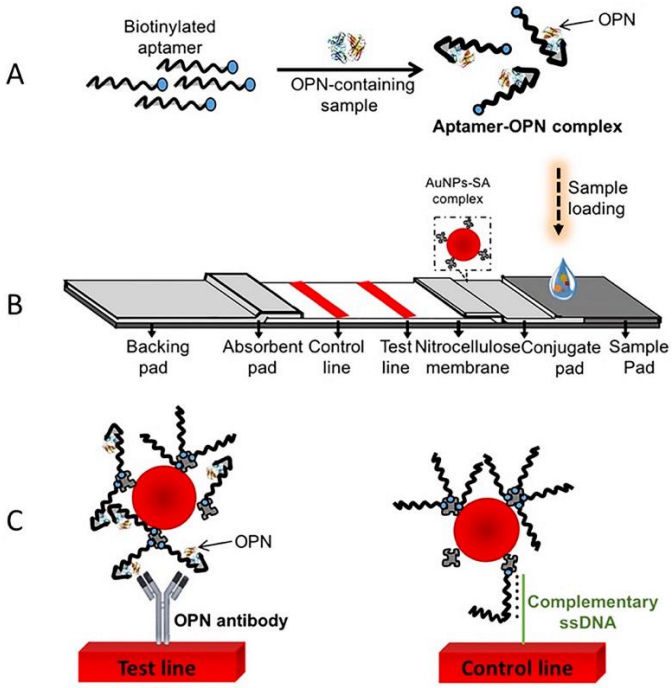

Figure 6. 1 Illustrative scheme of the OPN LFB.

(A) The biotinylated aptamer was incubated with OPN-containing samples to obtain a stable aptamer-OPN complex and applied on the sample pad (reversed arrow). (B) The OPN LFB assembly with AuNPs-SA on the conjugate pad, immobilized OPN antibody and a probe complementary to the aptamer on the nitrocellulose membrane. (C) OPN-aptamer complex containing samples subjected to the LFB sample pad flow and react with AuNPs-SA on the conjugate pad, then subsequently captured by the anti-OPN antibody at the test line. Then, the excess biotinylated OPN aptamers are captured by the partially complementary ssDNA probes immobilized on the control line.

6.2 Materials and methods

6.2.1 Materials

Human recombinant OPN protein expressed in HEK 293 cell lines, rabbit polyclonal/monoclonal anti-OPN were purchased from Abcam (Shanghai, China), and anti-rabbit secondary antibody (with HRP) was purchased from Bioroyee (Beijing, China). DNA probe and aptamer were synthesized by Sangon (Shanghai, China). Human serum albumin (HSA), bovine serum albumin (BSA), ovum albumin (OVA), thrombin, trisodium

citrate, $HAuCl_4.3H_2O$, and SA were purchased from Sigma–Aldrich (Steinheim, Germany). Absorbent and fiberglass papers and nitrocellulose membranes were purchased from Millipore (Billerica, Massachusetts). Dispenser for antibody, conjugates and probes immobilization and a paper strip cutter were purchased from Shanghai Kinbio (Shanghai, China). A portable strip reader is from Goldbio Technology Co. (Shanghai, China). All buffer solutions were prepared in our lab. Other reagents of high analytical grade and purity were obtained from other commercial sources.

6.2.2 Preparation of AuNPs and its conjugates

AuNPs of 15 nm average diameter were prepared by citrate reduction method as previously described (Fang et al., 2011) with slight modifications. Briefly, 350 mL of 1 mM aqueous gold chloride solution ($HAuCl_4$) was boiled and continuously stirred in a flask, followed by subsequent addition of 3.5 mL of 1% sodium citrate solution. The resulting colorless solution turned to a wine red-like color after 10 minutes boiling. The solution was then cooled at room temperature to form AuNPs and subsequently kept at 4 ◦C until use.

AuNPs–SA conjugate was prepared according to (D'Agata et al., 2017) with some modifications. Briefly, 1 mL of the prepared AuNPs solution was collected and concentrated in multiple of two by centrifugation (12000 rpm, 25 min). The resulted AuNPs red pellets were resuspended in 1 mL double distilled water (ddH_2O), and subsequently mixed with 6 µL of K_2CO_3 (0.1 M in ddH_2O) and 10 µL of SA (50 µg mL^{-1} in 10 mM phosphate-buffered saline (PBS). The solution was gently shaken for 3 hours at room temperature and then centrifuged at 12000 rpm, 25 min. The AuNPs-SA complex was resuspended in 100 µL of suspension buffer (0.1% NaN_3, 0.25% Tween-20, 5% BSA, 10% sucrose, and 20 mM Na_3PO_4), and then dispensed on the conjugate pad.

Furthermore, different LFBs were constructed using different concentrations of the AuNPs–SA conjugates by applying 200 ng mL^{-1} of OPN-containing samples (Salem, 2013). The six-times concentrated AuNPs were used for further experiments because they displayed a stable sensitivity and peak areas and tested, as shown in Figure S6.1.

6.2.3 Construction of lateral flow biosensor

The recognition molecules were immobilized on LFB as previously reported (Fang et al., 2011) with slight modifications as follows. 30 µL of both rabbit polyclonal anti-OPN (0.7 mg mL^{-1}) and ssDNA capture probe 5'-AAAAAAAAAAAAAAAATAAAAAAAAAA AAAAAAAATA A-3' (50 µM) were dispensed on the nitrocellulose membrane of the strip

(25 mm in width) using a LFB dispenser to form a test and control zone, respectively. The membrane was then dried at room temperature for 12 h and stored at 4 ◦C until use.

To assemble the detection strip, a fiberglass sample pad (16 mm in width) was immersed in sample pad buffer (1% Triton, 1% BSA, 2% glucose, 50 mM boric acid, pH 8.0), dried and then stored at low-humidity room temperature. The conjugate and absorbent pads (6mm and 17 mm in width, respectively) were used without buffer treatment. As shown in Figure 6.1b, all pads were sequentially assembled along the adhesive part of the nitrocellulose membrane with an overlap of 2 mm and then cut into 0.4 cm-wide strips.

6.2.4 Lateral flow biosensor detection of OPN protein

Prior to sample analysis, biotinylated aptamer (5'–biotin-TGTGTGCGGCACTCCA GTCTGTTACGCCGC**TTTTTTTTTATTTT**-3') were used. This aptamer is linked to biotin at the 5' and extended at the 3'-end with TsATs (bolded), a sequence complementary to the control line of the LFB. To detect OPN by the LFB, an optimized biotinylated aptamer of 20 µL (1µM) was selected from a wide range of concentrations (Figure S6.2). The aptamers were diluted in aptamer binding (AB) buffer (10 mM Tris (pH 7.5), 150 mM NaCl, 1 mM $MgCl_2$, 1 mM dithiothreitol (DTT), and 4% glycerol), heat-treated at 95 ◦C for 2 min, and then chilled on ice for 5 min. The aliquots were incubated with 20 µL of different concentrations of purified OPN, OPN-spiked or clinical samples within the AB buffer. The mixtures were then incubated for 30-60 minutes with gentle agitation (500 rpm) at 25 ◦C (Figure S6.2). Then, 20 µL of the loading buffer (150 mM NaCl, 20 mM Tris–HCl (pH 8.0)) was mixed with samples prior for subsequent loading to the LFB sample pad. After 5 minutes, the LFB was read using a portable LFB reader and peak intensities were analyzed using ImageJ (NIH Research Services, US), which provided peak areas for plotting and sensitivity calculation as described previously (Fang et al., 2019; Toley et al., 2015). Clinical breast cancer patient and normal serum samples were collected from the biological sample bank of Central South University. The normal serum was used to prepare a batch of six different concentrations of OPN-spiked serum and heated serum (50 ◦C, 30 min).

6.2.5 Statistical analysis

Each result presented is the mean ± SE of the triplicate samples from three independent experiments. Student's T-test was performed using Excel and the differences between samples were considered significant at $*p < 0.05$ or $**p < 0.01$.

6.3 Results and discussion

6.3.1 Principle of the OPN lateral flow for detection

AuNPs was conjugated to SA and then dispensed on a conjugate pad. The OPN antibody and an ssDNA probe complementary to one part of the biotin-labeled aptamer sequence were dispensed at the test and control zone of the nitrocellulose membrane, respectively. OPN containing samples incubated with biotinylated aptamer results in aptamer-OPN complex samples (Figure 6.1). Upon loading samples on the LFB, the OPN was captured on the LFB by the AuNPs-SA complex on the conjugated pad and subsequently by an anti-OPN antibody immobilized at the test line, generating visible red lines (Figure 6.1c). The semi-quantitation was analyzed using a portable strip reader that provided the plotted test lines' intensities responding to the concentration of OPN in purified OPN and OPN-spiked serum. Furthermore, the reproducibility of the assay was assessed by analysis of each sample three times at last twice.

6.3.2 Sensitivity of the OPN lateral flow biosensor

OPN overexpresses in cancer patients ranging from 100 to 336 (or 495) ng mL^{-1} in serum and plasma (Vaschetto et al., 2008; Bache et al., 2010), and this dramatic increase is related with tumor progression and severity (Salem, 2013; Simão et al., 2015). However, recent reports show that plasma OPN levels is associated with poor cancer prognosis (El-Din Bessa et al., 2010). Therefore, to investigate the sensitivity of the LFB, different concentrations of commercial OPN (0, 0.01, 0.1, 1, 10, 50, 100, 500 ng mL^{-1}), as well as OPN-spiked serum were subjected to the LFB. As shown in Figure 6.2a, no positive result was observed in the controls. The purified OPN higher than 0.01 ng mL^{-1} displayed a red test line optical response on the LFB within 5 minutes. The test line directly correlated with the concentration of OPN with a detection as low as 0.1 ng mL^{-1} (Figure 6.2b). Consistently, the band intensities of the test lines increased with the concentration of OPN with linear relationship between peak areas and OPN concentration in tested range of 0-500 ng mL^{-1} and the R^2 value was 0.89 (Figure 6.2c). The calculated mean peak areas from imageJ of each test line loaded with 3 controls (0 ng mL^{-1}) was 7.3±0.5, which was used to calculate the sensitivity according to LOD = Mean (M) + 3* standard deviation (SD) (Fang et al., 2019; Toley et al., 2015). The calculated LOD value of 8.8 ng mL^{-1} was then taken into the equation y= 332.74x - 780.87 to obtain an approximate LOD concentration of 11.1 ng mL^{-1}. Notably, the sensitivity of the

LFB was confirmed by SDS-PAGE, which was less sensitive but showed a similar trend of band intensity that changed with the loaded concentrations of OPN (Figure S6.3).

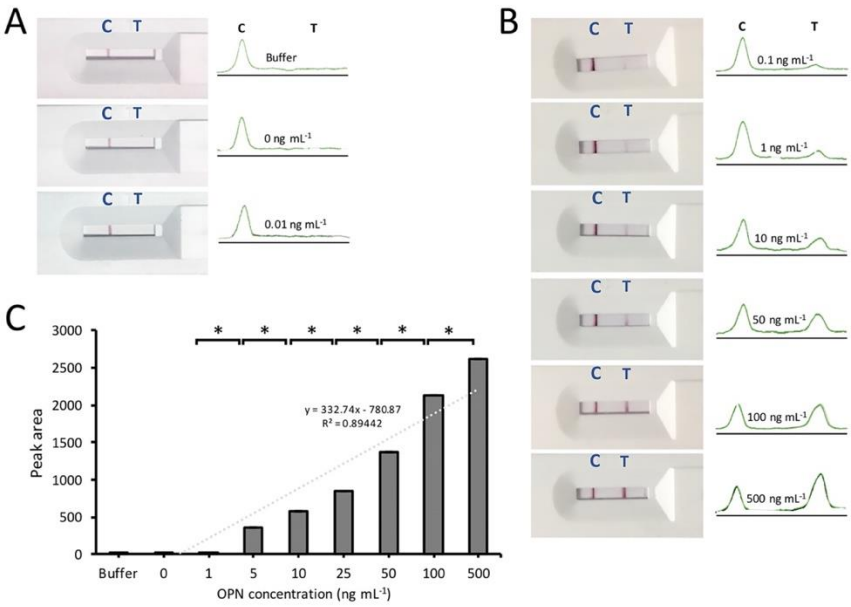

Figure 6. 2 (AB) Side-by-side analysis of LFB images (left) and corresponding intensities (right) loaded with buffer and different concentrations of purified OPN (0, 0.1, 1, 10, 50, 100, 500 ng mL^{-1}).

(C) LFB portable reader peaks corresponding to the LFB test line intensities at different concentrations of purified OPN. The peak areas of the LFB test lines of the purified OPN in (A) were calculated and plotted. Data presented are the mean ± SE of three independent samples. (*$p < 0.05$, **$p < 0.01$; n=3).

The sensitivity of our biosensor was confirmed using serum spiked with different concentrations of OPN (0, 5, 10, 50, 100, 500 ng mL^{-1}). As shown in Figure 6.3A, this LFB detected as low as 10 ng mL^{-1} in spiked serum with visible detection bands from 10-500 ng mL^{-1}, and the corresponding peak areas are shown in Figure 3B. The LOD was calculated as previously described, which provided an estimated LOD concentration of 10.3 ng mL^{-1} according to the equation y= 571.01x - 893.01. This sensitivity was obtained within 5 minutes, and is much faster than previously reported methods for OPN detection (Meirinho et al., 2014; Chakraborty et al., 2018b). Though less than 5 ng mL^{-1} OPN were not recovered, the LFB met the cut-off values for OPN biomarker-based cancer detection (El-Din Bessa et al., 2010; Simão et al., 2015; Zhao et al., 2012). We furthermore validated the assay by conventional ELISA according to the antibodies' source[1] using the serum samples spiked with OPN. As expected, the absorbance increased with increasing the amount of OPN in

spiked serum samples (Figure 6.3C), and the trend was similar to that of the LFB test lines (Figure 6.3A). The resulting plots of both our LFB and ELISA showed a linear relationship between plots and the spiked OPN concentrations of 0.91 and 0.94, respectively. Although the conventional ELISA showed higher sensitivity, our method met the cut-off level with a much fast performance (within 5 minutes) than ELISA (>2 hours) and other methods for OPN detection (Chakraborty et al., 2018a).

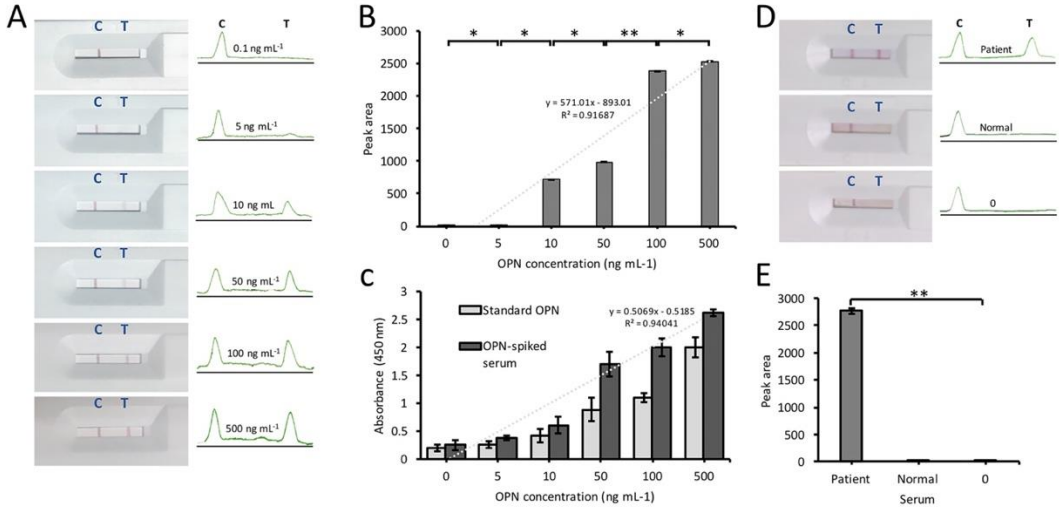

Figure 6. 3 Biosensor sensitivity for OPN concentrations spiked in serum and clinical samples.

(A) From top down is the gradual increase of the test line intensity respective to the applied concentrations of OPN and clinical samples. (B) The peak areas of the LFB test lines in (A) corresponding to the concentrations of OPN spiked in the serum. (C) Conventional ELISA detection for the purified OPN (standard OPN) and OPN-spiked serum. (D) Photo images (left) and corresponding intensities (right) of the biosensors loaded with clinical serum. (E) The peak areas of the LFB test lines in (D) corresponding to serum samples of breast cancer patient, normal people and buffer (0). Data presented are the mean ± SE of three independent samples. (*$p < 0.05$, **$p < 0.01$; n=3).

Finally, our essay was validated using clinical breast cancer serum and normal samples. As shown in Figure 6.3 d, e; no detectable test line was observed from normal people, while a visible red line was observed at the test line in a breast cancer patient. This activity was also confirmed using ELISA, which showed a similar trend as our biosensor but slightly increased

signals in the normal sample (Figure S6.4). This robust performance of our LFB could be attributed to the stable reaction between AuNPs and biotinylated aptamer through SA-biotin linkage on the conjugate pad. Distinct from our previous finding (Fang et al., 2011), this LFB was leveraged to use an inbuilt conjugate pad containing AuNPs-SA complex, allowing direct loading of samples without pretreatment with AuNPs-biotinylated aptamer complex. Thus, this method does not require the storage of AuNPs conjugates, which could cause aggregation or dissociation of the complex. Moreover, this linkage is stable and doesn't depend on nucleotide base contents of affinity probes, as for direct linkage of DNA probes to AuNPs have more affinity to adenine and cytosine than thymine (Kalra et al., 2018b). Furthermore, apart from fluorescent dyes, the usage of AuNPs enabled the visualization of the results by naked eye. Nevertheless, further assays from various and additional cancer patient's serum samples would be indispensable to validate the proposed LFB. Thus, it may be useful for rapid and reliable on-site diagnosis of other biomarkers.

6.3.3 Specificity of the OPN lateral flow biosensor

This LFB showed high specificity towards various interfering compounds, including OVA, BSA, HSA, thrombin, and heated serum. The interference test was performed using 200 µg of interfering proteins dissolved in PBS/serum. The red test line was only observed in the OPN spiked solution, rather than in the non-target proteins and heated serum (Figure 6.4A). Consistently, a detectable peak was only observed in the OPN containing solutions (Figure 6.4B).

As OPN is found in various complex body fluids such as blood (Razmi et al., 2018; Chang et al., 2008), we furthermore investigated the interference of other components using OPN spiked with the same interfering proteins in serum. As shown in Figure 6.5A, the red test line was observed in all OPN-interferants spiked serum, and the corresponding peak areas test lines signals are shown in Figure 6.5C. The results suggest that only OPN was pre-captured by the aptamer, and visually detected after binding to the OPN antibody on the LFB test line. This LFB performance showed no observable interference of serum components on the test line, thus discounting steric hindrance as found in electrochemical aptasensors for OPN (Meirinho et al., 2017). The specificity of this LFB can be attributed to two main reasons: one is the AuNPs-SA complex that captures OPN-Aptamer complex through biotin-SA reaction within a short time of conjugation, and another factor could be the

OPN antibody specificity immobilized on the test line. Thus, OPN is captured by both aptamers and its antibody, offering a dual specificity.

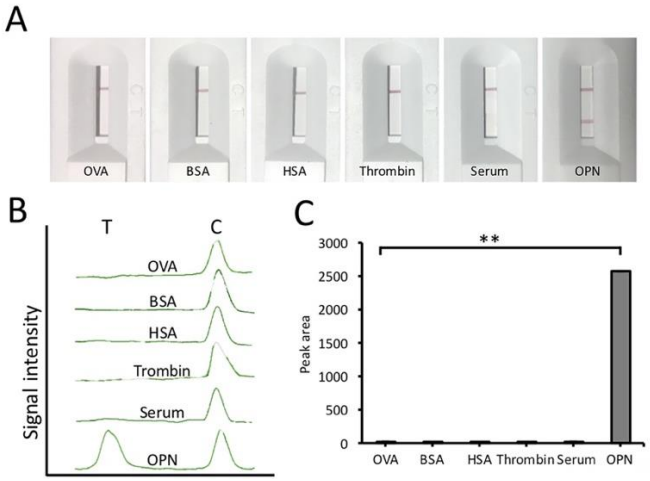

Figure 6. 4 (A) Side-by-side analysis of LFB images loaded with interfering proteins such as OVA, BSA, HSA, thrombin, serum dissolved in PBS and heated serum containing 200 ng mL^{-1} purified OPN solutions.

(B) Portable LFB reader peak intensities corresponding to different concentrations of interfering proteins in PBS and purified OPN on the test line. (C) The peak areas of the LFB test lines in (A) were measured and plotted. The absence of OPN and usage of heated serum generated neither test line nor a peak. Data presented are the mean ± SE of three independent samples. (*$p < 0.05$, **$p < 0.01$; n=3).

Noteworthy, OPN possesses multiple sites of post-translational modification and cleavage (Razzouk et al., 2002). OPN is prone to be cleaved, in particular, by thrombin, which is detected in high level (360-611 nM) in cancer patients with different tumor sites and stages; and monitored patients undergoing treatment (surgery, chemotherapy, radiotherapy) presented lower concentrations (Ay et al., 2011). Thus, patients with cancer are at high risk of developing venous thromboembolism (an increase of thrombin), with a hazard ratio of the continuous peak thrombin are given per 100 nM increase. Interestingly, the biosensor was challenged with additional concentrations of thrombin in OPN/serum and the interferant proteins, retained the actual activity (Figure 6.5A). However, weak test line signals were observed at higher concentrations of thrombin (Figure 6.5B, C). The specificity of the LFB was maintained because the used anti-OPN targets peptide corresponding to human OPN amino acid ^{170}CKSKKFRRPDIQYPD^{183} rather than at thrombin cleavage site ^{160}R and ^{169}S. Of main interest, thrombin couldn't interfere significantly with the OPN aptamer owing to its specific

targeting of the OPN N-terminal (Meirinho et al., 2017). Thus, this assay could be important for sepsis, intensive care unit setting, and emergency departments as it is quick, easy, and reliable for osteopontin quantitation.

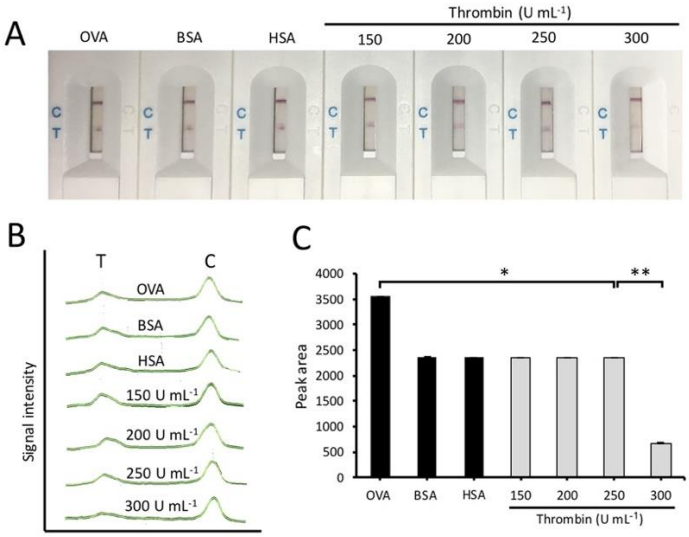

Figure 6. 5 (A) The reaction mixture of 200 ng mL^{-1} purified OPN solutions mixed with interfering proteins such as OVA, BSA, HSA, and thrombin within the heated serum.

(B) Portable LFB reader peaks on the test line corresponding to detectable OPN in the presence of interferants. (C) The peak areas of the LFB test lines in (A) were measured and plotted. Data presented are the mean ± SE of three independent samples. (*$p < 0.05$, **$p < 0.01$; n=3).

In conclusion, a simple, rapid, sensitive, and highly specific biosensor was developed for human osteopontin (OPN) detection. The biosensor successfully detected both purified OPN and OPN-spiked complex samples such as serum. Compared with other available OPN methods such as ELISA (Chakraborty et al., 2018a) and electrochemical biosensor (Meirinho et al., 2017). It is reasonable to conclude that this biosensor is of low cost, straightforward, simple to use, and provides a fast-visual detection response within 5 min. In addition, it is highly specific given that no background was obtained on the test line in the presence of interfering proteins, which can be explained by the pre-binding of aptamer on the target OPN and the specific OPN antibody fixed on the test line. Our biosensor can be employed for qualitative and semi-quantitative detection of OPN in simple and complex samples such as serum. More importantly, the developed method can be used to detect rapidly and conveniently several other biomarkers by replacing target recognition elements (antibody, aptamer, etc.).

Chapter 7: General conclusion, key innovation and recommendation

7.1 General conclusion

This work demonstrated a novel CRISPR/Cas12a/b based LFB for the detection of Human papilloma virus and *Pseudomonas aeruginosa*. The concept of this approach is a non-detectable test line on the LFB when Cas12 collaterally cleaves cognate target and ssDNA reporter sequences. By integrating LAMP amplification of target DNA to the CRISPR/Cas system, we developed a CRISPR/Cas and loop-mediated Isothermal Amplification (CIA) based LFB, which achieved high specificity and a single copy sensitivity for LAMP based CRISPR detection assays, and ~ thousands copies for PCR preamplification based reactions. Our system is robust because it doesn't require traditional DNA/RNA extraction, post product analysis like gel electrophoresis/instruments analysis, difficulty in multi-looped band analysis, use of toxic dyes, longer amplification time, and is less prone to carryover contamination. Moreover, our CIALFB is simple, portable, cheaper, and background-free compared with previously reported CRISPR-Cas based approaches that require expensive antibodies, reverse transcriptase (Gootenberg et al., 2018; Myhrvold et al., 2018), fluorescence detection apparatuses (Chen et al., 2018a; Li et al., 2018a). Furthermore, CIALFB is highly reproducible, rapid, and inexpensive with a cost below $0.5 per test and is applicable both in pure and complex samples. Notwithstanding that CRISPR-based techniques for ASFV and EBV detection using required PCR-preamplification, which increased cost due to the thermocycler. In addition, CRISPR-based diagnosis may display some promiscuous or no trans-cleavage; thus, thorough buffer and activator optimization are of great importance. In the future, it could be programmable and multiplexed for point-of care detection of other pathogens, SNPs and genotyping by using specific crRNA(s) and necessary amplification reagents such as primers, and reverse transcriptase (for RNA detection).

Furthermore, we developed the rapid determination of human osteopontin (OPN) protein, a potential cancer biomarker, which holds substantial promise for point-of-care diagnostics and biomedical applications. We showed that the most reported platforms for OPN detection are apparatus-dependent, time-consuming, and expensive. Our established lateral flow biosensor (LFB) for OPN detection achieved as low as 0.1 ng mL^{-1} OPN sensitivity with a good dynamic detection between 10-500 ng mL^{-1} within 5 minutes. Intriguingly, the LFB allowed a qualitative and semi-quantitative detection of OPN in serum at clinically cut-off

levels as in cancer patients, and can discriminate OPN from interfering proteins with high specificity. Thus, it is a promising alterative approach for point-of-care OPN screening and detection.

7.2 Key innovation

Our study demonstrated that nucleic acids can be detected rapidly, inexpensively and accurately. Apart from developing diagnostics with CRISPR-Cas system, the established universal biosensor that can be used for in vitro study of Cas enzyme trans-cleavage.

7.3 Recommendation

We use our CIALFB system to detect viruses and bacteria. The future work could be useful for SNPs detection, since its applicability have been reported by previous fluorescence based detection.

Supplementary data

Supplementary data (HPV)

Table S2. 1 Reporter and capture probe sequences involved in this study.

Name	Sequence (5'-3')	Label
Bio-2T-A-2T	TTATT	/5'6-Biotin
Bio-3T-A-2T	TTTATT	/5'6-Biotin
Bio-4T-A-2T	TTTTATT	/5'6-Biotin
Bio-5T-A-2T	TTTTTATT	/5'6-Biotin
Bio-6T-A-2T	TTTTTTATT	/5'6-Biotin
Bio-7T-A-2T	TTTTTTTATT	/5'6-Biotin
Bio-8T-A-2T**	TTTTTTTTATT	/5'6-Biotin
8T-A-2T-FQ**	TTTTTTTTATT	/5'6-FAM/3'-TAMRA
Bio-9T-A-2T	TTTTTTTTTATT	/5'6-Biotin
Bio-10T-A-2T	TTTTTTTTTTATT	/5'6-Biotin

**Optimum reporter sequences with efficient collateral cleavage activity and response on the LFB. Red stands for poly-T extension of reporter.

Table S2. 2 Capture probes of reporters immobilized on the LFB test line.

Name	Sequence (3'-5')
3A-T-2A	AAATAAAAATAA
4A-T-2A	AAAATAAAAATAA
5A-T-2A	AAAAATAAAAAATAA
6A-T-2A	AAAAAATAAAAAAATAA
7A-T-2A	AAAAAAATAAAAAAAATAA
8A-T-2A	AAAAAAAATAAAAAAAAATAA
9A-T-2A	AAAAAAAAATAAAAAAAAAATAA
10A-T-2A	AAAAAAAAAATAAAAAAAAAAATAA
16A-T-2A***	AAAAAAAAAAAAAAAATAAAAAAAAAAAAAAAATAA

Capture probe sequence in blue was repeated twice and immobilized on the LFB test line.

*** Corresponds to the optimum capture probe used in this study.

Table S2. 3 Target sequences involved in this study for HPV16 and HPV18.

Oligonucleotide	Sequence (5'-3')	Reference
HPV16 cloned DNA	GTTCCTAAAGTATCAGGATTACAATACAGGGTATTTAG AATACATTTACCTGACCCCAATAAGTTTGGTTTTCCTG ACACCTCATTTTATAATCCAGATACACAGCGGCTGGTT TGGGCCTGTGTAGGTGTTGAGGTAGGTCGTGGTCAGC CATTAGGTGTGGGCATTAGTGGCCATCCTTTATTAAAT AAATTGGATGACACAGAAAATGCTAGTGCTTATGCAG CAAATGCAGGTGTGGATAATAGAGAATGTATATCTATG GATTACAAACAAACACAATTGTGTTTAATTGGTTGCA AACCACCTATAGGGGAACACTGGGGCAAAGGATCCC CATGTACCAATGTTGCAGTAAATCCAGGTGATTGTCC ACCATTAGAGTTAATAAACACAGTTATTCAGGATGGT GATATGGTTGATACTGGCTTTGGTGCTATGGAC**TTTAC** **TACATTACAGGCTAACAAA**AGTGAAGTTCCACTGGA TATTTGTACATCTA	This study
HPV18 cloned DNA	GATGACACTGAAAGTTCCCATGCCGCCACGTCTAATG TTTCTGAGGACGTTAGGGACAATGTGTCTGTAGATTAT AAGCAGACACAGTTATGTATTTTGGGCTGTGCCCCTG CTATTGGGGAACACTGGGCTAAAGGCACTGCTTGTAA ATCGCGTCCTTTATCACAGGGCGATTGCCCCCCTTTAG AACTTAAAAACACAGTTTTGGAAGATGGTGATATGGT AGATACTGGATATGGTGCCATGGAC**TTTAGTACATTG** **CAAGATACTAAA**TGTGAGGTACCATTGGATATTTGTC AGTCTATTTGTAAATATCCTGATTATTTACAAATGTCTG CAGATCCTTATGGGGATTCCATGTTTTTTTGCTTACGG CGTGAGCAGCTTTTTGCTAGGCATTTTTGGAATAGAG CAGGTACTATGGGTGACACTGTGCCTCAATCCTTATAT ATTAAAGGCACAGGTATGCGTGCTTCACCTGGCAGCT GTGTGTATTCTC	

[a] Underline bold sequence represents PAM region.
[b] Bold represents crRNA targeting sequences.

Table S2. 4 1-20 mutations in pUC57-HPV16 cloned DNA (red letter (s)).

1	……...GCTATGGACTTTaCTACATTACAGGCTAACAAAAGTGAA…….
2	……..GCTATGGACTTTAcTACATTACAGGCTAACAAAAGTGAA…….
3	……...GCTATGGACTTTACtACATTACAGGCTAACAAAAGTGAA…….
4	……...GCTATGGACTTTACTaCATTACAGGCTAACAAAAGTGAA…….
5	……...GCTATGGACTTTACTAcATTACAGGCTAACAAAAGTGAA…….
6	……...GCTATGGACTTTACTACaTTACAGGCTAACAAAAGTGAA…….
7/8	…...……GCTATGGACTTTACTACAtTACAGGCTAACAAAAGTGAA…….
8	……...GCTATGGACTTTACTACATTaCAGGCTAACAAAAGTGAA…….
10	……...GCTATGGACTTTACTACATTAcAGGCTAACAAAAGTGAA…….
11	……..…GCTATGGACTTTACTACATTACaGGCTAACAAAAGTGAA…….
12/13	……..…GCTATGGACTTTACTACATTACAgGCTAACAAAAGTGAA…….
14	……..…GCTATGGACTTTACTACATTACAGGcTAACAAAAGTGAA…….
15	……..…GCTATGGACTTTACTACATTACAGGCtAACAAAAGTGAA…….
16/17	……..…GCTATGGACTTTACTACATTACAGGCTaACAAAAGTGAA…….
18	……..…GCTATGGACTTTACTACATTACAGGCTAAcAAAAGTGAA…….
19	……..…GCTATGGACTTTACTACATTACAGGCTAACaAAAGTGAA…….
20	……..…GCTATGGACTTTACTACATTACAGGCTAACAaAAGTGAA…….
-PAM	……..GCTATGGAC t t t ACTACATTACAGGCTAACAAAAGTGAA…….

Figure S2. 1 10 % SDS-PAGE gel of the commercial human LbaCas12a (left) and our purified AaCas12b (right) enzymes ran using gel filtration fractions.

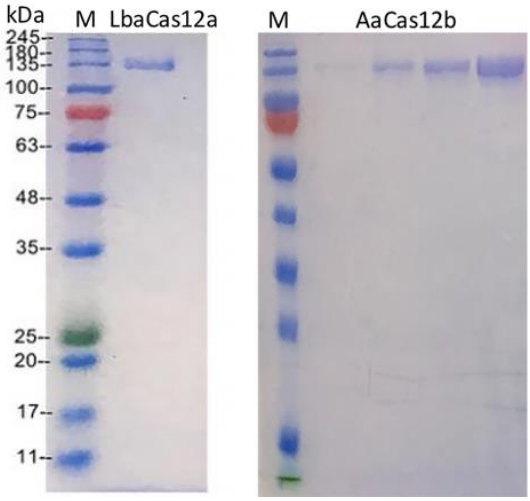

Supplementary data (*P. aeruginosa*)

Table S3. 1 Sequences involved in this study for *P. aeruginosa*.

Name	Sequence (5'-3')
Target dsDNA (*P. aeruginosa* acyltransferase)	CAAGGCACCGGCGCGGCTGGTGCGGCTGAGTCTGAGCGGG GAGGATGTCGGGCGCGCACGTTTTC**CCTTCGCTGAGCACG CTGCGCGCG**TCGCCTACGTGAATGCGCTGTTCGATGCGTTG GCCGAAGGCAACCCGCGGGTGAGCGTGCTCGACCCCTCCA GCGTGCTCTGCGATGGCCTGGATTGTTTCGCCGAACGTGAT GGCTGGTCGCTGTACATGGATAACAACCACCTTTCGACCCA GGGGGCCCATGAACTCGGGCCT
LAMP primers	
F3	TGGTGCGGCTGAGTCTGA
B3	GTCGAAAGGTGGTTGTTATCC
FIP(F1c+F2)	GCCAACGCATCGAACAGCTTTCCCTTCGCTGAGCAC
BIP(B1c+B2)	TCCAGCGTGCTCTGCGATGTACAGCGACCAGCCATC
PCR primers	
Forward	GTTTTCCCTTCGCTGAGCAC
Reverse	CGAAACAATCCAGGCCATCG
crRNA	UAAUUUCUACUAAGUGUAGAU**CCUUCGCUGAGCACGCU GCGCGCG**
Activator	GGCGCGCACGTTTTC**CCTTCGCTGA**

Underline indicates the PAM region. Bold characters represent a crRNA binding region and targeted PAM-proximal truncate sequence.

Figure S3. 1 Test line signal intensity depends on the length and concentration of reporters and capture probes.

(A) 100 nM reporter with various poly-Ts (number in red) was dissolved in water and loaded on the LFB to bind the corresponding poly-A capture probes (number in blue). (B) Peak area showing 9Ts and 10Ts reporter slight binding on peer capture probes. (C) LFB showing various reporters (3Ts-8Ts) binding to capture probes (10As and 16As) with an efficient binding of 8Ts to 16 As. (D) Peak area showing the optimized lengths of the reporter and capture probe. (E) Determination of the optimum concentration of 8Ts reporters on 16As capture probes.

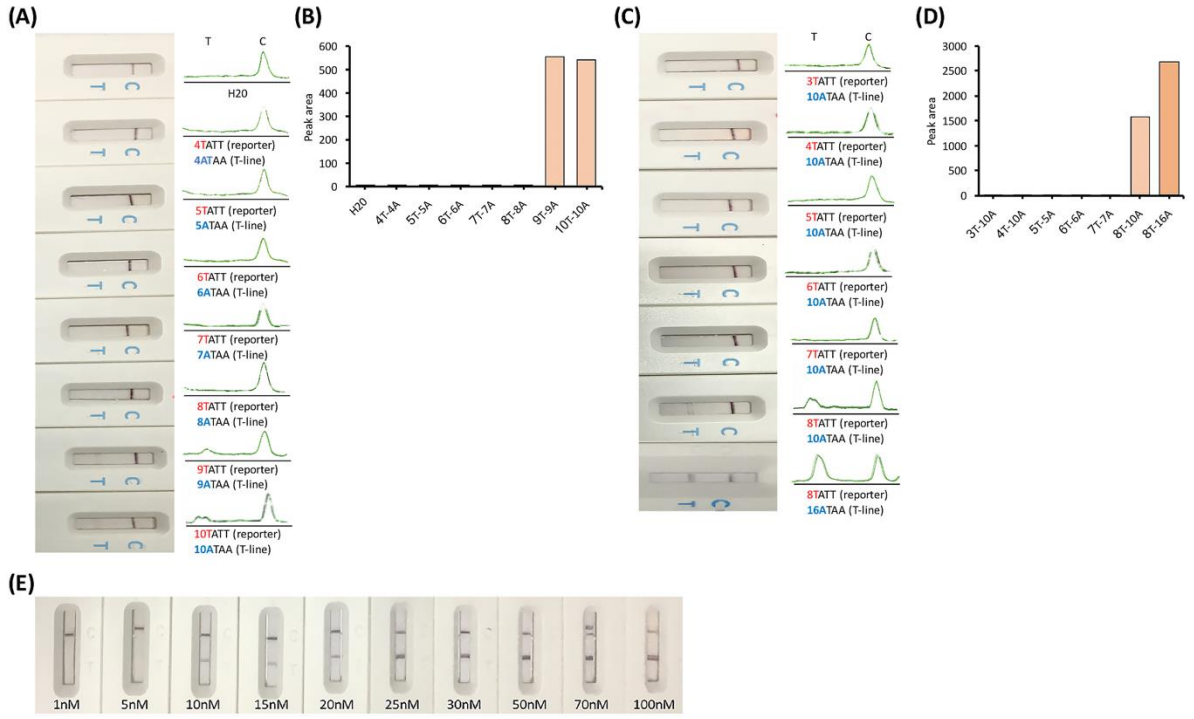

Figure S3. 2 CIALFB detection using LAMP amplified P. aeruginosa target sequence at various time points.

(A-D) CIALFB detection using 15 min LAMP amplification (A) and 30 min (C) with corresponding peak area intensities of the test lines (B, D). (E) Exclusion of activator or Cas12a-crRNA complex or target from the reaction mixture with reporter collateral cleavage. (F) The calculated peak areas corresponding to the test line signals in (E).

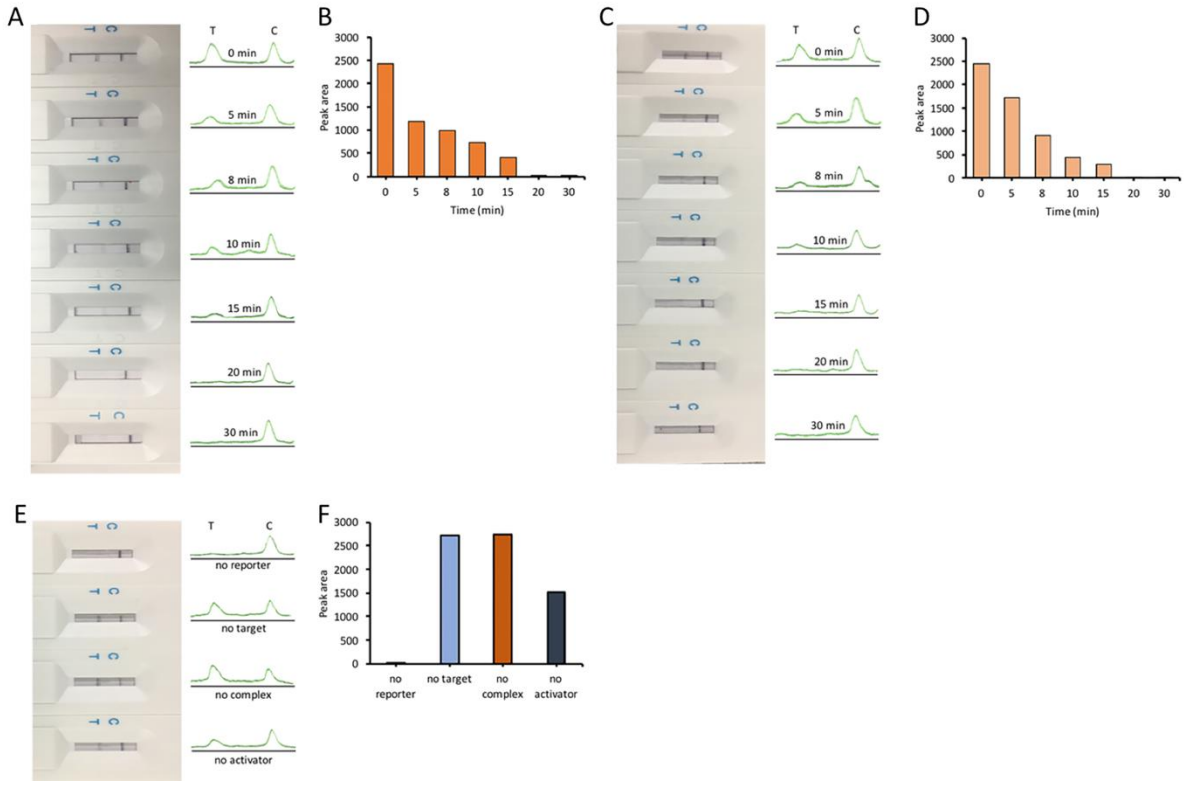

Figure S3. 3 High-fidelity CIALFB and fluorescence detection at different concentrations of cloned *P. aeruginosa* acetyltransferase sequence containing plasmid and clinical samples.

(A) LFB detection with different CIA reaction time (0 to 30 min) and 5 min readout using 1 cfu/ml of the target bacteria (as described in the methods section). (B) Fluorescence detection of different concentrations of cognate bacteria using FAM-TAMRA labeled reporter. (C) Standard PCR for clinical samples. Lanes P1-P4 correspond to positive samples; Lanes N1-N5 correspond to negative samples; Lane PC corresponds to the positive control (recombinant plasmid DNA) and NC is the negative control (ddH_2O), and M is a 1kb marker.

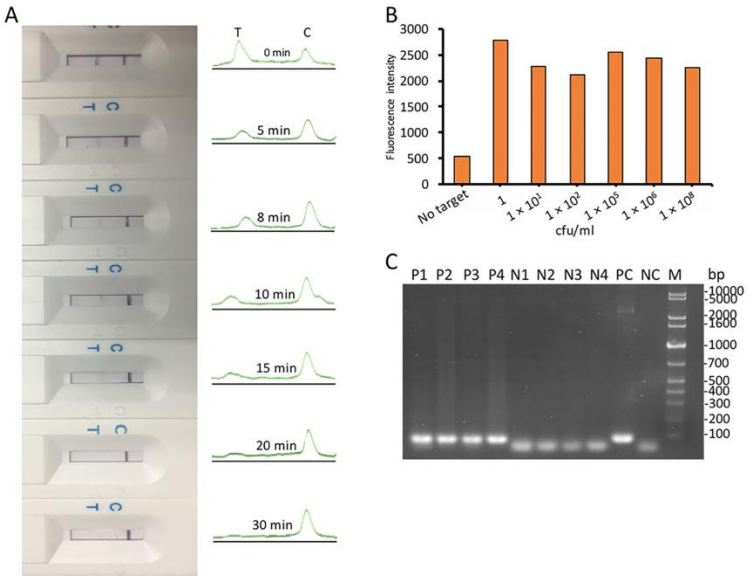

Figure S3. 4 High temperature inhibits CIALFB by using Cas12a in a one-pot reaction.

(A) LFB detection of 3.4 aM *P. aeruginosa* template at different temperatures and their corresponding signal intensities. (B) Peak area intensities of the test lines based on the magnitude of Cas12a trans-cleavage.

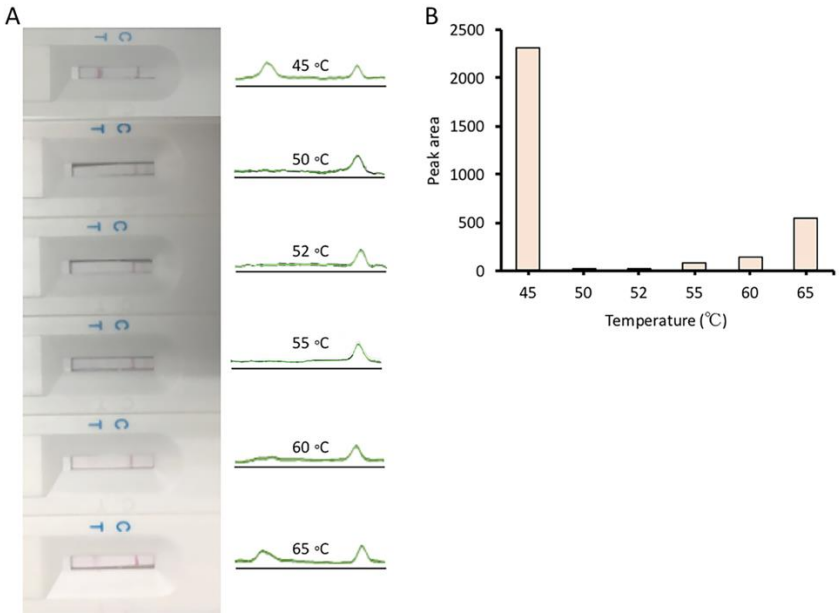

Supplementary data (ASFV)

Figure S4. 1 Sensitivity assay using different concentrations of recombinant plasmids (ng/μl).

M stands for 1kb marker, while red is the sensitivity achieved by CRISPR/Cas-LFB method.

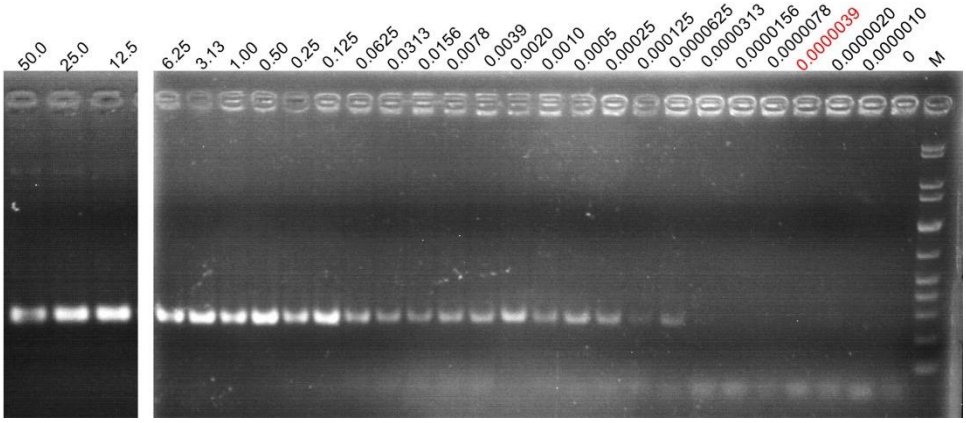

Figure S4. 2 PCR amplification confirmation of 6 ASFV clinical samples.

ASFV P1-P4: ASFV positives; ASFV P1-P2: ASFV negatives; NC: negative control; M: 1kb marker.

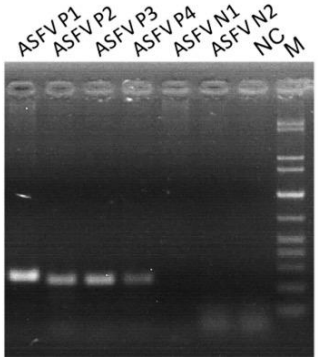

Figure S4. 3 Selectivity assay using different strains co-incubated with ASFV.

Biosensor images with test and control lines responses corresponding to the subjected 10^4 cfu/ml strains.

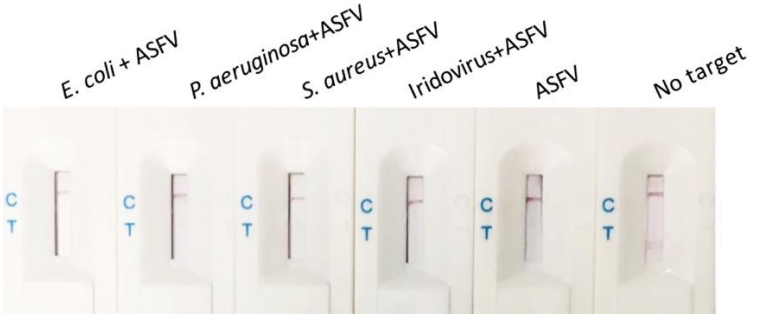

Supplementary data (EBV)

Figure S5. 1 Reporter concentration.

(A) LFB images of different reporter concentrations diluted in ddH_2O. (B) Calculated peak area intensities corresponding to LFB test line in (A).

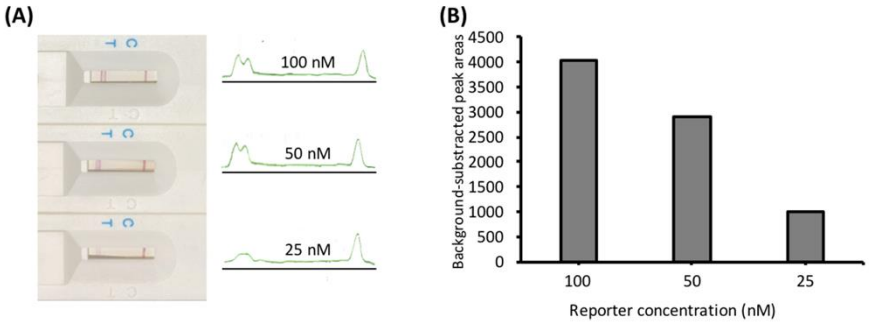

Fig. S5.2 Amplification of 2 µl EBV recombinant plasmid (40 ng/µl) and clinical serum samples.

Lanes 1-3 to positive control (PC), EBV positive sample (PS, arrow), 10 negative samples (NS1-10), respectively and lane M is 1-kb marker, respectively.

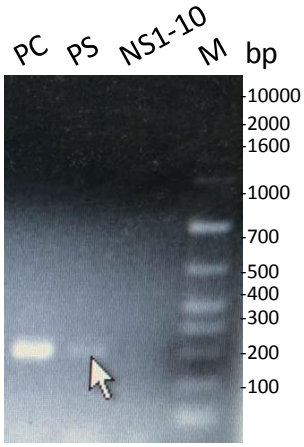

Figure S5.3 Sensitivity assay for the CRISPR based LFB without PCR pre-amplification. (A)

LFB images of different concentrations of EBV recombinant plasmid subjected to CRISPR/Cas12a. (B) Peak intensities corresponding to LFB test line (T) and control line (C) in figure (A). (C) Calculated peak area intensities corresponding to LFB test line in figure (A).

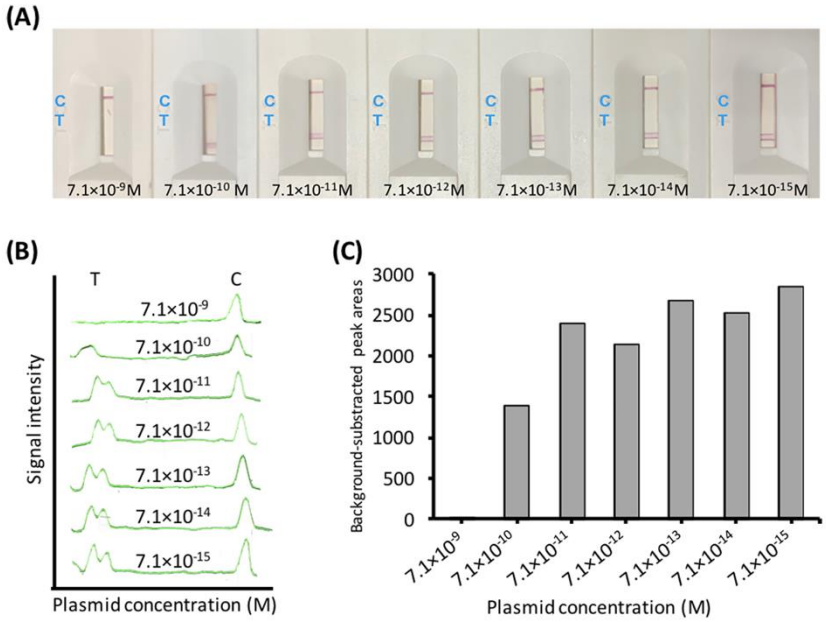

Supplementary data (Osteopontin apatasensor)

Figure S6. 1 Optimization of AuNPs concentration of the biosensor.

(A) The sensitivity increased proportionally with the increase of AuNPs from 6 to 10 times concentrated AuNPs. (B) Calculated peak areas corresponding to the concentrations of AuNPs on test line. *$p < 0.05$; **$p < 0.01$; NS, not significant; n=3.

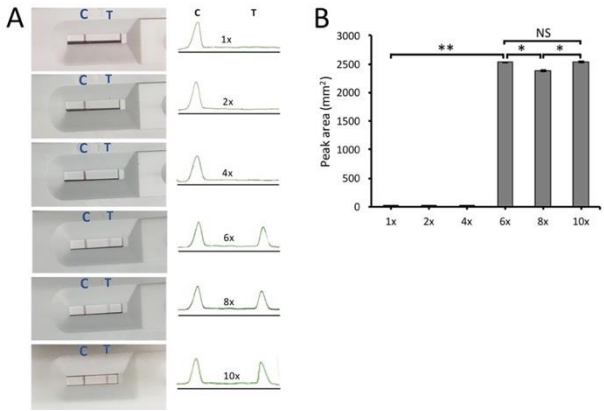

Figure S6. 2 Optimization of aptamer concentration for 200 ng mL^{-1} OPN detection and peak area of the test line.

(A) The sensitivity at different concentration of aptamers from 10 nM to 10 μM. (B) The sensitivity at different incubation time (10-90 min) of 1 μM aptamers.

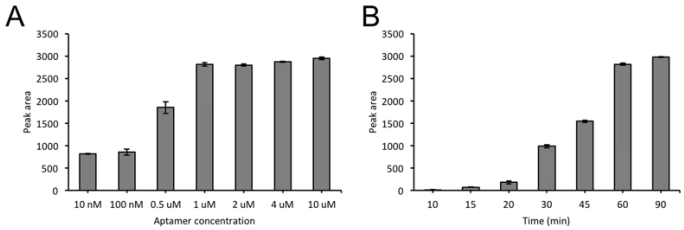

Figure S6. 3 SDS-PAGE analysis of the commercial human OPN protein at different concentrations (left) and anti-OPN antibody (right).

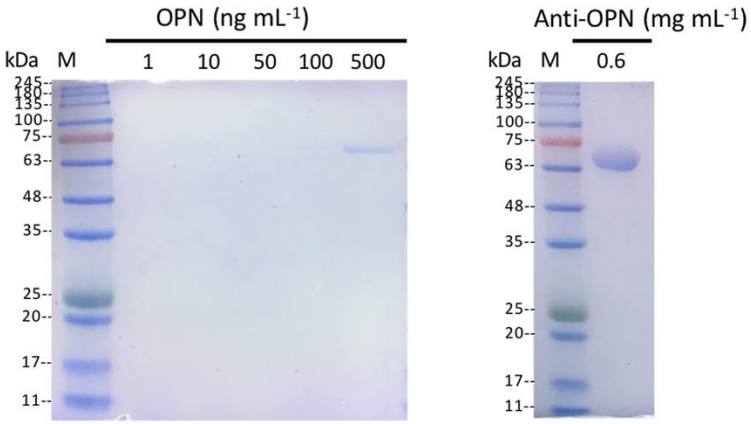

Figure S6. 4 ELISA for clinical serum from breast cancer patient and normal samples.

($p < 0.05$, $n = 3$).

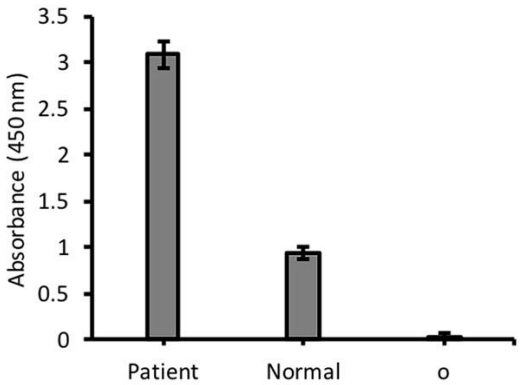

References

Barrangou R, Fremaux C, Deveau H, et al. CRISPR provides acquired resistance against viruses in prokaryotes [J]. Science, 2007, 315(5819): 1709-12.

Jinek M, Chylinski K, Fonfara I, et al. A programmable dual-RNA-guided DNA endonuclease in adaptive bacterial immunity [J]. Science, 2012, 337(6096): 816-21.

Jinek M, Jiang F, Taylor D W, et al. Structures of Cas9 endonucleases reveal RNA-mediated conformational activation [J]. Science, 2014, 343(6176): 1247997.

Tang Y, Fu Y. Class 2 CRISPR/Cas: an expanding biotechnology toolbox for and beyond genome editing [J]. Cell & Bioscience, 2018, 8(1): 59.

Ishino Y, Krupovic M, Forterre P. History of CRISPR-Cas from Encounter with a Mysterious Repeated Sequence to Genome Editing Technology [J]. Journal of bacteriology, 2018, 200(7):

Makarova K S, Haft D H, Barrangou R, et al. Evolution and classification of the CRISPR-Cas systems [J]. Nature reviews Microbiology, 2011, 9(6): 467-77.

Strecker J, Jones S, Koopal B, et al. Engineering of CRISPR-Cas12b for human genome editing [J]. Nature Communications, 2019, 10(1): 212.

Chen J S, Ma E, Harrington L B, et al. CRISPR-Cas12a target binding unleashes indiscriminate single-stranded DNase activity [J]. Science, 2018a, 360(6387): 436-9.

Gootenberg J S, Abudayyeh O O, Kellner M J, et al. Multiplexed and portable nucleic acid detection platform with Cas13, Cas12a, and Csm6 [J]. Science, 2018, 360(6387): 439-44.

Li L, Li S, Wang J. CRISPR-Cas12b-assisted nucleic acid detection platform [J]. bioRxiv, 2018a, 362889.

Myhrvold C, Freije C A, Gootenberg J S, et al. Field-deployable viral diagnostics using CRISPR-Cas13 [J]. Science, 2018, 360(6387): 444-8.

Li S Y, Cheng Q X, Wang J M, et al. CRISPR-Cas12a-assisted nucleic acid detection [J]. Cell discovery, 2018b, 4(20.

Notomi T, Okayama H, Masubuchi H, et al. Loop-mediated isothermal amplification of DNA [J]. Nucleic Acids Research, 2000a, 28(12): e63-e.

Huang X-Y, Hu X-N, Ma H, et al. Detection of new bunyavirus RNA by reverse transcription-loop-mediated isothermal amplification [J]. Journal of clinical microbiology, 2014a, 52(2):

531-5.
E. Tacconelli E C, A. Savoldi, D. Kattula, F. Burkert. Global priority list of antibiotic-resistant bacteria to guide research, discovery, and development of new antibiotics [J]. WHO report, 2017,
Tacconelli E, Carrara E, Savoldi A, et al. Discovery, research, and development of new antibiotics: the WHO priority list of antibiotic-resistant bacteria and tuberculosis [J]. The Lancet Infectious diseases, 2018, 18(3): 318-27.
Xu Z, Li M, Li Y, et al. Native CRISPR-Cas mediated in situ genome editing reveals extensive resistance synergy in the clinical multidrug resistant <em>Pseudomonas aeruginosa</em&gt [J]. bioRxiv, 2018a, 496711.
Pawluk A, Staals R H J, Taylor C, et al. Inactivation of CRISPR-Cas systems by anti-CRISPR proteins in diverse bacterial species [J]. Nature Microbiology, 2016, 1(16085.
Van Belkum A, Soriaga L B, Lafave M C, et al. Phylogenetic Distribution of CRISPR-Cas Systems in Antibiotic-Resistant Pseudomonas aeruginosa [J]. MBio, 2015, 6(6): e01796.
Yan, Lei, Zhou, et al. Isothermal amplified detection of DNA and RNA [J]. Molecular BioSystems, 2014,
Lobato I M, O'sullivan C K. Recombinase polymerase amplification: Basics, applications and recent advances [J]. TrAC Trends in Analytical Chemistry, 2018, 98(19-35.
Ali M M, Li F, Zhang Z, et al. Rolling circle amplification: a versatile tool for chemical biology, materials science and medicine [J]. Chemical Society reviews, 2014a, 43(10): 3324-41.
Xu G, Hu L, Zhong H, et al. Cross Priming Amplification: Mechanism and Optimization for Isothermal DNA Amplification [J]. Scientific reports, 2012a, 2(1): 246.
Wang Y, Li H, Li D, et al. Multiple Cross Displacement Amplification Combined with Gold Nanoparticle-Based Lateral Flow Biosensor for Detection of Vibrio parahaemolyticus [J]. Frontiers in Microbiology, 2016a, 7(2047):
Liu W, Dong D, Yang Z, et al. Polymerase Spiral Reaction (PSR): A novel isothermal nucleic acid amplification method [J]. Scientific reports, 2015a, 5(1): 12723.
Compton J. Nucleic acid sequence-based amplification [J]. Nature, 1991, 350(6313): 91-2.
Vincent M, Xu Y, Kong H. Helicase-dependent isothermal DNA amplification [J]. EMBO Rep, 2004a, 5(8): 795-800.
Geng Y, Wu J, Shao L, et al. Sensitive colorimetric biosensing for methylation analysis of p16/CDKN2 promoter with hyperbranched rolling circle amplification [J]. Biosens Bioelectron, 2014, 61(593-7.
Hamidi S V, Ghourchian H. Colorimetric monitoring of rolling circle amplification for detection of H5N1 influenza virus using metal indicator [J]. Biosens Bioelectron, 2015, 72(121-6.
Oh S J, Park B H, Jung J H, et al. Centrifugal loop-mediated isothermal amplification microdevice for rapid, multiplex and colorimetric foodborne pathogen detection [J]. Biosens Bioelectron, 2016, 75(293-300.
Hu B, Guo J, Xu Y, et al. A sensitive colorimetric assay system for nucleic acid detection based on isothermal signal amplification technology [J]. Anal Bioanal Chem, 2017a, 409(20): 4819-25.
Baek Y H, Cheon H S, Park S J, et al. Simple, Rapid and Sensitive Portable Molecular Diagnosis of SFTS Virus Using Reverse Transcriptional Loop-Mediated Isothermal Amplification (RT-LAMP) [J]. J

Microbiol Biotechnol, 2018, 28(11): 1928-36.
Ding S, Chen R, Chen G, et al. One-step colorimetric genotyping of single nucleotide polymorphism using probe-enhanced loop-mediated isothermal amplification (PE-LAMP) [J]. Theranostics, 2019, 9(13): 3723-31.
Yang Y, Qin X, Wang G, et al. Development of a fluorescent probe-based recombinase polymerase amplification assay for rapid detection of Orf virus [J]. Virol J, 2015, 12(206.
Jiang H X, Liang Z Z, Ma Y H, et al. G-quadruplex fluorescent probe-mediated real-time rolling circle amplification strategy for highly sensitive microRNA detection [J]. Anal Chim Acta, 2016, 943(114-22.
Li J, Sun K, Chen Z, et al. A fluorescence biosensor for VEGF detection based on DNA assembly structure switching and isothermal amplification [J]. Biosens Bioelectron, 2017a, 89(Pt 2): 964-9.
Shirato K, Semba S, El-Kafrawy S A, et al. Development of fluorescent reverse transcription loop-mediated isothermal amplification (RT-LAMP) using quenching probes for the detection of the Middle East respiratory syndrome coronavirus [J]. J Virol Methods, 2018, 258(41-8.
Lin Q, Ye X, Yang B, et al. Real-time fluorescence loop-mediated isothermal amplification assay for rapid and sensitive detection of Streptococcus gallolyticus subsp. gallolyticus associated with colorectal cancer [J]. Anal Bioanal Chem, 2019,
Wang J, Lu P, Yan J, et al. Rapid and Sensitive Detection of RNA Viruses Based on Reverse Transcription Loop-Mediated Isothermal Amplification, Magnetic Nanoparticles, and Chemiluminescence [J]. J Biomed Nanotechnol, 2016b, 12(4): 710-6.
Kober C, Niessner R, Seidel M. Quantification of viable and non-viable Legionella spp. by heterogeneous asymmetric recombinase polymerase amplification (haRPA) on a flow-based chemiluminescence microarray [J]. Biosens Bioelectron, 2018, 100(49-55.
Cheng W, Zhang W, Yan Y, et al. A novel electrochemical biosensor for ultrasensitive and specific detection of DNA based on molecular beacon mediated circular strand displacement and rolling circle amplification [J]. Biosens Bioelectron, 2014, 62(274-9.
Barreda-Garcia S, Gonzalez-Alvarez M J, De-Los-Santos-Alvarez N, et al. Attomolar quantitation of Mycobacterium tuberculosis by asymmetric helicase-dependent isothermal DNA-amplification and electrochemical detection [J]. Biosens Bioelectron, 2015, 68(122-8.
Del Rio J S, Svobodova M, Bustos P, et al. Electrochemical detection of Piscirickettsia salmonis genomic DNA from salmon samples using solid-phase recombinase polymerase amplification [J]. Anal Bioanal Chem, 2016, 408(30): 8611-20.
Tabata M, Yao B, Seichi A, et al. Electrochemical Biosensors Combined with Isothermal Amplification for Quantitative Detection of Nucleic Acids [J]. Methods Mol Biol, 2017, 1572(135-51.
Islam M N, Moriam S, Umer M, et al. Naked-eye and electrochemical detection of isothermally amplified HOTAIR long non-coding RNA [J]. Analyst, 2018, 143(13): 3021-8.
Kampeera J, Pasakon P, Karuwan C, et al. Point-of-care rapid detection of Vibrio parahaemolyticus in seafood using loop-mediated isothermal amplification and graphene-based screen-printed electrochemical sensor [J]. Biosens Bioelectron, 2019, 132(271-8.
Draz M S, Lu X. Development of a Loop Mediated Isothermal Amplification (LAMP) - Surface Enhanced Raman spectroscopy (SERS) Assay for the Detection of Salmonella Enterica Serotype

Enteritidis [J]. Theranostics, 2016, 6(4): 522-32.
Yao L, Ye Y, Teng J, et al. In Vitro Isothermal Nucleic Acid Amplification Assisted Surface-Enhanced Raman Spectroscopic for Ultrasensitive Detection of Vibrio parahaemolyticus [J]. Anal Chem, 2017, 89(18): 9775-80.
Gervais L, De Rooij N, Delamarche E. Microfluidic chips for point-of-care immunodiagnostics [J]. Advanced materials (Deerfield Beach, Fla), 2011, 23(24): H151-76.
Chen J, Huang Z, Meng H, et al. A facile fluorescence lateral flow biosensor for glutathione detection based on quantum dots-MnO2 nanocomposites [J]. Sensors and Actuators B: Chemical, 2018b, 260(770-7.
Rodríguez M O, Covián L B, García A C, et al. Silver and gold enhancement methods for lateral flow immunoassays [J]. Talanta, 2016, 148(272-8.
Zhang X, Yu X, Wen K, et al. Multiplex lateral flow immunoassays based on amorphous carbon nanoparticles for detecting three Fusarium mycotoxins in maize [J]. Journal of agricultural and food chemistry, 2017, 65(36): 8063-71.
Xu H, Chen J, Birrenkott J, et al. Gold-nanoparticle-decorated silica nanorods for sensitive visual detection of proteins [J]. Anal Chem, 2014, 86(15): 7351-9.
Elif Burcu B, Mustafa Kemal S. Lateral flow assays: principles, designs and labels [J]. Trends in Analytical Chemistry, 2016,
Sander J D, Joung J K. CRISPR-Cas systems for editing, regulating and targeting genomes [J]. Nature biotechnology, 2014, 32(347.
Chen J S, Ma E, Harrington L B, et al. CRISPR-Cas12a target binding unleashes indiscriminate single-stranded DNase activity [J]. Science, 2018c, 360(6387): 436.
Mori Y, Notomi T. Loop-mediated isothermal amplification (LAMP): a rapid, accurate, and cost-effective diagnostic method for infectious diseases [J]. J Infect Chemother, 2009, 15(2): 62-9.
Notomi, Okayama, Masubuchi, et al. Loop-mediated isothermal amplification of DNA [J]. Nucleic Acids Research, 2000b,
Nagamine K, Kuzuhara Y, Notomi T. Isolation of single-stranded DNA from loop-mediated isothermal amplification products [J]. Biochem Biophys Res Commun, 2002, 290(4): 1195-8.
Byung Hyun P, Seung Jun O, Jae Hwan J, et al. An integrated rotary microfluidic system with DNA extraction, loop-mediated isothermal amplification, and lateral flow strip based detection for point-of-care pathogen diagnostics [J]. Biosensors and Bioelectronics, 2016,
Xueran M, Xiwen Z, Changwei L, et al. Development and application of a visual loop-mediated isothermal amplification combined with lateral flow dipstick (LAMP-LFD) method for rapid detection of Salmonella strains in food samples [J]. Food Control, 2019,
Reona T, Yukari K, Yasutaka M, et al. Rapid Screening Detection of Genetically Modified Crops by Loop-Mediated Isothermal Amplification with a Lateral Flow Dipstick [J]. Journal of Agricultural and Food Chemistry, 2018,
Yin H, Fang T, Wen H. Combined multiplex loop-mediated isothermal amplification with lateral flow assay to detect sea and seb genes of enterotoxic Staphylococcus aureus [J]. Letters in applied

microbiology, 2016, 63(1): 16-24.
Liu W, Dong D, Yang Z, et al. Polymerase spiral reaction (PSR): a novel isothermal nucleic acid amplification method [J]. Scientific reports, 2015b, 5(12723.
Ji J, Xu X, Wang X, et al. Novel polymerase spiral reaction assay for the visible molecular detection of porcine circovirus type 3 [J]. BMC veterinary research, 2019, 15(1): 322.
He S, Jang H, Zhao C, et al. Rapid visualized isothermal nucleic acid testing of Vibrio parahaemolyticus by polymerase spiral reaction [J]. Analytical and Bioanalytical Chemistry, 2020, 412(1): 93-101.
Xu G, Hu L, Zhong H, et al. Cross priming amplification: mechanism and optimization for isothermal DNA amplification [J]. Scientific reports, 2012b, 2(246.
Huang X, Zhai C, You Q, et al. Potential of cross-priming amplification and DNA-based lateral-flow strip biosensor for rapid on-site GMO screening [J]. Analytical and bioanalytical chemistry, 2014b, 406(17): 4243-9.
Gao Y, Meng X-Y, Zhang H, et al. Cross-priming amplification combined with immunochromatographic strip for rapid on-site detection of African swine fever virus [J]. Sensors and Actuators B: Chemical, 2018, 274(304-9.
Wang Y, Wang Y, Ma A-J, et al. Rapid and sensitive isothermal detection of nucleic-acid sequence by multiple cross displacement amplification [J]. Scientific reports, 2015, 5(11902.
Hu S, Niu L, Zhao F, et al. Identification of Acinetobacter baumannii and its carbapenem-resistant gene bla OXA-23-like by multiple cross displacement amplification combined with lateral flow biosensor [J]. Scientific Reports, 2019, 9(1): 1-11.
Wang Y, Deng J, Liu D, et al. Nanoparticles-based lateral flow biosensor coupled with multiple cross displacement amplification Plus for simultaneous detection of nucleic acid and prevention of carryover contamination [J]. Sensors and Actuators B: Chemical, 2018a, 255(3332-43.
Wang Y, Wang Y, Zhang L, et al. Visual and multiplex detection of nucleic acid sequence by multiple cross displacement amplification coupled with gold nanoparticle-based lateral flow biosensor [J]. Sensors and Actuators B: Chemical, 2017a, 241(1283-93.
Piepenburg O, Williams C H, Stemple D L, et al. DNA detection using recombination proteins [J]. PLoS Biol, 2006, 4(7): e204.
Fu M, Chen G, Zhang C, et al. Rapid and sensitive detection method for Karlodinium veneficum by recombinase polymerase amplification coupled with lateral flow dipstick [J]. Harmful Algae, 2019, 84(1-9.
Saxena A, Pal V, Tripathi N K, et al. Development of a rapid and sensitive recombinase polymerase amplification-lateral flow assay for detection of Burkholderia mallei [J]. Transbound Emerg Dis, 2019, 66(2): 1016-22.
Sun N, Wang Y, Yao X, et al. Visual signal generation for the detection of influenza viruses by duplex recombinase polymerase amplification with lateral flow dipsticks [J]. Anal Bioanal Chem, 2019, 411(16): 3591-602.
Du X J, Zang Y X, Liu H B, et al. Recombinase Polymerase Amplification Combined with Lateral Flow Strip for Listeria monocytogenes Detection in Food [J]. J Food Sci, 2018, 83(4): 1041-7.

Li T, Jalbani Y M, Zhang G, et al. Rapid authentication of mutton products by recombinase polymerase amplification coupled with lateral flow dipsticks [J]. Sensors and Actuators B: Chemical, 2019, 290(242-8.

Xu Y, Wei Y, Cheng N, et al. Nucleic Acid Biosensor Synthesis of an All-in-One Universal Blocking Linker Recombinase Polymerase Amplification with a Peptide Nucleic Acid-Based Lateral Flow Device for Ultrasensitive Detection of Food Pathogens [J]. Analytical Chemistry, 2018b, 90(1): 708-15.

Walker, G T, Fraiser, et al. Strand displacement amplification--an isothermal, in vitro DNA amplification technique [J]. Nucleic Acids Research, 1992a,

Walker, G T, Little, et al. Isothermal in vitro amplification of DNA by a restriction enzyme/DNA polymerase system [J]. PNAS, 1992b,

Fang, Zhiyuan, Wu, et al. Lateral flow biosensor for DNA extraction-free detection of Salmonella based on aptamer mediated strand displacement amplification [J]. Biosensors and Bioelectronics, 2014a,

Wu, Wei, Zhao, et al. A sensitive lateral flow biosensor for Escherichia coli O157:H7 detection based on aptamer mediated strand displacement amplification [J]. Analytica Chimica Acta, 2015a,

Wu W, Mao Y, Zhao S, et al. Strand displacement amplification for ultrasensitive detection of human pluripotent stem cells [J]. Analytica Chimica Acta, 2015b, 881(124-30.

Blanco, Bernad, Lazaro, et al. Highly efficient DNA synthesis by the phage phi 29 DNA polymerase. Symmetrical mode of DNA replication [J]. Journal of Biological Chemistry, 1989,

Banér J, Nilsson M, Mendel-Hartvig M, et al. Signal amplification of padlock probes by rolling circle replication [J]. Nucleic Acids Research, 1998, 26(22): 5073-8.

Yao M, Lv X, Deng Y, et al. Specific and simultaneous detection of micro RNA 21 and let-7a by rolling circle amplification combined with lateral flow strip [J]. Anal Chim Acta, 2019a, 1055(115-25.

Chunyun Z, Guofu C, Yuanyuan W, et al. Establishment and application of hyperbranched rolling circle amplification coupled with lateral flow dipstick for the sensitive detection of Karenia mikimotoi [J]. Harmful Algae, 2019,

Liu F G, Chen G F, Zhang C Y, et al. Exponential rolling circle amplification coupled with lateral flow dipstick strips as a rapid and sensitive method for the field detection of Karlodinium veneficum [J]. Journal of Applied Phycology, 2019, 31(4): 2423-36.

Deiman B, Van Aarle P, Sillekens P. Characteristics and applications of nucleic acid sequence-based amplification (NASBA) [J]. Mol Biotechnol, 2002, 20(2): 163-79.

Park C, Kwon E Y, Shin N Y, et al. Evaluation of nucleic acid sequence based amplification using fluorescence resonance energy transfer (FRET-NASBA) in quantitative detection of Aspergillus 18S rRNA [J]. Med Mycol, 2011, 49(1): 73-9.

Niazi A, Jorjani O N, Nikbakht H, et al. A nanodiagnostic colorimetric assay for 18S rRNA of Leishmania pathogens using nucleic acid sequence-based amplification and gold nanorods [J]. Mol Diagn Ther, 2013, 17(6): 363-70.

Vincent M, Xu Y, Kong H. Helicase-dependent isothermal DNA amplification [J]. EMBO Rep, 2004b, 5(8): 795-800.

Kolm C, Martzy R, Fuhrer M, et al. Detection of a microbial source tracking marker by isothermal

helicase-dependent amplification and a nucleic acid lateral-flow strip test [J]. Sci Rep, 2019, 9(1): 393.
Aslanzadeh J. Preventing PCR amplification carryover contamination in a clinical laboratory [J]. Annals of Clinical & Laboratory Science, 2004, 34(4): 389-96.
Qian W, Meng Y, Lu Y, et al. Rapid, sensitive, and carryover contamination-free loop-mediated isothermal amplification-coupled visual detection method for 'Candidatus Liberibacter asiaticus' [J]. Journal of agricultural and food chemistry, 2017, 65(38): 8302-10.
Hsieh K, Mage P L, Csordas A T, et al. Simultaneous elimination of carryover contamination and detection of DNA with uracil-DNA-glycosylase-supplemented loop-mediated isothermal amplification (UDG-LAMP) [J]. Chemical communications, 2014, 50(28): 3747-9.
Ma C, Wang F, Wang X, et al. A novel method to control carryover contamination in isothermal nucleic acid amplification [J]. Chemical Communications, 2017, 53(77): 10696-9.
Wang Y, Liu D, Deng J, et al. Loop-mediated isothermal amplification using self-avoiding molecular recognition systems and antarctic thermal sensitive uracil-DNA-glycosylase for detection of nucleic acid with prevention of carryover contamination [J]. Analytica chimica acta, 2017b, 996(74-87.
Qian C, Wang R, Wu H, et al. Uracil-Mediated New Photospacer-Adjacent Motif of Cas12a To Realize Visualized DNA Detection at the Single-Copy Level Free from Contamination [J]. Analytical chemistry, 2019, 91(17): 11362-6.
Singh M, Pal D, Sood P, et al. Loop-mediated isothermal amplification assays: Rapid and efficient diagnostics for genetically modified crops [J]. Food Control, 2019, 106(106759.
Li Y, Fan P, Zhou S, et al. Loop-mediated isothermal amplification (LAMP): A novel rapid detection platform for pathogens [J]. Microbial Pathogenesis, 2017b, 107(54-61.
Qi H, Yue S, Bi S, et al. Isothermal exponential amplification techniques: From basic principles to applications in electrochemical biosensors [J]. Biosensors and Bioelectronics, 2018, 110(207-17.
Dong Q, Liu Q, Guo L, et al. A signal-flexible gene diagnostic strategy coupling loop-mediated isothermal amplification with hybridization chain reaction [J]. Analytica Chimica Acta, 2019, 1079(171-9.
Gao H, Zhang K, Teng X, et al. Rolling circle amplification for single cell analysis and in situ sequencing [J]. TrAC Trends in Analytical Chemistry, 2019, 121(115700.
Yao M, Lv X, Deng Y, et al. Specific and simultaneous detection of micro RNA 21 and let-7a by rolling circle amplification combined with lateral flow strip [J]. Analytica Chimica Acta, 2019b, 1055(115-25.
Deng H, Gao Z. Bioanalytical applications of isothermal nucleic acid amplification techniques [J]. Analytica Chimica Acta, 2015, 853(30-45.
Dunbar S, Das S. Amplification chemistries in clinical virology [J]. Journal of Clinical Virology, 2019, 115(18-31.
Mayboroda O, Katakis I, O'sullivan C K. Multiplexed isothermal nucleic acid amplification [J]. Analytical Biochemistry, 2018, 545(20-30.
Zhao Y, Chen F, Li Q, et al. Isothermal Amplification of Nucleic Acids [J]. Chemical Reviews, 2015a, 115(22): 12491-545.
Shen X, Chen D, Fu Y, et al. 42. RETROSPECTIVE PGT-A ANALYSIS FOR MULTIPLE DISPLACEMENT AMPLIFICATION (MDA) PRODUCTS OF EMBRYOS CORRESPONDING TO 21

SPONTANEOUS ABORTIONS BY NGS [J]. Reproductive BioMedicine Online, 2019, 39(e52-e3.

Wang Y, Yan W, Wang Y, et al. Rapid, sensitive and reliable detection of Klebsiella pneumoniae by label-free multiple cross displacement amplification coupled with nanoparticles-based biosensor [J]. Journal of Microbiological Methods, 2018b, 149(80-8.

Chen Y, Yang M, Xiang Y, et al. Ligase chain reaction amplification for sensitive electrochemiluminescent detection of single nucleotide polymorphisms [J]. Analytica Chimica Acta, 2013, 796(1-6.

Zhang B, Xia Q, Wang Q, et al. Detecting and typing target DNA with a novel CRISPR-typing PCR (ctPCR) technique [J]. Analytical Biochemistry, 2018, 561-562(37-46.

Jia C, Huai C, Ding J, et al. New applications of CRISPR/Cas9 system on mutant DNA detection [J]. Gene, 2018, 641(55-62.

Liang X, Potter J, Kumar S, et al. Rapid and highly efficient mammalian cell engineering via Cas9 protein transfection [J]. Journal of Biotechnology, 2015, 208(44-53.

Sternberg S H, Redding S, Jinek M, et al. DNA interrogation by the CRISPR RNA-guided endonuclease Cas9 [J]. Nature, 2014, 507(7490): 62-7.

Swarts D C, Van Der Oost J, Jinek M. Structural Basis for Guide RNA Processing and Seed-Dependent DNA Targeting by CRISPR-Cas12a [J]. Molecular cell, 2017, 66(2): 221-33.e4.

Gao P, Yang H, Rajashankar K R, et al. Type V CRISPR-Cas Cpf1 endonuclease employs a unique mechanism for crRNA-mediated target DNA recognition [J]. Cell research, 2016, 26(8): 901-13.

Brouns S J, Jore M M, Lundgren M, et al. Small CRISPR RNAs guide antiviral defense in prokaryotes [J]. Science, 2008, 321(5891): 960-4.

Deltcheva E, Chylinski K, Sharma C M, et al. CRISPR RNA maturation by trans-encoded small RNA and host factor RNase III [J]. Nature, 2011, 471(7340): 602-7.

Samai P, Pyenson N, Jiang W, et al. Co-transcriptional DNA and RNA Cleavage during Type III CRISPR-Cas Immunity [J]. Cell, 2015, 161(5): 1164-74.

Sogo J M, Lopes M, Foiani M. Fork Reversal and ssDNA Accumulation at Stalled Replication Forks Owing to Checkpoint Defects [J]. Science, 2002, 297(5581): 599.

Tsou J-H, Leng Q, Jiang F. A CRISPR Test for Detection of Circulating Nuclei Acids [J]. Translational Oncology, 2019, 12(12): 1566-73.

Mukama O, Wu J, Li Z, et al. An ultrasensitive and specific point-of-care CRISPR/Cas12 based lateral flow biosensor for the rapid detection of nucleic acids [J]. Biosensors and Bioelectronics, 2020, 112143.

Fukuma A, Kurosaki Y, Morikawa Y, et al. Rapid detection of Lassa virus by reverse transcription-loop-mediated isothermal amplification [J]. Microbiology and immunology, 2011, 55(1): 44-50.

Blomstrom A L, Hakhverdyan M, Reid S M, et al. A one-step reverse transcriptase loop-mediated isothermal amplification assay for simple and rapid detection of swine vesicular disease virus [J]. Journal of virological methods, 2008, 147(1): 188-93.

Ferlay J E M, Lam F, Colombet M, Mery L, Piñeros M, Znaor A, Soerjomataram I, Bray F Global

Cancer Observatory: Cancer Today. Lyon, France: International Agency for Research on Cancer. [J]. WHO, https://gcoiarcfr/today, 2018,

Lowy D R, Schiller J T. Reducing HPV-associated cancer globally [J]. Cancer Prev Res (Phila), 2012, 5(1): 18-23.

Burd E M. Human papillomavirus and cervical cancer [J]. Clin Microbiol Rev, 2003, 16(1): 1-17.

Gustafsson L, Ponten J, Zack M, et al. International incidence rates of invasive cervical cancer after introduction of cytological screening [J]. Cancer causes & control : CCC, 1997, 8(5): 755-63.

Dickinson J A, Stankiewicz A, Popadiuk C, et al. Reduced cervical cancer incidence and mortality in Canada: national data from 1932 to 2006 [J]. BMC public health, 2012, 12(992.

Ferdous M, Lee S, Goopy S, et al. Barriers to cervical cancer screening faced by immigrant women in Canada: a systematic scoping review [J]. BMC women's health, 2018, 18(1): 165.

Cuzick J, Arbyn M, Sankaranarayanan R, et al. Overview of human papillomavirus-based and other novel options for cervical cancer screening in developed and developing countries [J]. Vaccine, 2008, 26 Suppl 10(K29-41.

Kumar A A, Hennek J W, Smith B S, et al. From the Bench to the Field in Low-Cost Diagnostics: Two Case Studies [J]. Angewandte Chemie International Edition, 2015, 54(20): 5836-53.

Halliday J E B, Hampson K, Hanley N, et al. Driving improvements in emerging disease surveillance through locally relevant capacity strengthening [J]. Science, 2017, 357(6347): 146.

Corey A S, Hudgins P A. Radiographic imaging of human papillomavirus related carcinomas of the oropharynx [J]. Head Neck Pathol, 2012, 6 Suppl 1(Suppl 1): S25-S40.

Abreu A L P, Souza R P, Gimenes F, et al. A review of methods for detect human Papillomavirus infection [J]. Virol J, 2012, 9(262-.

Mariano V S, Lorenzi A T, Scapulatempo-Neto C, et al. A Low-Cost HPV Immunochromatographic Assay to Detect High-Grade Cervical Intraepithelial Neoplasia [J]. PLoS One, 2016, 11(10): e0164892-e.

Siti-Aishah M A, Isahak I, Sabil D, et al. Detection of human papillomavirus using in situ hybridization technique in vulvo-vaginal warts [J]. Malays J Med Sci, 2000, 7(2): 27-31.

Lu W, Yuan Q, Yang Z, et al. Self-primed isothermal amplification for genomic DNA detection of human papillomavirus [J]. Biosensors and Bioelectronics, 2017, 90(258-63.

Ma B, Fang J, Lin W, et al. A simple and efficient method for potential point-of-care diagnosis of human papillomavirus genotypes: combination of isothermal recombinase polymerase amplification with lateral flow dipstick and reverse dot blot [J]. Analytical and Bioanalytical Chemistry, 2019, 411(28): 7451-60.

Ali M M, Li F, Zhang Z, et al. Rolling circle amplification: a versatile tool for chemical biology, materials science and medicine [J]. Chemical Society reviews, 2014b, 43(10): 3324-41.

Kim D, Kim J, Hur J K, et al. Genome-wide analysis reveals specificities of Cpf1 endonucleases in human cells [J]. Nature biotechnology, 2016a, 34(8): 863-8.

Kleinstiver B P, Tsai S Q, Prew M S, et al. Genome-wide specificities of CRISPR-Cas Cpf1 nucleases in human cells [J]. Nature biotechnology, 2016a, 34(8): 869-74.

Fang Z, Wu W, Lu X, et al. Lateral flow biosensor for DNA extraction-free detection of salmonella

based on aptamer mediated strand displacement.amplification [J]. Biosensors & Bioelectronics, 2014b, 56(192-7.

Kodaka H, Iwata M, Yumoto S, et al. Evaluation of a new agar medium containing cetrimide, kanamycin and nalidixic acid for isolation and enhancement of pigment production of Pseudomonas aeruginosa in clinical samples [J]. Journal of basic microbiology, 2003, 43(5): 407-13.

Jami Al-Ahmadi G, Zahmatkesh Roodsari R. Fast and specific detection of Pseudomonas Aeruginosa from other pseudomonas species by PCR [J]. Ann Burns Fire Disasters, 2016, 29(4): 264-7.

Zeng L, Lie P, Fang Z, et al. Lateral Flow Biosensors for the Detection of Nucleic Acid [M]//KOLPASHCHIKOV, GERASIMOVA. Nucleic Acid Detection: Methods and Protocols. Totowa, NJ; Humana Press. 2013: 161-7.

Seaman W T, Andrews E, Couch M, et al. Detection and quantitation of HPV in genital and oral tissues and fluids by real time PCR [J]. Virol J, 2010, 7(194-.

Gootenberg J S, Abudayyeh O O, Lee J W, et al. Nucleic acid detection with CRISPR-Cas13a/C2c2 [J]. Science, 2017, 356(6336): 438-42.

Kim D, Kim J, Hur J K, et al. Genome-wide analysis reveals specificities of Cpf1 endonucleases in human cells [J]. Nature biotechnology, 2016b, 34(863.

Kleinstiver B P, Tsai S Q, Prew M S, et al. Genome-wide specificities of CRISPR-Cas Cpf1 nucleases in human cells [J]. Nature biotechnology, 2016b, 34(869.

Kleiboeker S B, Scoles G A, Burrage T G, et al. African swine fever virus replication in the midgut epithelium is required for infection of Ornithodoros ticks [J]. Journal of virology, 1999, 73(10): 8587-98.

Parker J, Plowright W, Pierce M A. The epizootiology of African swine fever in Africa [J]. The Veterinary record, 1969, 85(24): 668-74.

Gomez-Villamandos J C, Bautista M J, Sanchez-Cordon P J, et al. Pathology of African swine fever: the role of monocyte-macrophage [J]. Virus research, 2013, 173(1): 140-9.

Gallardo C, Fernández-Pinero J, Pelayo V, et al. Genetic variation among African swine fever genotype II viruses, eastern and central Europe [J]. Emerg Infect Dis, 2014, 20(9): 1544-7.

Ruiz-Fons F, Segalés J, Gortázar C. A review of viral diseases of the European wild boar: Effects of population dynamics and reservoir rôle [J]. The Veterinary Journal, 2008, 176(2): 158-69.

Gogin A, Gerasimov V, Malogolovkin A, et al. African swine fever in the North Caucasus region and the Russian Federation in years 2007-2012 [J]. Virus research, 2013, 173(1): 198-203.

Śmietanka K, Woźniakowski G, Kozak E, et al. African Swine Fever Epidemic, Poland, 2014-2015 [J]. Emerg Infect Dis, 2016, 22(7): 1201-7.

Sanchez-Vizcaino J M, Mur L, Martinez-Lopez B. African swine fever (ASF): five years around Europe [J]. Veterinary microbiology, 2013, 165(1-2): 45-50.

Liu J, Liu B, Shan B, et al. Prevalence of African Swine Fever in China, 2018-2019 [J]. Journal of Medical Virology, n/a(n/a):

Cubillos C, Gomez-Sebastian S, Moreno N, et al. African swine fever virus serodiagnosis: a general review with a focus on the analyses of African serum samples [J]. Virus research, 2013, 173(1): 159-67.

Agüero M, Fernández J, Romero L, et al. Highly sensitive PCR assay for routine diagnosis of African swine fever virus in clinical samples [J]. Journal of clinical microbiology, 2003, 41(9): 4431-4.

Harrington L B, Burstein D, Chen J S, et al. Programmed DNA destruction by miniature CRISPR-Cas14 enzymes [J]. Science, 2018, 362(6416): 839-42.

Smatti M K, Al-Sadeq D W, Ali N H, et al. Epstein-Barr Virus Epidemiology, Serology, and Genetic Variability of LMP-1 Oncogene Among Healthy Population: An Update [J]. Frontiers in oncology, 2018, 8(211.

Chou J, Lin Y-C, Kim J, et al. Nasopharyngeal carcinoma--review of the molecular mechanisms of tumorigenesis [J]. Head Neck, 2008, 30(7): 946-63.

Niedobitek G, Meru N, Delecluse H J. Epstein-Barr virus infection and human malignancies [J]. Int J Exp Pathol, 2001, 82(3): 149-70.

Wu L, Li C, Pan L. Nasopharyngeal carcinoma: A review of current updates [J]. Exp Ther Med, 2018, 15(4): 3687-92.

Hu J, Kong L, Gao J, et al. Use of Radiation Therapy in Metastatic Nasopharyngeal Cancer Improves Survival: A SEER Analysis [J]. Scientific reports, 2017b, 7(1): 721-.

Cai Y, Song Y, Cen D, et al. Novel ELISA for serodiagnosis of nasopharyngeal carcinoma based on a B cell epitope of Epstein-Barr virus latent membrane protein 2 [J]. Oncology letters, 2018, 16(4): 4372-8.

Van Beek J, Zur Hausen A, Kranenbarg E K, et al. A Rapid and Reliable Enzyme Immunoassay PCR-Based Screening Method to Identify EBV-Carrying Gastric Carcinomas [J]. Modern Pathology, 2002, 15(8): 870-7.

Wu W, Zhao S, Mao Y, et al. A sensitive lateral flow biosensor for Escherichia coli O157:H7 detection based on aptamer mediated strand displacement amplification [J]. Analytica Chimica Acta, 2015c, 861(62-8.

Fang Z, Wu W, Lu X, et al. Lateral flow biosensor for DNA extraction-free detection of salmonella based on aptamer mediated strand displacement amplification [J]. Biosensors and Bioelectronics, 2014c, 56(192-7.

Chan K H, Ng M H, Seto W H, et al. Epstein-Barr Virus (EBV) DNA in Sera of Patients with Primary EBV Infection [J]. Journal of clinical microbiology, 2001, 39(11): 4152.

Ai J-W, Zhou X, Xu T, et al. CRISPR-based rapid and ultra-sensitive diagnostic test for Mycobacterium tuberculosis [J]. Emerg Microbes Infect, 2019, 8(1): 1361-9.

Limeres Posse J, Diz Dios P, Scully C. Viral Diseases Transmissible by Kissing [J]. Saliva Protection and Transmissible Diseases, 2017, 53-92.

Haylock D N, Nilsson S K. Osteopontin: a bridge between bone and blood [J]. British Journal of Haematology, 2006, 134(5): 467-74.

Das R, Mahabeleshwar G H, Kundu G C. Osteopontin stimulates cell motility and nuclear factor kappaB-mediated secretion of urokinase type plasminogen activator through phosphatidylinositol 3-kinase/Akt signaling pathways in breast cancer cells [J]. The Journal of biological chemistry, 2003, 278(31): 28593-606.

Reinholt F P, Hultenby K, Oldberg A, et al. Osteopontin--a possible anchor of osteoclasts to bone [J].

Proc Natl Acad Sci U S A, 1990, 87(12): 4473-5.
Takahashi F, Takahashi K, Shimizu K, et al. Osteopontin is strongly expressed by alveolar macrophages in the lungs of acute respiratory distress syndrome [J]. Lung, 2004, 182(3): 173-85.
Strom A, Franzen A, Wangnerud C, et al. Altered vascular remodeling in osteopontin-deficient atherosclerotic mice [J]. Journal of vascular research, 2004, 41(4): 314-22.
Bautista D S, Denstedt J, Chambers A F, et al. Low-molecular-weight variants of osteopontin generated by serine proteinases in urine of patients with kidney stones [J]. Journal of cellular biochemistry, 1996, 61(3): 402-9.
Teramoto H, Castellone M D, Malek R L, et al. Autocrine activation of an osteopontin-CD44-Rac pathway enhances invasion and transformation by H-RasV12 [J]. Oncogene, 2005, 24(3): 489-501.
Wai P Y, Kuo P C. The role of Osteopontin in tumor metastasis [J]. The Journal of surgical research, 2004, 121(2): 228-41.
Hu Z, Lin D, Yuan J, et al. Overexpression of osteopontin is associated with more aggressive phenotypes in human non-small cell lung cancer [J]. Clinical cancer research : an official journal of the American Association for Cancer Research, 2005, 11(13): 4646-52.
Bramwell V H, Tuck A B, Chapman J A, et al. Assessment of osteopontin in early breast cancer: correlative study in a randomised clinical trial [J]. Breast cancer research : BCR, 2014a, 16(1): R8.
He Y, Zeng K, Zhang S, et al. Visual detection of gene mutations based on isothermal strand-displacement polymerase reaction and lateral flow strip [J]. Biosensors and Bioelectronics, 2012, 31(1): 310-5.
Zhao M, Liang F, Zhang B, et al. The impact of osteopontin on prognosis and clinicopathology of colorectal cancer patients: a systematic meta-analysis [J]. Scientific reports, 2015b, 5(12713-.
Gotoh M, Sakamoto M, Kanetaka K, et al. Overexpression of osteopontin in hepatocellular carcinoma [J]. Pathology international, 2002, 52(1): 19-24.
Lorena D, Darby I A, Gadeau A P, et al. Osteopontin expression in normal and fibrotic liver. altered liver healing in osteopontin-deficient mice [J]. Journal of hepatology, 2006, 44(2): 383-90.
Zhao H, Chen Q, Alam A, et al. The role of osteopontin in the progression of solid organ tumour [J]. Cell Death & Disease, 2018, 9(3): 356.
Rittling S R, Wejse P L, Yagiz K, et al. Suppression of tumour growth by orally administered osteopontin is accompanied by alterations in tumour blood vessels [J]. British Journal Of Cancer, 2014, 110(1269.
Mi Z, Guo H, Russell M B, et al. RNA Aptamer Blockade of Osteopontin Inhibits Growth and Metastasis of MDA-MB231 Breast Cancer Cells [J]. Molecular Therapy, 2009, 17(1): 153-61.
Vaschetto R, Nicola S, Olivieri C, et al. Serum levels of osteopontin are increased in SIRS and sepsis [J]. Intensive Care Medicine, 2008, 34(12): 2176-84.
Meirinho S G, Dias L G, Peres A M, et al. Electrochemical aptasensor for human osteopontin detection using a DNA aptamer selected by SELEX [J]. Analytica Chimica Acta, 2017, 987(25-37.
Meirinho S G, Dias L G, Peres A M, et al. Development of an Electrochemical Aptasensor for the Detection of Human Osteopontin [J]. Procedia Engineering, 2014, 87(316-9.

Chakraborty D, Viveka T S, Arvind K, et al. A facile gold nanoparticle–based ELISA system for detection of osteopontin in saliva: Towards oral cancer diagnostics [J]. Clinica Chimica Acta, 2018a, 477(166-72.

Saad F A, Salih E, Glimcher M J. Identification of osteopontin phosphorylation sites involved in bone remodeling and inhibition of pathological calcification [J]. Journal of cellular biochemistry, 2008, 103(3): 852-6.

Lenton S, Grimaldo M, Roosen-Runge F, et al. Effect of Phosphorylation on a Human-like Osteopontin Peptide [J]. Biophysical journal, 2017, 112(8): 1586-96.

Christensen B, Schack L, Kläning E, et al. Osteopontin is cleaved at multiple sites close to its integrin-binding motifs in milk and is a novel substrate for plasmin and cathepsin D [J]. The Journal of biological chemistry, 2010, 285(11): 7929-37.

Chen H, Mei Q, Jia S, et al. High specific detection of osteopontin using a three-dimensional copolymer layer support based on electrochemical impedance spectroscopy [J]. Analyst, 2014, 139(18): 4476-81.

El-Din Bessa S S, Elwan N M, Suliman G A M, et al. Clinical Significance of Plasma Osteopontin Level in Egyptian Patients with Hepatitis C Virus-related Hepatocellular Carcinoma [J]. Archives of Medical Research, 2010, 41(7): 541-7.

Bramwell V H C, Tuck A B, Chapman J-A W, et al. Assessment of osteopontin in early breast cancer: correlative study in a randomised clinical trial [J]. Breast cancer research : BCR, 2014b, 16(1): R8-R.

Baryeh K, Takalkar S, Lund M, et al. Development of quantitative immunochromatographic assay for rapid and sensitive detection of carbohydrate antigen 19-9 (CA 19-9) in human plasma [J]. Journal of Pharmaceutical and Biomedical Analysis, 2017, 146(285-91.

Huang Y, Wen Y, Baryeh K, et al. Lateral flow assay for carbohydrate antigen 19–9 in whole blood by using magnetized carbon nanotubes [J]. Microchimica Acta, 2017, 184(11): 4287-94.

Mukama O, Sinumvayo J P, Shamoon M, et al. An Update on Aptamer-Based Multiplex System Approaches for the Detection of Common Foodborne Pathogens [J]. Food Analytical Methods, 2017, 10(7): 2549-65.

Sajid M, Kawde A-N, Daud M. Designs, formats and applications of lateral flow assay: A literature review [J]. Journal of Saudi Chemical Society, 2015, 19(6): 689-705.

Guo L, Jackman J A, Yang H-H, et al. Strategies for enhancing the sensitivity of plasmonic nanosensors [J]. Nano Today, 2015, 10(2): 213-39.

Kim H-S, Kim Y-J, Chon J-W, et al. Two-stage label-free aptasensing platform for rapid detection of Cronobacter sakazakii in powdered infant formula [J]. Sensors and Actuators B: Chemical, 2017, 239(94-9.

Oh S Y, Heo N S, Shukla S, et al. Development of gold nanoparticle-aptamer-based LSPR sensing chips for the rapid detection of Salmonella typhimurium in pork meat [J]. Scientific reports, 2017, 7(1): 10130-.

Fang Z, Ge C, Zhang W, et al. A lateral flow biosensor for rapid detection of DNA-binding protein c-jun [J]. Biosensors and Bioelectronics, 2011, 27(1): 192-6.

Kalra P, Dhiman A, Cho W C, et al. Simple Methods and Rational Design for Enhancing Aptamer

Sensitivity and Specificity [J]. Frontiers in Molecular Biosciences, 2018a, 5(41):

D'agata R, Palladino P, Spoto G. Streptavidin-coated gold nanoparticles: critical role of oligonucleotides on stability and fractal aggregation [J]. Beilstein journal of nanotechnology, 2017, 8(1-11.

Salem. Clinical Significance of Plasma Osteopontin Level as a Biomarker of Hepatocellular Carcinoma [M]. 2013.

Fang B, Hu S, Wang C, et al. Lateral flow immunoassays combining enrichment and colorimetry-fluorescence quantitative detection of sulfamethazine in milk based on trifunctional magnetic nanobeads [J]. Food Control, 2019, 98(268-73.

Toley B J, Covelli I, Belousov Y, et al. Isothermal strand displacement amplification (iSDA): a rapid and sensitive method of nucleic acid amplification for point-of-care diagnosis [J]. Analyst, 2015, 140(22): 7540-9.

Bache M, Kappler M, Wichmann H, et al. Elevated tumor and serum levels of the hypoxia-associated protein osteopontin are associated with prognosis for soft tissue sarcoma patients [J]. BMC Cancer, 2010, 10(1): 132.

Simão A, Madaleno J, Silva N, et al. Plasma osteopontin is a biomarker for the severity of alcoholic liver cirrhosis, not for hepatocellular carcinoma screening [J]. BMC gastroenterology, 2015, 15(73-.

Chakraborty D, Viveka T S, Arvind K, et al. A facile gold nanoparticle-based ELISA system for detection of osteopontin in saliva: Towards oral cancer diagnostics [J]. Clinica chimica acta; international journal of clinical chemistry, 2018b, 477(166-72.

Zhao L, Wang Y, Qu N, et al. Significance of Plasma Osteopontin Levels in Patients with Bladder Urothelial Carcinomas [J]. Molecular Diagnosis & Therapy, 2012, 16(5): 311-6.

Kalra P, Dhiman A, Cho W C, et al. Simple Methods and Rational Design for Enhancing Aptamer Sensitivity and Specificity [J]. Frontiers in molecular biosciences, 2018b, 5(41-.

Razmi N, Baradaran B, Hejazi M, et al. Recent advances on aptamer-based biosensors to detection of platelet-derived growth factor [J]. Biosensors and Bioelectronics, 2018, 113(58-71.

Chang P-L, Harkins L, Hsieh Y-H, et al. Osteopontin expression in normal skin and non-melanoma skin tumors [J]. The journal of histochemistry and cytochemistry : official journal of the Histochemistry Society, 2008, 56(1): 57-66.

Razzouk S, Brunn J C, Qin C, et al. Osteopontin posttranslational modifications, possibly phosphorylation, are required for in vitro bone resorption but not osteoclast adhesion [J]. Bone, 2002, 30(1): 40-7.

Ay C, Dunkler D, Simanek R, et al. Prediction of Venous Thromboembolism in Patients With Cancer by Measuring Thrombin Generation: Results From the Vienna Cancer and Thrombosis Study [J]. Journal of Clinical Oncology, 2011, 29(15): 2099-103.

Acknowledgements

Author’s resume, academic papers and research results published during the author's degree study

During my PhD, I have achieved to publish 4 SCI research articles as first author and 1 book with an overall impact factor of 23.327. Moreover, 2 other research articles have been submitted to SCI journals.